Development of a Mechanical Counter Pressure Bio-Suit System for Planetary Exploration

by

Zhe Liang Sim

B.E. in Mechanical Engineering
University of New South Wales, Sydney, Australia (2003)

Submitted to the Department of Aeronautics and Astronautics
in partial fulfillment of the requirements for the degree of

Master of Science in Aeronautics and Astronautics

at the

MASSACHUSETTS INSTITUTE OF TECHNOLOGY

February 2006

Author .....
Department of Aeronautics and Astronautics
15th February 2006

Certified by.... .....
Jeffrey A. Hoffman
Professor of the Practice of Aerospace Engineering
Thesis Supervisor

Accepted by..... .....
Jaime Peraire
Professor of Aeronautics and Astronautics
Chair, Committee on Graduate Students

Development of a Mechanical Counter Pressure Bio-Suit System for Planetary Exploration

by

Zhe Liang Sim

Submitted to the Department of Aeronautics and Astronautics
on 15th February 2006, in partial fulfillment of the
requirements for the degree of
Master of Science in Aeronautics and Astronautics

Abstract

Extra-vehicular activity (EVA) is critical for human spaceflight and particularly for human planetary exploration. The MIT Man Vehicle Laboratory is developing a Bio-Suit EVA System, based on mechanical counterpressure (MCP), that has the potential to maximize and even augment the EVA capabilities of future planetary explorers.

This thesis describes the design and implementation of novel MCP concepts for the Bio-Suit System. Two concepts known as the *detached bands* and *elastic bindings* were initially developed and tested in ambient conditions on a human leg. The elastic bindings proved superior to the detached bands and demonstrated greater mobility, comfort and ease of donning than previous MCP garments.

After refining the bindings design to improve the uniformity of its pressure distribution, five subjects donned bindings on one calf and exposed the suited calf to -30kPa (-225mmHg, -0.3atm) for up to an hour – a greater magnitude and longer duration of underpressure than previous MCP garment tests – to demonstrate the effectiveness of the bindings as a pressure garment. Changes in heart rate, skin temperature and blood pressure were recorded during these experiments. The bindings prevented the increase in blood pressure that occurs when the unprotected calf is exposed to underpressure, further demonstrating their efficacy as a pressure layer.

The elastic bindings concept in its current form is not a final design for an operational EVA system. However, it exhibits many of the attributes necessary for use in such a system and is thus extremely valuable for studying the engineering, physiological and practical issues associated with utilizing mechanical counterpressure as a cornerstone of the Bio-Suit.

Thesis Supervisor: Jeffrey A. Hoffman
Title: Professor of the Practice of Aerospace Engineering

Acknowledgments

I have wanted to be an astronaut since I was eight years old. Suppose, then, that I had stumbled across a magic lamp two years ago and the genie inside had told me, "Soon you will have the opportunity to journey to MIT to develop revolutionary spacesuits for future explorers on Mars. You will work with and learn from astronauts, fighter pilots, circumnavigational sailors and some of the world's most brilliant aerospace engineers and scientists. You will present your research in Rome, fly on NASA's zero-g training aircraft in Houston, and teach MIT Aero-Astro courses in China. On the side you will attend Nobel Laureate lectures a few times a year, go sailing and cycling with your professors, take French classes, make lifelong friends hailing from five continents and live in the heart of one of America's most vibrant cities. And oh, by the way, *they* will support *you* to do all this."

How would I have reacted to such outrageous claims – with astonishment, utter disbelief, fervent hope, or merely cynicism that the genie was only repeating exactly what I wished to hear?

And yet by summer 2006 I will have accomplished all these things after having spent less than two years at MIT. Where, or how, can I even begin to say thank you for such superlative experiences?

First, I am enormously grateful to my adviser, **Prof. Jeffrey A. Hoffman**, for the opportunity to join the Man Vehicle Laboratory. Naturally I was excited to discover that I would pursue spacesuit research with one of NASA's most experienced astronauts, but my most enduring impression of Jeff has been his passionate dedication to his students. Despite crushing responsibilities, Jeff's door has always been open to me for valuable guidance, expert knowledge and encouragement. Furthermore, he has repeatedly emphasized the importance of maintaining a balanced perspective – a life-saver in the hothouse that MIT often becomes: "You're a graduate student, and graduate students must have a life," he said to me during my first semester. Jeff has therefore been key in making my academic experience intense but immensely pleasurable and *manageable.*

I am also indebted to **Prof. Dava J. Newman** for many things: for swashbuckling through NASA red tape to maintain research funding; for sailing trips on the *Galatea* and dinners in Marblehead, Cambridge and Rome; for a meeting with Buzz Aldrin; for providing considerably more than 15 minutes of fame on Discovery Channel et al, and much more. Like most of us, I am convinced that Dava never sleeps, for she does so much for us and still finds time to sail through the Caribbean and beyond.

To all members of the Man Vehicle Laboratory, I humbly thank you. No one could ask for a more delightful group of colleagues and friends. I thank **Dr Chris Carr** for being an unfailing mentor – not only for patiently answering countless technical questions but also for moral support in times of crisis, valuable guidance on all aspects of graduate school, and being an excellent travel companion in Rome (how many gelatos?). I owe **Dr Alan Natapoff** as much for his crucial assistance in experimental design and statistical analysis as for his insider's tips on local restaurants and cafes.

I am enormously privileged for having **Kristen Bethke** not only as my trusty Bio-Suit partner-in-crime but also for lending a sympathetic ear at exactly the right times. It would also have been impossible for me to complete this thesis without my outstanding UROPS – **Brendan Smith**, **Amy Brzezinski**, **Becca Arvanites**, **Jordan Wirfs-Brock** and **Shambhavi Kadam** – all of whom I could always count on to get their hands dirty in the machine shop or to run a physiological experiment for hours on end. Finally, I offer my heartfelt appreciation to my brave test subjects – you know who you are! – for cheerfully enduring some discomfort in the name of science (or more accurately, for my thesis...)

Naturally, my greatest thanks are to Mum (biochemist) and Dad (physicist). Not only did they instill in me an appreciation of scholarship and the scientific method from day one, but they also allowed me unrestrained freedom to pursue my own, somewhat non-linear trajectory – a rare and significant liberty. This thesis is for you.

This work is supported by the NASA Institute of Advanced Concepts Contract 070605-003-006.

Contents

List of Figures

List of Tables

Chapter 1

Introduction

One of the key requirements of human planetary surface exploration is a spacesuit that enables astronaut locomotion. Since planetary traversal will involve loping, climbing, squatting and other locomotive activities, the mobility of spacesuits used for planetary traversal must greatly surpass that provided by any current or previous spacesuit.

Mechanical counterpressure (MCP) has been proposed as a technique for enhancing astronaut mobility as well as offering reduced mass, lower profile, improved safety and numerous other advantages for planetary EVA [4]. In a MCP-based spacesuit the body is pressurized using elastic tension in a skin-tight garment rather than by the gas in a traditional spacesuit. There have been numerous attempts in the last 35 years to create MCP spacesuits [3]; however, these have either been hindered by operational difficulties [1] or have only focused on creating MCP on small anatomical areas such as the hand [5, 6, 7, 8, 9].

The Bio-Suit System being developed at MIT's Man Vehicle Laboratory leverages new concepts and technologies to overcome obstacles encountered in previous MCP designs [10]. In particular, Bio-Suit subsystems are conceived to allow the explorer the same ease of use as ordinary clothing; eventually, the overall system is envisioned to provide a "second skin" capability, possibly incorporating biomechanic and cybernetic augmentation for enhanced human performance during planetary exploration.

This thesis describes the design and implementation of novel MCP concepts for

the Bio-Suit System. Two concepts known as the *detached bands* and *elastic bindings* were initially developed and tested in ambient conditions on a human leg. The elastic bindings permitted greater mobility than the detached bands and were also more comfortable and easier to don; however, the pressure distribution generated by the bindings on the leg was insufficiently uniform from a physiological perspective.

The bindings design was therefore refined and exhaustively tested on a cylindrical surface – an idealized model of the human leg – to improve the uniformity of the MCP it generated. Once the improved design was adapted for use on a human leg, five subjects wore custom-made bindings on their right calf and exposed the suited calf to -30kPa (-225mmHg, -0.3atm) for over an hour – a greater magnitude and longer duration of underpressure than previous MCP garment tests – to demonstrate the effectiveness of the bindings as a pressure garment. To further quantify the efficacy of the bindings in protecting the wearer against underpressure, changes in heart rate, skin temperature and blood pressure were recorded during the suited experiments and compared to the physiological response induced when an *unsuited* calf is exposed to underpressure.

This thesis is therefore structured as follows:

Chapter 2 discusses the motivation for MCP-based spacesuits and their potential advantages over traditional gas-pressure spacesuits. The chapter reviews previous efforts to develop partial- or whole-body MCP prototypes and provides an overview of the Bio-Suit System.

Chapter 3 reviews the accuracy of the Tekscan I-Scan pressure measurement system and describes experiments performed to quantify their accuracy on a cylindrical surface – an idealized leg model, as mentioned earlier. The I-Scan sensors are one of the most important means of measuring the performance of the MCP prototypes discussed in Chapter 4 and 6; these experiments were thus essential for interpreting the results of these chapters.

Chapter 4 describes the process by which the detached bands and elastic bindings prototypes were designed, fabricated and preliminarily tested. As mentioned above, the elastic bindings demonstrated the best performance and were thus chosen for use

in subsequent physiological experiments.

Chapters 5 and 6 then describe the physiological effects of using the elastic bindings as a pressure garment. **Chapter 5** provides context and background by reviewing the physiological implications of localized pressure variations that occur when using MCP in place of the gas pressure in a traditional spacesuit to pressurize the body surface. Finally, **Chapter 6** describes experiments in which five subjects wore the elastic bindings prototype in a low pressure leg chamber for an hour or more. These demonstrated the bindings' capability to protect the leg from underpressure and to mitigate physiological changes that occur with unprotected exposure to underpressure.

Chapter 2

Literature Review

2.1 Mechanical Counterpressure (MCP) Spacesuits

2.1.1 Motivation

One of the key requirements of human planetary surface exploration is a spacesuit that enables astronaut locomotion. Unlike microgravity EVA, which involves limited translation performed almost entirely with the hands and arms or via a robotic manipulator, future planetary surface EVA will require locomotion, long traverses, climbing, and extensive bending. These activities place new demands on spacesuit mobility and dexterity, especially in the lower body, that can only be attained by implementing designs that facilitate natural locomotion and minimize energetic expenditure.

The mobility permitted by future planetary spacesuits must therefore greatly surpass the mobility provided by current and previous spacesuits. High joint torques in the Apollo lunar suits forced astronauts on the Moon to walk with a considerably altered "bunny hop" gait to compensate for reduced knee and hip mobility [11], and hindered their ability to kneel or bend over to perform simple tasks such as picking up rock samples or performing a close-up inspection of the lunar surface. The current Space Shuttle Extravehicular Mobility Unit (EMU) and Russian Orlan suit are designed for work in weightlessness where lower body rigidity is actually beneficial in reducing the metabolic cost of producing counter-torques for body stabilization

during microgravity EVAs; however, this rigidity and the substantial mass (130 kg) of the EMU and similar gas pressurized spacesuits make these systems inadequate for planetary surface locomotion and exploration mission tasks [10].

Mechanical counterpressure (MCP) was first proposed by Annis and Webb in the late 1960s [12, 1] to greatly enhance astronaut mobility and dexterity, as well as offer improved safety and other advantages for planetary EVA. In a MCP-based spacesuit, the body is pressurized using elastic tension in a skin-tight garment rather than by the gas in a traditional spacesuit. Such a garment is conceptually similar to the compression garments worn by burn victims or patients with varicose veins and other circulatory problems; the challenge, however, is that the pressure that an MCP garment must generate is an order of magnitude higher than typical compression garments, as discussed in Section 2.1.2. The conceptual elegance of MCP not only has the potential to increase mobility but also simplify life support system design, reduce the astronaut's energy expenditure in using the suit, and greatly diminish the risk of depressurization and other EVA hazards [4].

An alternative method of pressurizing the body is a **hybrid** concept combining both gas-pressure and MCP elements whereby pressurized fluid bladders transduce MCP to the body via an inextensible restraint layer, much like a fighter pilot's g-suit or a blood pressure cuff. Hybrid garments are *not* "true" MCP garments because they still rely on fluid to transmit the pressure to the skin; as such, they do not enjoy many of the benefits inherent in an **elastic-only**[1] MCP garment. Most importantly, a hybrid garment, like a traditional gas-pressure suit, would suffer a loss of pressure that immediately propagates over the entire body in the event of a puncture anywhere on the suit; in contrast, loss of pressure in an elastic-only MCP garment would be limited to the region immediately around the puncture [4].

Hybrids are discussed in this thesis as they are relatively easy to develop and have been useful stepping stones for illustrating the practical and physiological issues associated with using MCP (Section 2.1.3). However, it cannot be over-emphasized

[1]In this thesis, an "elastic-only" MCP garment is defined as as one that does not use fluid to transmit pressure; it does not necessarily consist of an elastic material.

that a hybrid's reliance on fluid pressure prevents it from enjoying the safety and other benefits inherent in an elastic-only MCP garment; this, combined with other reasons[2], leads us to believe that operational MCP spacesuits of the future should avoid use of the hybrid concept as much as possible.

2.1.2 Engineering Requirements

Before reviewing previous MCP-based spacesuit development efforts it is necessary to discuss the engineering requirements that suits must satisfy. The function of a spacesuit (this term being used interchangeably with "EVA system") is to protect the wearer from the extreme environment of outer space (Earth orbit) or a planetary surface (Moon or Mars). The spacesuit must provide oxygen, pressurize the body surface with the same pressure as the breathing pressure, maintain the body at a comfortable temperature, and protect the body from radiation, micrometeorites and other hazards.

The MCP garment is only one of many spacesuit subsystems. Its function is primarily to pressurize the body surface, but it may also simplify thermal control by allowing the user to sweat through the garment if it is made of a porous material [1, 4]. Bio-Suit research to date, including this thesis, has focused on the pressurization function and assumes that other subsystems are modularly added to perform the thermal, radiation and other functions of the spacesuit [4, 13]. With this in mind, it is now possible to discuss the requirements for the pressurization function to be fulfilled by the MCP garment (sometimes referred to as a "pressure layer".)

First, the garment must apply MCP on the body that is equal to the pressure of the gas that the astronaut is breathing. We have assumed this to be 30kPa (225mmHg, 4.4psi) as this is the pressure of the pure oxygen atmosphere within the Shuttle EMU

[2]Hybrids do have a few inherent advantages over elastic-only MCP garments. The level of MCP they produce on the skin can easily be adjusted by varying the fluid pressure; furthermore, the MCP distribution tends to be more uniform than an elastic-only MCP suit as the pressure inside the fluid bladder is already perfectly uniform. However, the pressure distribution in a gas-pressure suit is *already* controllable and even more uniform than that produced by a hybrid garment since the former has no bladder confounding the pressure transmission from fluid to body surface. Considering this in conjunction with the aforementioned loss-of-pressure aspect, one might thus argue that hybrids suffer the major disadvantages inherent in *both* gas-pressure and MCP-only suits.

as well as the minimum oxygen pressure required for normal oxygen diffusion, or normoxia (with some safety margin [14]). Note, however, that a higher breathing pressure and corresponding MCP would be highly beneficial for EVA operations because it would substantially reduce pre-breathe times; in fact, a suit producing 55kPa (412mmHg, 8.0psi) MCP would eliminate the need for pre-breathe altogether in a spacecraft at sea level ambient pressure (101.3kPa, 760mmHg, 14.7psi) [14], which is the pressure used on the ISS and Shuttle for most operations. In short, the garment must produce at least 30kPa MCP but higher pressures up to 55kPa are desirable[3].

For hybrid garments, the requirement must be stated differently since the MCP applied by a hybrid garment varies with the pressure in its fluid bladder. Like a traditional gas-pressure spacesuit, this fluid pressure must be minimized in order to maximize the mobility of the hybrid garment whilst satisfying the 30kPa oxygen pressure mentioned above. The hybrid must therefore transform as much fluid pressure into MCP as possible, but it is inherently impossible for the MCP to be higher than the fluid pressure. As such, the requirement for a hybrid garment is that the MCP-to-fluid pressure ratio should be as close to the maximum value of 1 as possible.

As well as being at least 30kPa, it is extremely important that the applied MCP must be as uniform as possible to avoid adverse physiological effects such as bruising or edema that would be caused by spatial pressure variations across the body surface, as discussed in Chapter 5. Trevino and Carr [16] conservatively estimate that variations of less than 1.6kPa ($\pm$12mmHg) are unlikely to produce edema or restrict capillary blood flow, but are not certain as to the minimum magnitude or duration of variation that will produce edema or other adverse effects. This thesis has used $\pm$12mmHg as the design requirement.

Similarly, the garment must avoid exposing large areas of the skin to the external (low pressure) environment, unintentionally or otherwise, because such exposure would create a spatial pressure variation between the exposed and unexposed areas that is as great as the applied MCP. However, the garment should still be porous in

[3]See Gernhardt [15] for a far more detailed discussion on selection of breathing pressure and breathing gas composition.

order to allow the wearer to sweat, as discussed above. Webb showed that areas of skin as large as $1mm^2$ can be exposed to vacuum without adverse effects due to the inherent tensile strength of human skin [12]. We have thus included this maximum exposure limit in the requirements, but it may be possible to expose larger areas without unduly adverse effects[4].

The mobility requirement has previously been defined by stating the maximum torque required to bend a joint to a specified position [3]. A simpler method is to ask whether the wearer can comfortably initiate and maintain a deep knee squat using only his/her body weight – a fundamental requirement for planetary exploration that, as mentioned in Chapter 1, the Apollo lunar suits were unable to satisfy.

Finally, the number and frequency of EVAs on planetary missions will be orders of magnitude higher than that required to complete the ISS [11]; it would be impractical for the MCP garment to require as much pre-EVA preparation time as the EMU or Orlan. As such, we require that the wearer should be able to don or doff the suit in less than ten minutes without any assistance [10].

The next section reviews previous MCP development efforts using the aforementioned requirements (summarized in 2.1) as performance metrics.

Function	**Requirement**
Pressure Production	For elastic-only suits, apply at least 30kPa (225mmHg, 4.4psi) of average pressure at body surface. For hybrid garments, achieve a 1:1 ratio of MCP-to-fluid pressure.
	No more than 1.6kPa (±12mmHg) spatial variation in pressure [11].
	Locally expose no more than $1mm^2$ skin surface area to vacuum [1].
Mobility	Permit wearer to initiate and maintain deep knee squat without undue discomfort, using only body weight.
Operations	Don and doff in less than 10 minutes without assistance.

Table 2.1: Summary of engineering requirements for an MCP spacesuit (adapted from [3].)

[4]This is indirectly discussed in the literature review of Chapter 5.

2.1.3 Previous MCP Garments

Annis and Webb were the first to develop an MCP garment in the late 1960s [1]. Their Space Activity Suit utilized seven layers of highly elastic material in order to pressurize the body surface, while a bubble helmet and chest bladder provided adequate breathing pressure (Figure 2-1). While the SAS initiated the MCP concept and demonstrated advantages of mobility, low energy costs and a simplified life support system, the difficultly in donning/doffing the SAS was the largest limitation; NASA subsequently did not pursue MCP suit development.

Since then, however, several researchers have sustained the idea of MCP suits. In 1983 Clapp designed and tested an MCP glove and compared its performance to the A7L-B Skylab-era gas pressure glove [5]. Subjects who tested the elastic "skinsuit" glove in a partial vacuum of -24kPa (-180mmHg) for 30 continuous minutes[5] retained 90% of bare-skin finger mobility, compared to 30% mobility in the A7L-B gas pressure glove. Slight edema occurred over the palm of the hand after 30 minutes of wearing the glove in the partial vacuum, but no other health problems were observed.

In 2002 Korona et al developed a hybrid gas elastic glove (Figure 2-1) and compared its performance to a 4000-Series EMU glove, finding that the hybrid slightly outperformed the EMU glove in both mobility and perceived exertion levels [2]. More recently, Tourbier, Tanak et al [6, 7] examined the physiological effects of elastic MCP gloves using an a skintight elastic design augmented with an inflatable layer for the dorsum (back surface) of the hand. The glove produced the desired 27kPa (200mmHg) of MCP on the dorsum and finger regions. However, the pressure on the palm, which was not pressurized by a bladder, was significantly lower at 9kPa (70mmHg, 1.4psi) as the elastic material stretched over the palm concavity and was thus unable to exert pressure on it. Even so, the glove prevented the blood flow increase, tissue edema and finger swelling that occurred on a bare hand subjected to similar levels of underpressure, and thus provided evidence that the glove could protect the user from physiological effects of underpressure.

[5] All pressures quoted in this thesis are gauge pressures – i.e. pressure above the absolute sea-level atmospheric pressure of 101.3kPa.

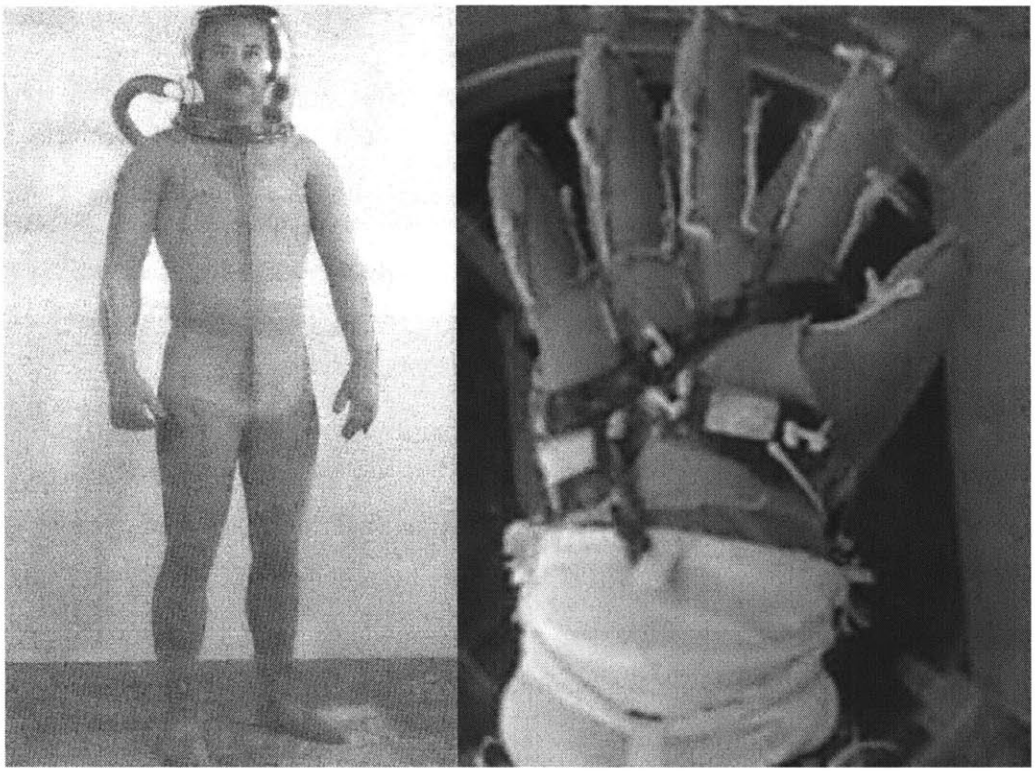

Figure 2-1: (Left) Annis' and Webb's Space Activity Suit [1]. (Right) Hybrid elastic glove of Korona et al [2].

The Tanaka group subsequently developed an elastic MCP sleeve for the full arm [9]. The pressure produced by the sleeve varied from 21kPa (160mmHg) at the forearm and upper arm to 31kPa (230mmHg) at the finger, dorsum of hand, and wrist. Despite the variations in pressure, the sleeve prevented adverse changes in skin blood flow and skin temperature during partial vacuum tests, and enabled subjects to tolerate underpressures of up to -20kPa (-150mmHg) for 5 minutes. These physiological results are discussed in further detail in Chapter 5.

In summary, the aforementioned efforts[6] have demonstrated the potential for MCP suits to provide considerably greater mobility and reduced metabolic cost compared to gas-pressure spacesuits; furthermore, they have provided preliminary evidence that

[6]Interestingly, the Soviets also made significant attempts to develop MCP suits [17, 18]; details of the program appear to be classified, but we have been told that the efforts were abandoned due to operational and practical difficulties similar to those experienced by the US-based researchers described above.

MCP can be realized without adverse physiological effects. However, these designs have been limited by one or more factors, particularly difficulty in donning and doffing, a non-uniform pressure distribution, and insufficient pressure on body concavities. Furthermore, their mobility is still somewhat less than that of an unsuited human. Table 2.2 compares the performance of these systems.

2.2 Bio-Suit: An MCP-based EVA System

The Bio-Suit System being developed by MIT's Man Vehicle Laboratory (MVL) is a MCP-based EVA system for planetary exploration that leverages new concepts and technologies to overcome obstacles encountered by previous MCP suits [10]. In particular, Bio-Suit subsystems are conceived to allow the explorer the same ease of use as ordinary clothing (Figure 2-2); eventually, the overall system is envisioned to provide a "second skin" capability, possibly incorporating biomechanic and cybernetic augmentation for enhanced human performance during planetary exploration.

Bio-Suit development has progressed along three major streams: definition of Bio-Suit System requirements, prototype development and testing, and physiological considerations of MCP and spacesuit simulation for planetary missions [19]. This thesis contributes to all three streams, with a focus on prototype development and physiological considerations.

The **requirements definition** work is motivated by the fact that the pressure layer of the Bio-Suit System is skin-tight and is envisioned to provide a "second skin" capability. It is therefore critical to understand the detailed stretching and deformation of human skin as well as the changes in volume, surface area and shape that occur during body movement, or locomotion. MVL has thus developed techniques for quantifying these changes using 3D laser scanning and digital image correlation and has subsequently demonstrated these techniques on a human leg at different joint angles [3].

Prototype development has been the primary focus of Bio-Suit research, the principal objective being to demonstrate the feasibility of the MCP concept by de-

Table 2.2: Description and performance of previous MCP garments. It is difficult to directly compare spatial pressure variation and mobility across different prototypes due to the different ways in which they are reported in the literature. "N/A" means "not available".

Group	Hybrid?	Target body area	Description	Average MCP[a] (mmHg)	MCP spatial variation (±mmHg)	Donning time (approx.)	Mobility
Annis and Webb (1971)	No	Whole body	Full-body elastic suit consisting of up to six skintight Spandex layers	Up to 170mmHg[a]	N/A	30min; two assistants required	Approx. halfway between that of unsuited and suited human
Clapp (1983)	No	Hand	Skintight glove	N/A	N/A	N/A	90% of bare hand
Korona et al (2002)	Yes	Hand	Hybrid glove	N/A	N/A	N/A	Approx 50% of bare hand[g]
Tourbier, Waldie et al (2002)	Partial	Hand	Skintight glove augmented with air bladder on hand dorsum	50-213mmHg[b]	24[f]	N/A	Not measured
Tanaka et al (2003)	Partial	Hand and arm	Skintight glove and arm sleeve augmented with air bladder on hand dorsum	173-222mmHg[c]	11[f]	N/A	Not measured
Pitts (2003)	Yes	Lower leg	Single-channel hybrid	~1:1[b,d]	2.5[g]	<30s	Not applicable (garment does not cover knee joint)
Pitts (2003)	Yes	Lower leg	Multi-channel hybrid	~2:1[b,d]	N/A	2min per calf	
Pitts (2003)	Yes	Lower leg	Spray-on urethane layered foam	~1:1[b,d]	N/A	2min per calf	
Bethke (2005)	Yes	Full leg	Spray-on urethane layered foam	~3:1[b,d,e]	N/A	15min; two assistants required	Knee bends limited to 90°
Bethke (2005)	No	Full leg	Lines of non-extension	50-62[h]	N/A	~30s	Slight discomfort when knee bends >100°

Notes
a. Measured only at a few discrete points (rather than a pressure distribution map) using inflatable bladder between garment and joint.
b. Measured using Tekscan I-Scan sensors
c. Measured using Tekscan I-Scan sensors; palm pressures for this prototype that were extremely low in the glove-only prototype (above) not reported.
d. Hybrid bladder input-output pressure ratio, as described in text.
e. Excluding inside thigh where pressure ratio was ~20:1.
f. Standard error from average.
g. RMS deviation from row-means.
h. Based on Korona Figs 19 and 20.

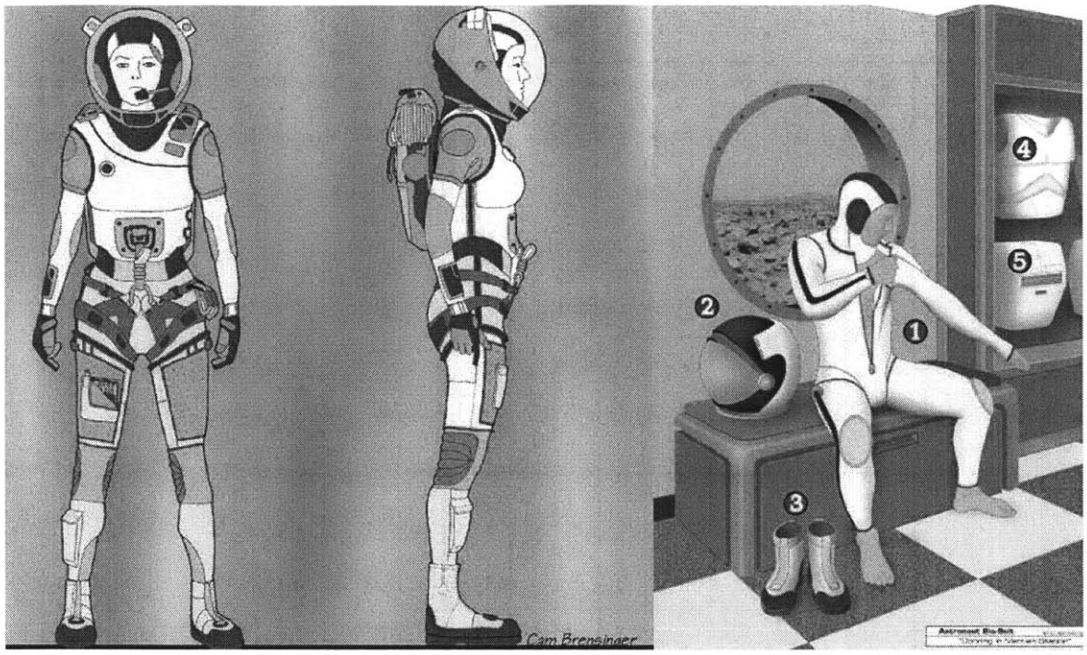

Figure 2-2: (Left) Artist's concept of an operational Bio-Suit System, envisaged to be far lighter and lower profile than current gas-filled spacesuits. (Right) An astronaut on Mars is depicted donning the Bio-Suit MCP pressure layer (1). A lightweight life support system (5) supplies breathing gas into the helmet (2) and possibly through elastic tubes to hybrid MCP glove and boots (3). A hard upper torso (4) on top of the MCP layer provides a structural foundation on which the life support system and other suit system elements can be mounted. Images courtesy of Cam Brensinger.

veloping comfortable, high-mobility prototypes that can protect the wearer from the effects of underpressure. MVL has concentrated on developing prototypes for the lower body due to the relative lack of leg mobility in current and previous spacesuits [10] and to demonstrate a revolutionary locomotion capability for exploration missions in partial gravity environments; however, the leg prototypes are directly applicable to the arm with relatively few modifications.

Pitts developed two types of hybrid prototype for the lower leg and used these to demonstrate the basic feasibility of MCP and gain practical insight into using MCP garments [14]. The first featured one or more longitudinal channels between the skin and garment that expand as it fills with gas (Figure 2-3(a) and (b)), similar to some partial pressure suits for fighter pilots (Bethke [3], p22.) The second was a highly innovative design comprising an inflatable foam layer sealed by spray-on urethane

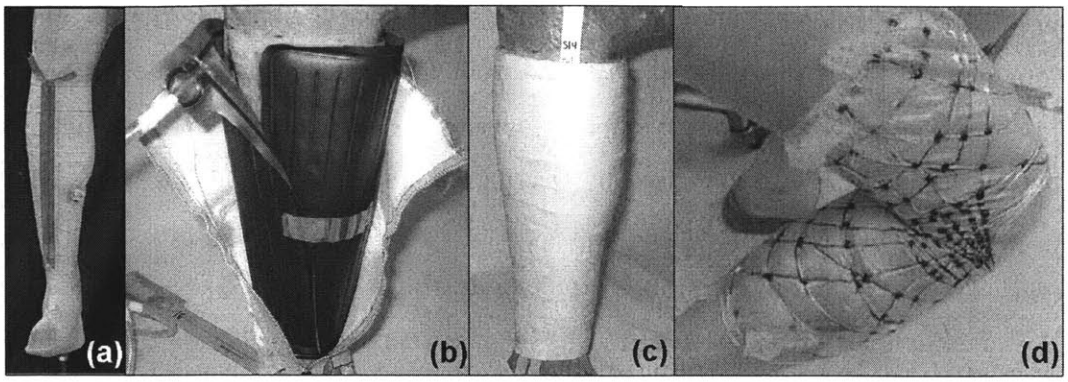

Figure 2-3: Previous Bio-Suit prototypes: (a) single-channel prototype with longitudinal zipper for quick donning and doffing; (b) multi-channel prototype showing inner multi-channel inflation layer in black and white sailcloth restraint layer in white; (c) paint-on urethane layer of open-cell foam prototype; (d) lines of non-extension prototype fabricated using inextensible Kevlar fibers.

layers, the result being a skintight garment that conforms very well to the wearer's body shape (Figure 2-3(c)).

As mentioned earlier, however, the preferred approach is to pressurize the body using only elastic tension without relying on any form of fluid pressure. As such, MVL has also developed elastic-only prototypes based on several different concepts. Bethke [3] developed a leg garment patterned along the body's lines of non-extension (LoNE), empirical lines along the body surface that remain the same length as the body moves. The LoNE concept was originally proposed by Iberall in the 1950s for use as restraint layers of gas-filled pressure suits [20]; Bethke adopted the concept to develop a minimum energy–maximum mobility MCP prototype made of inextensible Kevlar fibers and demonstrated their ability to provide excellent leg mobility (Figure 2-3(d)).

Finally, there are several motivations for research into the **physiological considerations** of using MCP. First, a major problem with current and previous MCP prototypes is that the wearer must endure overpressure on one body part while the rest of the suit is being donned. This causes considerable discomfort even for garments that can be donned or doffed in a few minutes; adverse physiological effects may occur if the donning time is longer than 20-30 minutes [1]. Additionally, wear-

ing MCP suits for extended periods may induce some adverse effects on the body – for example, if the MCP generated on the body is not uniform or does not match the breathing pressure. Previous research has measured changes in blood flow, skin temperature and other effects caused by wearing MCP garments and has provided some evidence that MCP can be realized without excessively adverse physiological effects [1, 9], as reviewed in detail in Chapters 5 and 6.

MVL research has extended these results by quantitatively considering the effects of pressure differentials between different parts of the body, as it is unlikely that an MCP suit will produce a pressure distribution as uniform as that in a gas pressure suit. Trevino and Carr derived a theoretical first-order estimate of the differential that can be supported by the cardio-pulmonary system without causing edema [16]. Carr has also begun developing non-invasive experimental methods for assessing edema in a human subject wearing an MCP garment using a thermal diffusion probe [21].

Chapter 3

Tekscan I-Scan Sensors for Pressure Distribution Measurements

3.1 Introduction and Motivation

The I-Scan Pressure Sensor System (Tekscan, South Boston MA) is used to measure the mechanical counterpressure distribution generated by Bio-Suit prototypes. The I-Scan system pressure sensor is a flexible printed circuit with individual sensing elements, or sensels, arranged in a rectangular array. Each sensel acts as a variable resistor in an electrical circuit; the resistance decreases as the applied pressure increases. Tekscan offers I-Scan pressure sensors in a wide variety of geometries; for Bio-Suit work, the most commonly used sensor has been the Model 9801 sensor consisting of 96 12.7mmx12.7mm (0.5"x0.5") sensels arranged in a 16x6 rectangular array (Figure 3-1).The 9801 sensor, in conjunction with the I-Scan software that controls its operation and collects its pressure measurements, will hereafter be collectively known simply as "I-Scan".

At first glance, the I-Scan system seems particularly appropriate for measuring MCP for several reasons. First, the sensors are extremely thin (0.1mm) and thus

cause minimal interference or pressure points between the garment and skin. The sensors can also measure the pressure distribution of a given area in real time, as opposed to many other thin sensors that can only take pressure measurements at a few discrete points, measure the mean pressure over the given area, or cannot make measurements in real time. Finally, the sensors can be cut into strips to increase their conformance to curved surfaces such as the leg.

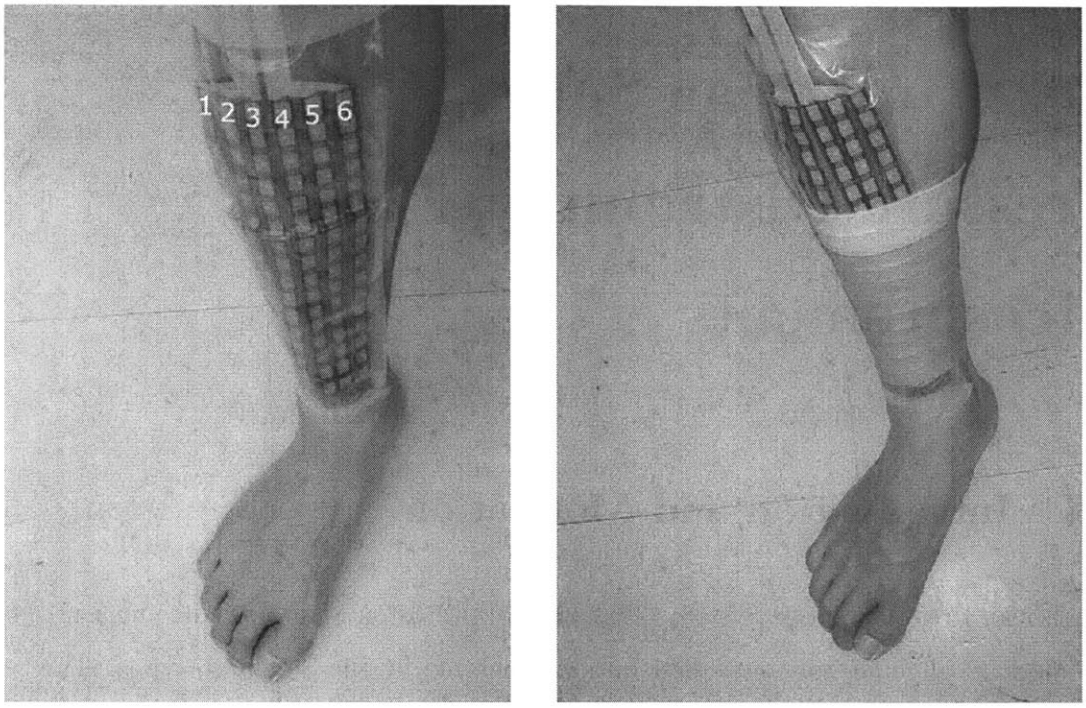

Figure 3-1: (Left) Tekscan I-Scan Model 9801 sensor on calf. The sensor has been cut into six strips (labelled 1-6) to improve conformity to the curved leg surface. Being extremely thin, the sensor causes minimal interference when used for measuring pressure applied by an MCP garment to the calf (right).

However, when using the sensors to test Bio-Suit calf prototypes [13] the I-Scan measurements were suspected to be an inaccurate representation of the actual garment pressure. Most problematically, pressure spikes were observed at individual sensels that were 4-5 times higher than the pressure measured by surrounding sensels; these were almost undoubtedly false as they were not felt by the wearer and because there was no physical reason for the garment to produce such sharp and localized spikes. Additionally, minor pressure variations between the sensels could be observed even

under ideal loading conditions such as when the sensor was being calibrated between two flat plates, despite the sensor having been equilibrated before measurement to compensate for these variations. The I-Scan system also repeatedly exhibited 5-10% hysteresis, even during calibration, that was difficult to predict and to compensate for in field measurements. Finally, the sensors exhibited an extremely slow response time – despite their 8Hz maximum sampling frequency – requiring more than a minute to correctly read a change in the applied pressure.

Before using the sensors to measure the MCP produced by Bio-Suit garments (Chapters 4 and 6) a literature review was undertaken to quantify their accuracy as determined by other I-Scan users (Section 3.2). This review also investigated the use of alternative pressure measurement systems to avoid the problems of the I-Scan sensors.

The experiments described in the literature review tested I-Scan accuracy on a flat surface; however, for Bio-Suit work the I-Scan sensors are being used on the curved surface of a human leg. A series of experiments was therefore performed to measure and compare the accuracy of the sensors on cylindrical and flat surfaces (Section 3.3.)

3.2 Literature Review

3.2.1 Accuracy of I-Scan Sensors

Tekscan [22] claims that the "overall"[1] accuracy of the I-Scan system is approximately 10% and depends on the care taken by user to calibrate the sensors. However, they acknowledge that under non-ideal conditions I-Scan suffers further inaccuracies including:

- Temperature – for every deg F the calibration temperature differs from application, the sensor reading will err by up to 0.25%.
- Creep – 3% per log time, depending on the duration of applied load during calibration.

[1] However, "overall" is not clearly defined in the document.

- Hysteresis – up to 5%[2].

- False pressure spikes when the sensor is crimped or wrinkled.

McWilliams [23] suggested that many of these errors are likely to be caused by sensor crimping. He therefore suggested that for pressure garment testing the subject should wear pantyhose to protect the sensor from moisture and shear against the skin and cutting the sensor into strips to improve its conformity to the curved surface of the leg. These countermeasures had already been previously attempted [14, 3] with little success; false pressure spikes could still be clearly observed. He also suggested putting conformal plastic plates between the sensor and skin to reduce crimping; however, this was unsuitable because it would alter the suit characteristics and pressure production.

Wilson et al [24] quantified I-Scan accuracy by statically loading the sensors with a known pressure (1-7MPa) in an Instron testing machine between rubber-backed aluminum plates and showed that I-Scan measures the mean pressure with <10% error. They also loaded the sensor with two different loads to crudely determine how well I-Scan measured the local, as opposed to mean, pressure. In this case they found the error to be less than 1% – surprisingly better than that of the mean pressure. The authors acknowledged that the system displays other inaccuracies such as hysteresis and creep, which were deliberately minimized in this experiment, and that further inaccuracies may arise when measuring the asymmetrical geometry and changing compliance of human joints.

Matsuda et al [25] measured the accuracy of I-Scan sensors in measuring contact area and stress under ideal static loading conditions using an Instron machine and a circular steel indenter. Between the calibration loads the I-Scan overestimated contact area by about 10% but measured the applied force to within <5%, giving the system a better than 10% accuracy in pressure measurement under ideal conditions, similar to that reported by Wilson.

Mann et al [26] used I-Scan to measure the pressure provided by compression gloves and sleeves. In calibrating the sensors they determined that its accuracy in

[2]However, the quantity against which this 5% is measured is not defined.

measuring a 15lb weight was 3%.

Kirstukas [27] measured the accuracy of I-Scan force measurements in repeated deforming use by applying 80 cycles of a 900N peak force using polyurethane and rubber indenter balls. Foam rubber up to 1" thick was placed between the sensor and load cell to simulate tissue between a patient's skin and skeletal frame. The author qualitatively claimed that I-Scan was accurate in measuring contact force if well calibrated. However, the sensor exhibited 5-10% creep as measured by calibration coefficients as well as false pressure spikes when wrinkled, especially on thick substrates at lower contact pressures.

DeMarco et al [28] measured the accuracy of I-Scan sensors in measuring contact pressure and area by applying calibration loads of up to 2500psi to Tekscan Model 5051 sensors. Loads were transferred through a spherical joint adapted to a cylindrical Delrin peg with a rubber damping layer on the end of the peg; the sensor was placed between this damper and a smooth aluminum plate. They found that the Tekscan calibrated at three points had an mean pressure measurement error of over 11% while that of a sensor with eleven calibration points was about 4%. Unfortunately, Tekscan no longer offers the software to calibrate I-Scan with eleven points because it was found to be too time consuming for most users [23]; as such, Bio-Suit I-Scan measurements only use two calibration points (Appendix B).

McPoil et al [29] loaded F-Scan sensors (similar to I-Scan but designed specially for the foot) to 150kPa for 10min to test creep performance. The F-Scan exhibited 11.6% creep in a non-linear fashion.

Fregly et al [30] measured the magnitude of discretization errors in K-Scan sensors (K-Scan being a subset of I-Scan sensors designed for knee applications) by subjecting them to Hertzian and uniform pressure distributions. The measured errors were up to 4% for contact force and peak pressure and up to 9% for mean pressure and contact area. The authors suggested that discretization error was on the same order of magnitude as other sources of error (sensor insertion, pressure truncation) and should thus be considered when evaluating sensor accuracy. However, when compared to the results from other researchers (Table 3.1) Fregly's results suggest that the majority

of sensor error arises only from discretization.

Considering discretization error raises the question of whether the resolution of an I-Scan array is sufficiently fine, i.e. whether each sensel (0.5"x0.5") is sufficiently small to accurately measure pressure differentials that have physiological consequences. Stated differently, could pressure differentials within a 0.5" square patch of skin cause adverse physiological effects? Bio-Suit prototypes have the potential to produce such small-scale differentials; if so, the resolution of the I-Scan system would not be sufficiently fine to detect them.

Finally, Harris et al [31] used K-Scan sensors to measure the contact pressure and area in prosthetic knees. The K-Scan could not accurately track a calibration curve between 1500-3000N, being 5% too low at the 3500N mark; however, this could have been due to a poor calibration method. Similar inaccuracies were found in measuring a calibrated contact area.

Unit	Accuracy	Reference
"Overall"	10%	[22, 32]
Mean pressure	4–11% depending on number of calibration points	[24, 28, 30]
Contact area	10%	[25, 30]
Total force	3–5%	[25, 26, 31]
Creep	12% in 10min; 5–10% after 80 loading cycles; 3% per log time depending on calibration duration	[22, 27, 29]
Hysteresis	5%	[22, 32]
Temperature-caused offset	0.25% per °F of difference between calibration and application temperature	[22]

Table 3.1: Summary of I-Scan accuracy metrics.

3.2.2 Capacitive Systems as an Alternative to I-Scan

As far as is known, Tekscan is the only company that produces resistive ink-based pressure sensors thin enough for measuring pressure under compression garments. Similarly thin sensors based on capacitance are considered by some to be more accurate than resistance-based sensors because they exhibit improved linearity, reduced sensitivity to temperature and humidity, reduced hysteresis and creep, increased durability and improved conformity to curved surfaces [32]. A few commercially available

systems with sensor thicknesses less than 1mm were thus briefly investigated.

Pressure Profile Systems (Los Angeles, CA) manufactures "TactArray" conformable sensor arrays with sensel sizes as small as 2mm. PPS claims [33] that PPS sensors are more accurate than I-Scan because the conductive cloth from which they are made is softer than the Mylar used by I-Scan and is thus more conformable to curved surfaces, reducing false pressure spikes. Although each PPS sensor is considerably more expensive ($2,500) than I-Scan sensors ($100) they are claimed to last far longer and are less prone to wear and tear. The basic TactArray system costs $16,000. Unfortunately there is almost no academic literature citing use of PPS in medical applications as it is used mostly in industrial research [33].

Novel (St. Paul, MN) manufactures a "Pliance" sensor array <1mm thick with 10x10mm sensel size – slightly smaller than I-Scan (12.7x12.7mm). As with PPS, Novel [34] claims that Pliance sensors are more accurate than I-Scan due to their higher conformance with curved surfaces. The Pliance system costs approximately $40,000.

McPoil et al [29] compared the validity and reliability of normal force and pressure measurements obtained using Novel EMED and Tekscan F-Scan sensors (both the EMED and F-Scan systems being similar to the Pliance and I-Scan systems respectively but designed specially for the foot) from measurements obtained in treadmill walking tests. In applying calibration pressures of 50-500kPa for 2s the EMED exhibited <5% error across the entire pressure range while the F-Scan underestimated the pressure by up to 30% at 500kPa. However, much of this error may be due to the authors only using a single calibration point, rather than the two recommended by Tekscan; additionally, 2s is too short for the slow response time (10-30s) of I-Scan sensors that has often been observed in Bio-Suit work. In [29] the sensors were also loaded to 150kPa for 10min to test creep performance; the Novel creep was 3% (i.e. for a constant load, the measured pressure increased 3%) and linear over the 10min test while the F-San creep was 12% and non-linear.

Xsensor (Calgary, AB, Canada) manufactures an "X2 Medical Pressure Bandage Sensor" <1mm thick with 2.5x11mm sensel size for measuring pressure applied by

compression bandages. Xsensor [35] makes identical claims about the accuracy of Xsensor vs I-Scan as the PPS and Novel representatives and provides identical reasons. The system costs approximately $9,000 [36] – considerably less than the aforementioned systems but still a major investment.

Mitchell et al [37] tested F-Scan and Xsensor sensors on flat and curved surfaces under static and dynamic loading conditions. In curved surface testing the F-Scan overestimated the applied force by 72% while the Xsensor underestimated by 2%. In flat testing the F-Scan overestimated forces by 156% while the Xsensor underestimated by 15%. The methodologies and statistical analysis in this paper are somewhat questionable; however, the authors' conclusion that Xsensor sensors are more accurate than F-Scan appears correct.

In summary, capacitive sensors are considerably more accurate than I-Scan sensors; however, they appear to have been less frequently used for medical applications, particularly for pressure garment measurements, than I-Scan. Further investigation would be required to determine their suitability for Bio-Suit use, especially given the significant expense involved in purchasing a new system and that the sensors, despite being softer and more conformable than I-Scan sensors, are also considerably thicker (1mm vs 0.1mm).

3.2.3 Alternative Methods for Measuring Pressure under Compression Garments

A number of companies manufacture flexible pressure sensors for medical and industrial pressure measurement applications such as on the foot during walking, on the buttocks during sitting etc. based on capacitive, piezo-resistive and other technologies [32, 38]. These are generally unsuitable for Bio-Suit work because the sensor is too thick (>1mm) and / or consists of only a few discrete sensels rather than a complete "matrix" that can produce a pressure map of a given area in real time.

Harris et al [31] list a number of in vitro methods for measuring contact areas and pressures in prosthetic joints including dye injection, stereophotogrammetry, Fuji

pressure-sensitive film and piezoelectric transducers. However, these methods cannot provide the same level of information in real time as I-Scan or other capacitive sensor arrays. For example, dye injection and stereophotogrammetry only provide information about contact area and not pressure [39]; Fuji film is not reusable and cannot provide realtime dynamic data [28]; and piezoelectric transducers can only provide pressure information at discrete points (one per transducer) rather than the pressure distribution over a given area [40].

Giele et al [41] note that many studies that attempt to measure the pressure generated by medical compression garments either extrapolate the results from garment tension or measure the interface pressure between garment and skin using sensors such as balloon transducers and "electronic monitors" (presumably I-Scan-type sensors). These methods cause several problems including sensor interference and poor conformity to the skin.

The paper describes a novel method to overcome these problems by using a needle connected to a pressure transducer and inserted under the skin to measure the subdermal pressure (i.e. that just below the skin). The authors evaluated this method at several sites on a leg and found that pressure garments produce a higher measured pressure over bony prominences than over soft tissue sites. However, the authors could not make any claims as to the accuracy of the method because they could not compare the measured results to a known, calibrated control measurement; furthermore, they could not provide a correlation between the subdermal (measured) pressure and the external pressure applied to the skin (the desired measurement). Finally, the method is invasive and time-consuming.

In summary, I-Scan and capacitive thin flexible pressure sensors are the most suitable systems for Bio-Suit work because, unlike other systems, they are able to create pressure maps in real time with minimal interference to the garment and wearer.

3.2.4 Review Summary and Conclusions

Tekscan I-Scan sensors measure mean pressure to within 10% accuracy under ideal, flat-plate static loading conditions. However, the accuracy of individual sensels, es-

pecially for measuring pressure underneath a compression garment, is considerably poorer because the sensels suffer from creep, hysteresis, temperature and humidity sensitivity (e.g. when placed next to skin) and false pressure spikes when crimped (e.g. on a curved surface). Despite these shortcomings, however, I-Scan has been used extensively to measure pressure distributions in medical applications such as prosthetic limb joints and pressure garments.

Capacitive sensor arrays may be more accurate than I-Scan for measuring pressure distributions on the leg because the conductive cloth from which they are made is more flexible, conformable on curved surfaces and durable than the printed circuits of I-Scan. However, none of the capacitive systems investigated to date have been used for medical research applications nearly as widely as I-Scan has except in a few specific fields such as contact pressures on the foot during ambulation. Additionally, a new capacitive system would be extremely expensive (up to $40,000) and its capabilities must therefore be studied in considerably greater detail before a potential purchase.

Resistive and capacitive sensor arrays are the only systems that can create pressure maps of a given area in real time. Other pressure measurement systems can only take pressure measurements at a few discrete points, measure the mean pressure over the given area, or cannot create pressure maps in real time – all of which are essential requirements for Bio-Suit research.

It is therefore recommended that I-Scan sensors continue to be used for Bio-Suit research despite their inherent inaccuracies. In doing so the accuracy of the sensors must be maximized by performing frequent equilibration and calibration on a curved surface (to replicate the shape of the human leg), using as many equilibration and calibration points as possible, minimizing sensor crimping, and using new sensors whenever possible. The next section discusses these practical issues in greater detail.

3.3 Experimental Work

The experiments described in the literature review measured I-Scan accuracy on a flat surface; however, the I-Scan sensors are being used for Bio-Suit research on the

curved surface of a human leg. This section describes experiments that measured the accuracy of the sensors in measuring pressure distribution on a cylindrical surface – an idealized model of a human leg. The experiments were then repeated on a flat surface in order to verify the results of the literature review and to provide a comparison with the cylindrical surface results.

3.3.1 Method

An I-Scan Model 9801 sensor was preconditioned, equilibrated and calibrated[3] using a cylindrical calibration rig (Figure 3-2).

The rig was then used to apply a load-unload cycle as follows (all measurements in mmHg): 0, +50, +100, +150, +200, +250, +300, +250, +200, +150, +100, +50, 0. Such a cycle permitted the level of hysteresis to be estimated. Each pressure level was applied for 60s, after which the next load was immediately applied. Two such load-unload cycles were performed[4]. In order to measure sensor drift, the pressure distribution being measured by the I-Scan sensor was recorded twice at each pressure level: the first reading immediately upon reaching the new pressure level, and the second 60s later, just before the next pressure level was applied. For each reading, 10s of data was collected at 8Hz[5] and averaged [42].

The entire procedure was then repeated using a flat-plate, rather than cylindrical, calibration rig (Figure 3-3) to verify the results of the literature review and to provide a comparison with the cylindrical surface results.

[3]In these experiments, as well as all other experiments in this thesis involving Tekscan sensors, the sensor calibration protocol described in Appendix B was used.

[4]This procedure assumes that the air pressure in the inflated bladder, as measured by the pressure gage, is uniform and equal to the pressure applied on the sensor, i.e. the pressure applied by the bladder pressing the sensor against the wall of the calibration rig. This is reasonable because the 10mm-wide space in which the sensor and bladder are located is far too narrow for the bladder to inflate sufficiently for its walls to stretch. The bag's expansion is thus being restrained by the rigid walls of the cylinder or flat plates, not elastic tension in the bladder walls. With no elastic tension in the bladder walls, the air pressure on the side of the bladder wall inside the bladder is thus equal to that on the other side where the sensor is.

[5]This is the maximum frequency for the most recent version of I-Scan software available in the Man Vehicle Lab (I-Scan v4.23, Tekscan Inc., South Boston MA); more recent versions of this software can achieve considerably higher rates.

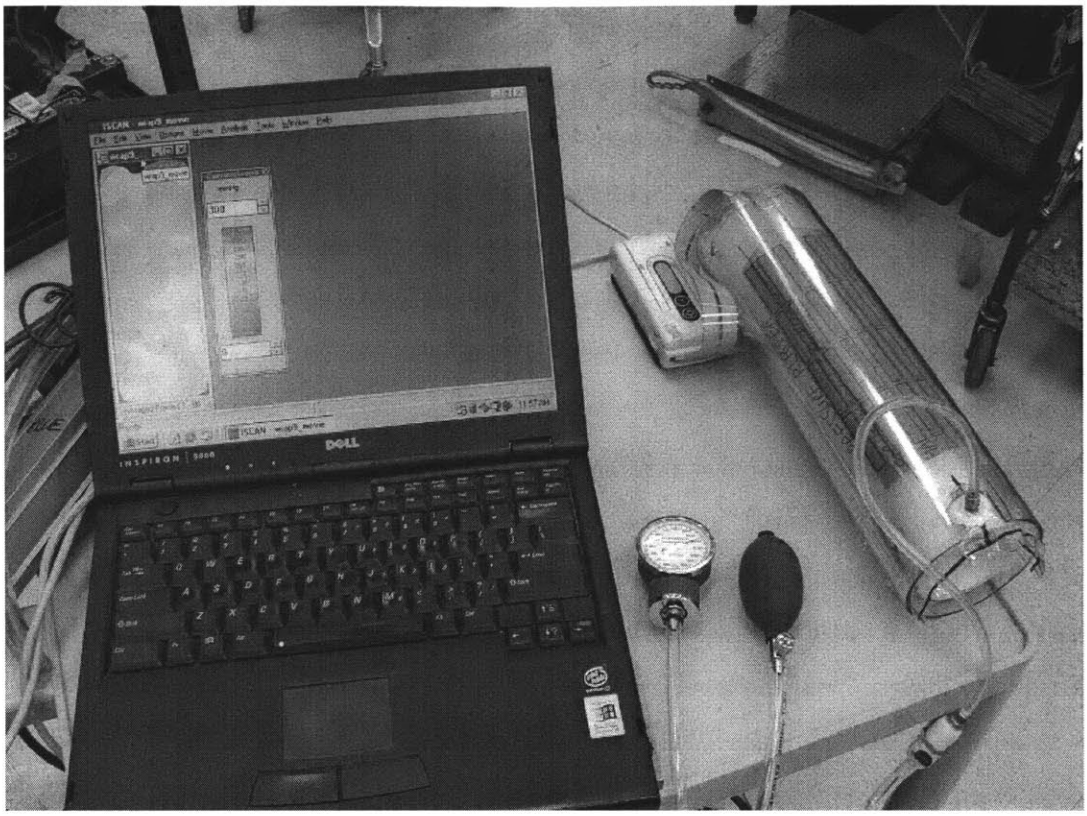

Figure 3-2: Tekscan I-Scan system undergoing calibration in the cylindrical calibration rig, consisting of two concentric rigid cylinders separated by a 10mm channel (right). A known load is being applied to the sensors by inflating a plastic bag inside the channel to a known pressure using the black hand pump (center), as measured by the rotary pressure gage (center). The pressure distribution being measured by the sensors is recorded and displayed graphically on the computer screen (left).

3.3.2 Results

Each pressure measurement consists of 96 individual pressure measurements, one from each sensel. The average of these 96 measurements (hereafter "average measured pressure") was calculated and compared to the air pressure inside the inflated plastic bladder (hereafter "applied pressure"). The difference between the average measured pressure and applied pressure was then calculated and plotted in Figures 3-4 and 3-5. For a perfect I-Scan sensor, all data points would thus lie on the x-axis in these Figures. There are two adjacent points at each pressure level, the first being the the measurement taken immediately upon reaching that pressure level, and the second

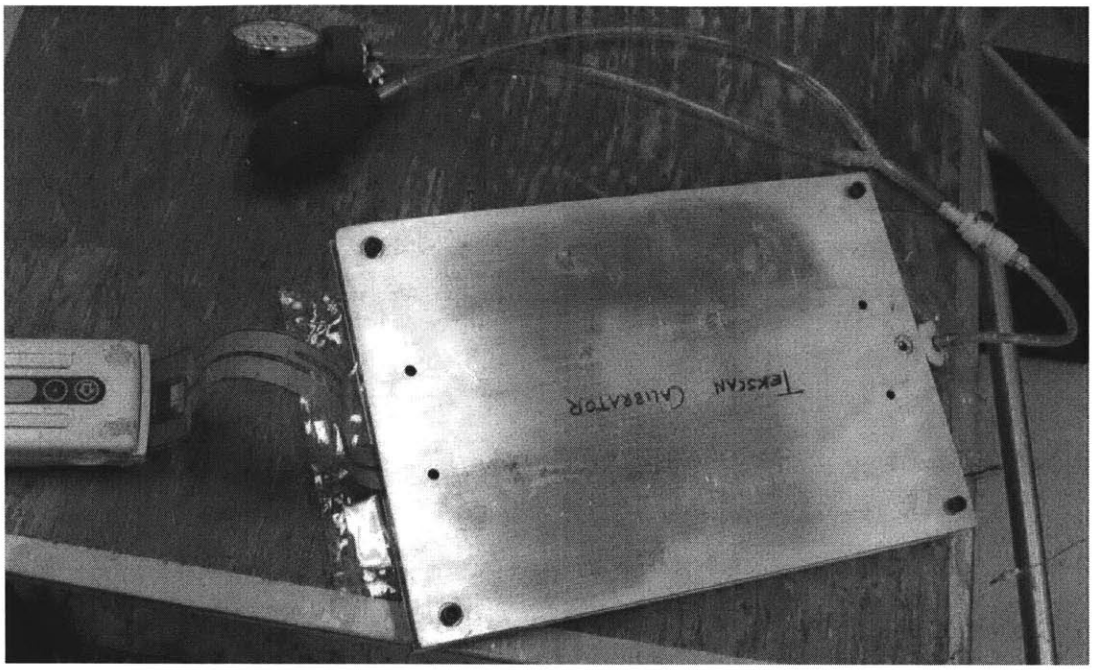

Figure 3-3: Flat-plate calibration rig consisting of two concentric aluminum plates separated by a 10mm channel in which the Tekscan sensor and inflatable bladder are positioned.

being that at the same pressure level 60s later, just before the next pressure level is applied. The arrows indicate the direction in which the load cycle was applied.

For each pressure distribution measurement, the standard deviation of the 96 sensel measurements was also calculated and is shown as horizontal error bars[6] in Figures 3-4 and 3-5. For a perfect sensor, every sensel measurement would be identical since since the applied pressure across the sensor is uniform; in this case, the standard deviation would then be zero.

3.3.3 Discussion – Implications for Use in Measuring Mechanical Counterpressure

A comparison of Figures 3-4 and 3-5 shows that the shape and magnitude of the load-unload curves for the cylindrical and flat-plate calibration rigs are very similar; in other words, the I-Scan performance is not affected by the sensor being flexed

[6]Vertical error bars caused the Figures to be excessively cluttered.

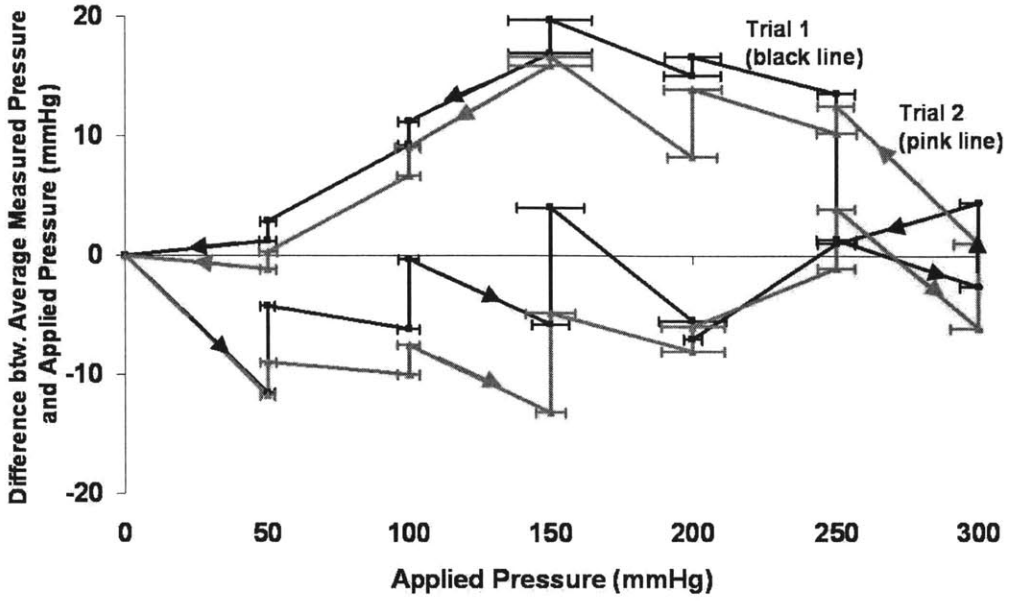

Figure 3-4: Difference between average measured pressure and applied pressure for I-Scan in the **cylindrical** rig. See text for full explanation.

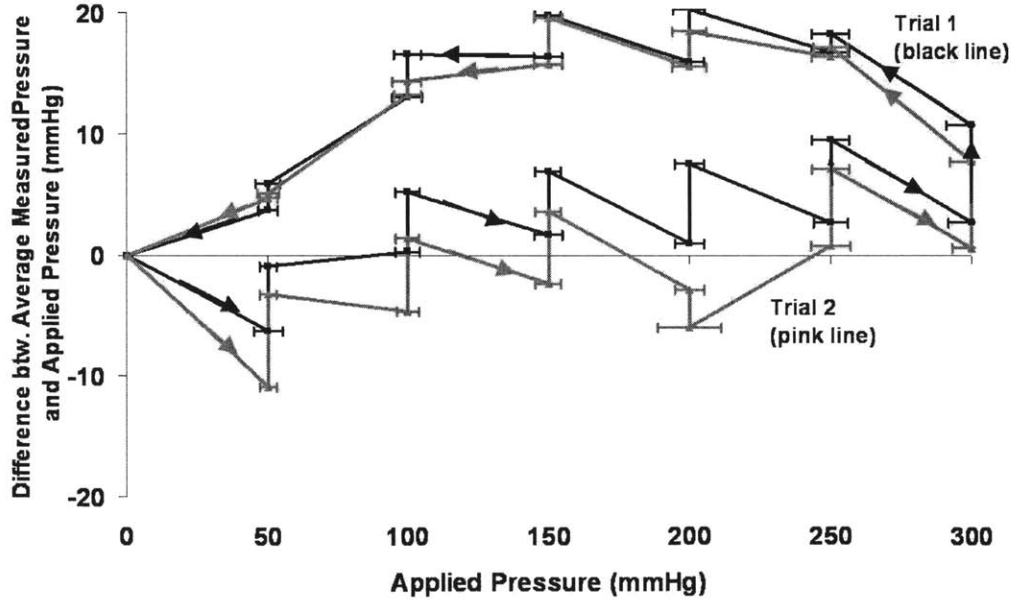

Figure 3-5: Difference between average measured pressure and applied pressure for I-Scan in the **flat-plate** rig. See text for full explanation.

onto a curved surface rather than its natural (flat) shape. The circumference of the cylindrical rig was 315mm, which is slightly larger than the 303mm calf circumference of a 5th percentile Japanese female[7]; as such, the similarity between the cylindrical and flat results suggests that the accuracy of the sensor is not affected by curvatures larger than this circumference – as long as it is calibrated in a rig as similar as possible to the geometry that the sensor will be operating in. For Bio-Suit research on human limbs, the sensors are therefore calibrated using the cylindrical, rather than flat-plate, rig (Appendix B.)

The results of Figures 3-4 and 3-5 are also similar to those from the literature review (Table 3.1). First, the error in mean pressure is up to ±20mmHg, in agreement with the 10% error stated in Table 3.1. It is not surprising that the highest errors occur at 150, 200 and 250mmHg since these are away from the pressure levels at which the sensor was calibrated (100 and 300mmHg – see Appendix B). Unfortunately it is impossible to utilize more than two calibration points to improve accuracy across the whole range of pressures since the Tekscan software does not permit this[8].

Most of the error in mean pressure appears to be caused by hysteresis, as the shape of the load-unload cycle clearly demonstrates. Up to ±20mmHg hysteresis occurs at 150mmHg and 200mmHg – more than the 5% claimed by Tekscan (Table 3.1). The hysteresis appears to be quite repeatable, as the similarity between the two trials in both the cylindrical and flat-plate rigs shows. Further trials would be necessary to determine the number of cycles for which this repeatability continues.

The sensors also display creep: in Figures 3-4 and 3-5 the second measurement for each pressure level, taken 60s after that pressure was initially applied, is usually closer to the (correct) applied pressure than the initial measurement. However, there does not appear to be a pattern regarding the magnitude of the creep.

Its presence is both advantageous and disadvantageous. It is beneficial that the sensor measurement creeps in the correct direction, thus reducing hysteresis error.

[7]NASA-STD-3000 Man-Systems Integration Standards Volume 1 Section 3, Rev B (July 1995).

[8]In fact, previous versions of the Tekscan software did permit multi-point calibration but the feature was removed at the request of Tekscan users who claimed that the time necesary to calibrate extra points did not result in greater accuracy [23].

However, it reveals that the sensor has an extremely slow response – on the order of minutes, which is far slower than the 8Hz maximum sampling rate of the I-Scan system. From a practical perspective it suggests that one should wait for a minute or two after pressure is applied before making a pressure measurement. This is no problem for Bio-Suit work, in which MCP measurements do not vary significantly with time, but would be unsuitable for high-frequency applications such as impact or locomotion measurements.

The standard deviation in individual sensel measurements, indicated by the horizontal error bars on Figures 3-4 and 3-5, is significantly higher ($p = 0.003$ by pairwise comparison) for the cylindrical rig ($\pm$7.0mmHg) than the planar rig ($\pm$5.5mmHg). The reason for this difference is currently unknown; in any case, even the lower deviation is disadvantageous because it decreases the ability to accurately measure spatial variations in the MCP applied by a Bio-Suit garment. Unfortunately, it is difficult to reduce this deviation because the sensor is already equilibrated before calibration specifically to adjust for inherent differences in the sensitivity of individual sensels [22]. The current calibration procedure already utilizes *six* equilibration points, one for every 50mmHg between 50-300mmHg inclusive, which is considerably more than the 1-2 equilibration points used in previous Bio-Suit research [3, 14]; using even more points would be unlikely to add any significant benefits.

3.4 Summary and Conclusions

These experiments provide evidence that the performance of the I-Scan sensors is not adversely affected through use on a curved, rather than flat, surface. The mean pressure, hysteresis and creep performance for both the cylindrical and flat calibration rigs generally agree with those discussed in the literature review. However, the accuracy of individual sensels appears to be slightly lower on a curved surface compared to a flat surface; further investigation is required to determine the underlying causes, but it is unlikely that it can be improved since the sensels are already equilibrated before calibration to maximize the uniformity of their gain.

Similarly, there appears to be little more that can be done to improve other aspects of I-Scan sensor accuracy. The current calibration procedure (Appendix B) already maximizes sensor sensitivity within the necessary operating range and uses the maximum number of calibration points. Furthermore, the equilibration and calibration process is already performed on a cylinder to replicate the curved surface of a human leg [22]. Finally, the literature review suggests that hysteresis and creep are inherent and inevitable in resistive sensors such as I-Scan, and the experiments of this chapter support this hypothesis.

These factors, coupled with the lack of readily available alternative sensors (Section 3.2.4) means that inaccuracies in I-Scan measurements appear unavoidable; as such, I-Scan measurements must be interpreted with caution. In practical terms:

- Mean pressures measurements have an error of up to $\pm 10\%$.
- Additionally, individual sensel measurements have a standard deviation of up to $\pm 7\%$. Judgment (as well as subject feedback, if possible) is required to determine whether a sensor whose measurement is considerably different to its surrounding sensels is truly detecting a localized pressure variation or is merely faulty.
- Measurements taken immediately after the pressure load is first applied are prone to $\pm 10\%$ hysteresis error. As such, measurements should be taken at least a minute after the load application to allow the sensor measurement to creep towards the correct value.

These practical recommendations are in addition to those provided by Tekscan [22, 23] and have been applied in the work described in Chapters 4 and 6. Some further considerations for using I-Scan sensors are discussed briefly in Appendix A.

Chapter 4

MCP Prototype Development

4.1 Introduction

As described in Chapter 2, one of the primary objectives of the Bio-Suit Project is to develop comfortable, high-mobility MCP prototypes in order to demonstrate the basic concept feasibility and to illustrate mechanical and physiological issues associated with using MCP to pressurize the body surface. This chapter describes several full-leg MCP prototypes that were designed, fabricated and preliminarily tested as part of this ongoing development.

Previous Bio-Suit leg garments (Section 2.2) have utilized the hybrid concept in which a pressurized bladder transduces MCP to the body. As emphasized throughout Chapter 2, however, the preferred approach is to pressurize the body without relying on any form of fluid pressure. Sections 4.2 and 4.3 describe the development of two such elastic-only prototypes: the **detached bands** and **elastic bindings** respectively, both conceived by Prof. Jeffrey Hoffman (see Acknowledgments). The objective of these prototypes was to demonstrate higher comfort, mobility and ease of donning than previous MCP designs – challenges that have hindered previous elastic-only MCP designs from further development (Section 2.1.3). The elastic bindings demonstrated better performance than the detached bands, and were thus chosen for further development and use in subsequent physiological experiments described in Chapter 6.

Both the detached bands and elastic bindings rely on the fact that the limbs have an approximately circular cross section; as such, it was difficult to use them to apply MCP to the foot and ankle, which have considerably more irregular shapes. Section 4.5 thus describes a hybrid garment that was developed as a simple, effective means of providing the MCP on the foot for the experiments described in Chapter 6. Being a hybrid, this foot garment should be considered as a temporary solution only; further efforts should be made to develop elastic-only garments that can provide a uniform MCP distribution on the complex foot and ankle surface.

4.2 Detached Bands Concept

4.2.1 Introduction

To date, the only attempt at an elastic-only MCP leg garment has been the Space Activity Suit (Section 2.1.3). Two of its major limitations were don/doff difficulty and lack of joint mobility. The SAS consisted of up to six layers of elastic material covering the limbs and torso; as such, the donning process required over 30 minutes even with the support of two assistants. Furthermore, the longitudinal stress of six fabric layers reduced the maximum knee flexion from 140° unsuited to 80° suited [1]. These limitations were key in hindering the SAS from further development.

To overcome these difficulties, a concept consisting of thin (<25mm) elastic bands wrapped around the leg was investigated. The garment consists of discrete bands of varying size and strength that are physically detached from one another (Figure 4-1(a)). The bands create MCP through elastic circumferential stress only, thus minimizing longitudinal stresses and maximizing joint mobility [4]. First, elastic bands of appropriate dimensions and material properties are chosen to create a uniform pressure distribution based on the individual leg dimensions of the wearer. The mechanical counterpressure P generated by an elastic band of thickness t, radius r_t and Youngs Modulus E placed on a cylinder of radius r (where $r > r_t$) is

$$P = \frac{Et}{r_t}\left(\frac{r - r_t}{r}\right) \tag{4.1}$$

After selecting bands that produce the desired pressure, the wearer simply dons the bands in any preferred order. The inherent modularity in this design theoretically allows the precise local control of the MCP applied to the leg.

4.2.2 Methods and Materials

Leg circumference was measured at 10mm intervals between the ankle and upper thigh. From a range of standard detached bands (Dykema Inc., Pittsburgh PA; Keener Rubber, Alliance OH; Aero Rubber, BridgeView IL) Equation 4.1 was used to select bands with appropriate dimensions and material properties to provide the target pressure at each measured circumference. Multiple bands were used for circumferences where no single band could provide the target pressure to within ±20%.

To measure the pressure distribution generated by the garment, Tekscan I-Scan Model 9801 pressure sensors (Chapter 3) were placed at the calf anterior and posterior (Figure 4-1(b) and (c)). The selected bands were then donned starting from the ankle and progressing to the thigh, this order having been experimentally determined to be more comfortable than thigh-to-ankle.

Pressure measurements were taken with the initial target MCP being 13.3kPa (100mmHg, 1.93psi). This is lower than the 30kPa (225mmHg) target specified in Section 2.1.2 and was chosen for initial experiments to verify the basic concept feasibility without causing undue discomfort to the wearer, the severity of which was unknown *a priori*.

The subject performed knee squats whilst wearing the garment to determine mobility (maximum knee flexion angle) and comfort. Knee flexion angle was measured using a goniometer.

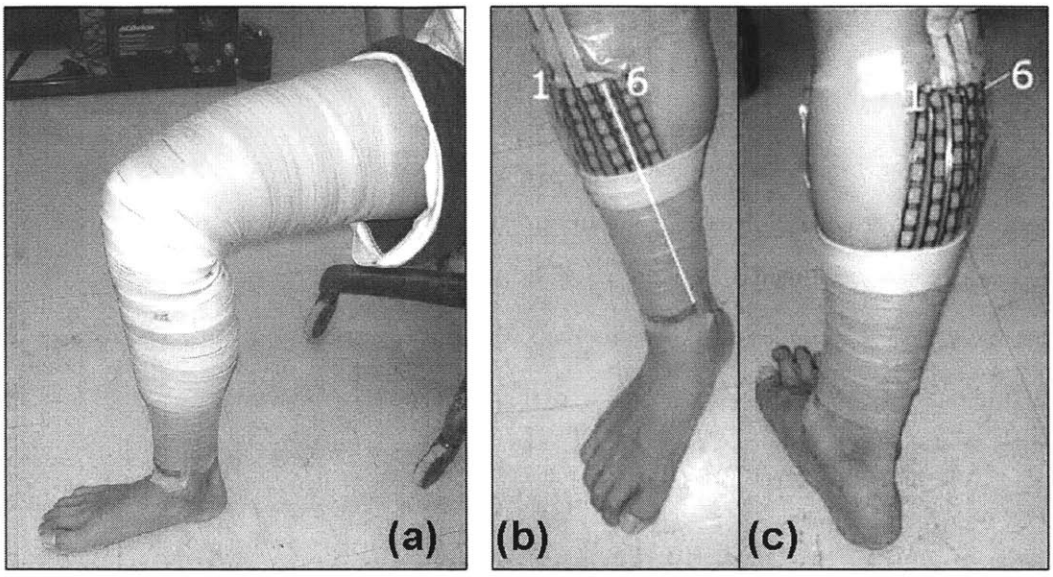

Figure 4-1: (a) Subject wearing detached bands prototype from ankle to thigh. (b) I-Scan sensors placed on calf anterior, with the sensor columns 1-6 defined as shown. The sensors on the anterior are positioned such that column 5 runs directly along the tibia, as indicated by the solid white line. (c) I-Scan sensors on calf posterior.

4.2.3 Results

Results were obtained for only one subject (male, age 24, height 170cm, mass 63kg) since the detached bands proved less successful than the elastic bindings concept (Section 4.3) and was therefore not pursued further.

With the target pressure set at 13.3kPa (100mmHg), the average MCP[1] generated by the bands was 14.0kPa (105mmHg) on the calf anterior and 15.1kPa (113mmHg) at the calf posterior. The standard deviation between the individual sensel measurements[2] was 7.2kPa (54mmHg) at the anterior and 5.6kPa (42mmHg) at the posterior. These results may change slightly each time the prototype is donned, or as the wearer moves his/her leg, but these changes were not investigated for this prototype.

The bands did not reduce the subjects mobility: knee flexion was approximately 150° for both the unsuited and suited leg. However, the bands caused considerable

[1] As in Section 3.3.2, "average MCP" is defined as the average of the 96 individual measurements of the I-Scan sensor array.

[2] Defined as the standard deviation between the I-Scan sensor's 96 sensel measurements; again, see Section 3.3.2 for details.

discomfort at the knee posterior above 120° as adjacent bands creased together to create high pressure points. Attempts were made to alleviate this by using bands that were tapered at the knee posterior; however, this did not alleviate the discomfort. Approximately 15 minutes per leg were required to don sufficient bands to provide the 13.3kPa average MCP profiles shown above. Plans to increase the target pressure to 26.7kPa (200mmHg, 3.76psi) were canceled since more bands, and thus more time, would have been required to achieve this, causing undue discomfort to the wearer.

4.2.4 Discussion

The detached bands prototype provided evidence that the concept of decoupling circumferential and longitudinal stresses increases joint mobility. However, the prototype suffered from numerous practical problems. Most importantly, the 15min per leg donning time was far lengthier than the target of 10 minutes for the entire (whole body) suit discussed in Section 2.1.2) and was due to the large number of differently sized bands that needed to be individually donned. Furthermore, the force necessary to stretch the larger bands during the donning process was difficult for the wearer to generate without assistance, and would be even higher if the target pressure were increased from the current 100mmHg to the 222mmHg operational target (Section 2.1.2). These limitations made it difficult to increase the target pressure beyond 13.3kPa within a reasonable donning time.

The pressure distribution generated by the bands was also highly non-uniform: the standard deviation of up to 7.2kPa was already more than 50% of the 13.3kPa initial target pressure. At the operational target of 30kPa this deviation is likely to be even higher, and is far greater than the 1.6kPa (±12mmHg) spatial variation limit of Section 2.1.2. The non-uniformity would be likely to cause adverse physiological effects if the prototype is worn for extended durations (Chapters 5 and 6).

To be fair, some of the non-uniformity was caused by inaccuracies in the I-Scan pressure sensors, as discussed in Chapter 3. In any case, no attempts were made to improve the uniformity of the pressure distribution because the lengthy donning time already hindered the detached bindings concept from further development, and

because the bulk of development efforts focused on the elastic bindings described in the next section.

4.3 Elastic Bindings Concept (Phase I)

4.3.1 Introduction

To overcome the cumbersome don-doff process inherent in the detached bands, a novel concept was conceived in which a single, long elastic binding, rather than many discrete elastic bands, is wrapped around the limb in a similar fashion to medical bindings. The wearer varies the force with which the binding is stretched as it is wrapped around the limb in order achieve a uniform pressure distribution. Friction permits different sections of a single binding to be stretched at different rates. The circumferential tension F with which a binding of width b must be stretched around a cylinder of radius r to generate a mechanical counterpressure P on the cylinder is[3]

$$F = Pbr \tag{4.2}$$

As such, the tension in an elastic binding producing uniform MCP is considerably greater at the top of the thigh than at the ankle.

The principal advantage of the elastic bindings is that they can be donned far more efficiently than the detached bands without any reduction in mobility or comfort, as the following sections show. Development occurred in two "phases", with discrete methods, materials and results for each. The following sections (4.3 and 4.4) present the development process chronologically, by phase.

4.3.2 Methods and Materials

Based on initial experiments by Prof. Jeffrey Hoffman, the first elastic bindings consisted of standard butyl rubber inner tubes for bicycle wheels slit circumferentially

[3]This is the equation in Appendix A of [3] but substituting F/b for T, the tension per unit width of band.

to form a flat binding approximately 2,000mm long and up to 40mm wide [13]. First, the wearer's leg circumference was measured at 10mm intervals between the ankle and upper thigh as for the detached bands. Equation 4.2 was then used to determine the circumferential tension necessary to produce the target pressure for a given limb circumference. The binding was attached to a spring scale and stretched to the appropriate tension as it was wrapped onto the leg (Figure 4-2(a)). As before, an I-Scan Model 9801 sensor was used to measure the pressure distribution generated by the bindings, and the wearer also performed knee squats to determine mobility.

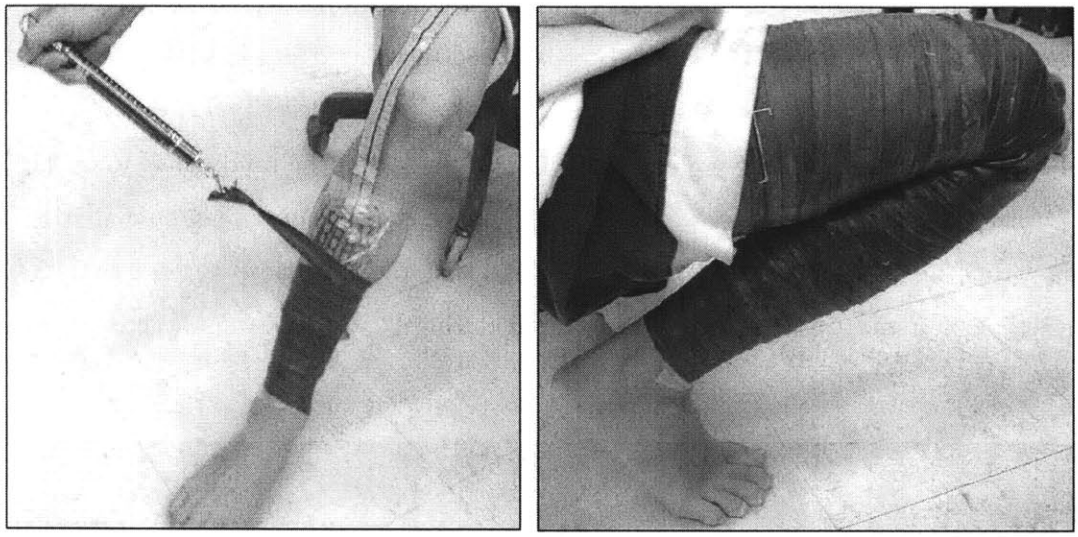

Figure 4-2: (a) Elastic bindings being donned over Tekscan sensors, with a spring scale being used to control the wrapping tension. (b) Subject demonstrating a deep knee squat while wearing elastic bindings.

4.3.3 Results

As before, most results for this preliminary phase were obtained for only one subject (male, age 24, height 170cm, mass 63kg). With the target pressure set at 26.7kPa (200mmHg, 3.8psi), the MCP generated by the bindings on the calf in ambient conditions was 23.3kPa (175mmHg) at the anterior and 22.5kPa (169mmHg) at the posterior. The standard deviation of individual sensel measurements was 10.0kPa (75mmHg) at the anterior and 7.5kPa (56mmHg) at the posterior.

As with the detached bands, the bindings did not reduce the subjects mobility; knee flexion angle remained at approximately 150° for both the unsuited and suited leg during squatting. The bindings caused some discomfort at high flexion angles (above 130°) as adjacent binding rows behind the knee creased together to create high pressure points. However, the discomfort was considerably less than that of the elastic bands and was alleviated further by placing a stiff rubber pad at the back of the knee between the skin and binding.

Donning time was approximately 8-10 minutes when the spring scale (Figure 4-2(a)) was used to measure the force with which the bindings needed to be stretched. However, a substantially faster method was devised in which the the spring scale is used only when the prototype is donned for the first time, as described above. Once donned, vertical lines are drawn along the length of the leg on the bindings (Figure 4-3). On subsequent dons, the wearer simply re-aligns corresponding alignment marks when wrapping the bindings. This method reduced the don time to less than 5 minutes per leg and was utilized and improved during later phases, as described in Section 4.4.

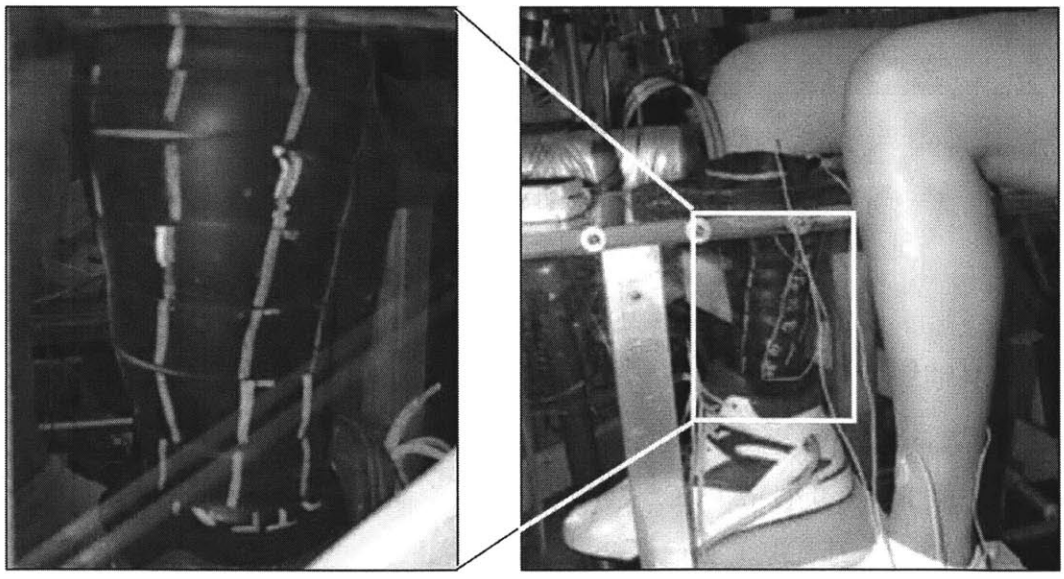

Figure 4-3: (a) Alignment marks along the length of the elastic bindings. (b) Alternate view of the alignment marks on bindings worn by a test subject in the low pressure leg chamber.

4.3.4 Discussion

This initial phase demonstrated the basic feasibility of the elastic bindings concept. First, the experiments demonstrated that that the elastic bindings could be donned and doffed far more rapidly than the detached bands and were also considerably more comfortable when donned, allowing the bindings to generate almost double the MCP achieved by the the detached bands. The assumption that friction between the binding and skin would allow the tension in the binding to be varied along its length also proved valid, demonstrating the potential for the bindings to create a uniform pressure distribution despite the change in circumference along the calf (pressure measurements on the thigh were not performed during these experiments.)

However, the pressure distribution was still not as uniform as desired: the 10kPa standard deviation of sensel measurements was still far greater than the 1.6kPa (12mmHg) limit of Section 2.1.2. The next phase of development therefore focused on improving the uniformity of the pressure distribution generated by the bindings.

4.4 Elastic Bindings Concept (Phase II)

4.4.1 Introduction

In seeking methods to improve the uniformity of the pressure distribution generated by the bindings, it was hypothesized that major improvements could be realized by focusing on two key aspects – the binding material, and the technique by which the bindings are wrapped.

An improved material was sought because the butyl rubber strips used in Phase I exhibited non-uniform material properties along its length: during characterization, applying the same tensile load on different sections of the band caused their strain to differ by as much as 10%. Furthermore, the bands exhibited 1-3% inelastic (permanent) elongation after 10-15 don-doff cycles.

The binding technique is almost unquestionably the most important variable affecting the uniformity of the pressure distribution. The objective was thus to refine

the alignment mark concept described in the previous section to improve uniformity without sacrificing the ease and speed of donning.

Once these new materials and methods were developed, the improved bindings were tested on the "ideal" surface of a rigid cylinder rather than a human leg, for two reasons. First, it would theoretically be easier to generate a uniform pressure on a cylinder than a leg because its cross-sectional circumference is constant, meaning that the necessary wrapping tension would also be constant throughout the binding. Second, its rigidity means that, unlike the leg, application of pressure would not deform or change the cylinders cross-sectional shape or circumference. It was thus felt that the new materials and methods should first be demonstrated successfully on a rigid cylinder before being applied to a human leg.

4.4.2 Improved Binding Material

The search for an elastic bindings with more uniform material properties and reduced creep was performed in collaboration with N. Jared Keegan of Midé Technology Corporation (Medford MA). According to Keegan [43], butyl rubber typically has low creep strength and are only used in bicycle inner tubes due to their low permeability and therefore air-tightness – a quality that is irrelevant, even disadvantageous, for an MCP garment as it prevents the wearer's perspiration from being wicked away[4].

Keegan suggested neoprene, latex or natural rubber strips as these have higher tensile strength and lower creep propensity than butyl rubber [43]. A search was therefore performed to find these types of rubber in a strip form that was empirically deemed appropriate for the elastic bindings – approximately 20-40mm wide, 1-2mm thick and up to 2,500mm long, these dimensions being based on Phase I experience with butyl rubber.

Several manufacturers were found to provide neoprene rubber in such a form, including Greene Rubber (Woburn MA) and New England Rubber (Dedham MA). One

[4]One of the potential advantages of a permeable MCP garment is its ability to reduce life-support system mass and complexity by passively allowing the wearer's perspiration to sublimate [4] through its pores, as long as these pores are not large enough to cause adverse physiological effects, as discussed in Section 2.1.2.

of the crucial advantages in the strips purchased from these manufacturers (Figure 4-4) is that they are cut from a large rubber sheet to the appropriate width using high-precision cutting machines. When stretched, such a well-cut strip has substantially greater strength than one cut using less accurate means (e.g. by hand, as the original butyl strips of Phase I were cut) because, under tension, the former would not suffer from stress concentrations that occur in the jagged, rough edges of the latter.

4.4.3 Development of Improved Wrapping Technique

The spring-scale wrapping technique described in Phase I was a cumbersome and inaccurate method for controlling the tension in the binding with any reasonable accuracy, for several reasons. First, the binding needed to be frequently re-tied to the scale's hook as it was wrapped onto the leg. Second, friction and hysteresis in the tension spring further reduced the accuracy and ability of the user to maintain the desired tension. The addition of alignment marks substantially increased donning speed on the second and subsequent dons, but their pressure distribution was still limited by the accuracy of the spring scale.

A method was therefore developed to eliminate the spring scale completely and measure alignment marks on the bindings *before* use. As well as avoiding the awkwardness associated with the scale, the pressure distribution achieved using this new method was surprisingly accurate when performed on a rigid cylinder – an idealized model of a human limb.

In this method, the material properties of the elastic bindings were first characterized in detail. The strain, width decrease and thickness decrease for a given tensile load (F in Equation 4.2) was measured at approximately 10N intervals between 0-50N[5] and a strain vs force per unit binding width ϵ-(F/b) curve calculated using these measurements.

Equation 4.2 was then used to calculate the force per unit width (F/b) necessary to generate the desired mechanical counterpressure P on the rigid test cylinder of

[5]From experience, 50N is the maximum force with which a typical wearer could reasonably stretch a binding without difficulty

radius r. This F/b value was substituted into the ϵ-(F/b) curve to calculate the strain necessary to produce the desired pressure, which for these experiments was set at 26.7kPa (200mmHg). This strain was in turn used to calculate the spacing between the alignment marks on the bindings (Figure 4-4(a)), based on the cylinder radius and number of longitudinal alignment lines on the cylinder. Generally, either four or eight equally spaced alignment lines were marked onto the cylinder (Figure 4-4(b))[6]. Finally, the bindings were then wrapped around the cylinder such that their alignment marks were aligned with the corresponding lines on the cylinder (Figure 4-4(c)).

In later trials, spiral alignment marks were were also drawn on the cylinder to guide the edges of the bindings as they were wrapped onto the cylinder (Figure 4-4(b)). Their pitch spacing was customized to the stretched width of the binding being wrapped around it, as determined from the binding's force-strain-width measurements. In summary, the combination of longitudinal and spiral alignment marks on the cylinder was intended to provide a well-defined guide along which the bindings could be wrapped in order to achieve a uniform, reproducible pressure distribution, as measured by the I-Scan sensors (Figure 4-4(d)).

Some difficulty was observed in using the alignment spiral to guide the binding edge. The spirals are intended to both to prevent adjacent binding edges from overlapping, which would create excessive pressure in the overlap area, as well as minimize any gaps between adjacent binding edges, which would expose part of the skin to the low pressure environment (Section 2.1.2). Clearly there is little middle ground between these two undesirable outcomes, an inherent flaw in the elastic bindings concept. In an attempt to overcome this, a "double wrap" concept was conceived as an alternative to the spiral, in which a centerline was drawn along the length of the binding (Figure 4-5(a)). The binding was then wrapped such that its edge followed the centerline, rather than the spiral; the leg or cylinder would then be pressurized by two intentionally overlapping layers, preventing gaps between binding edges. Another

[6]From practical experience, eight lines was deemed to be a suitable balance: Using only one or two lines resulted in inconsistent tension in different lengths of the binding [13] while it became impractical and time-consuming to align the bindings to more than eight lines.

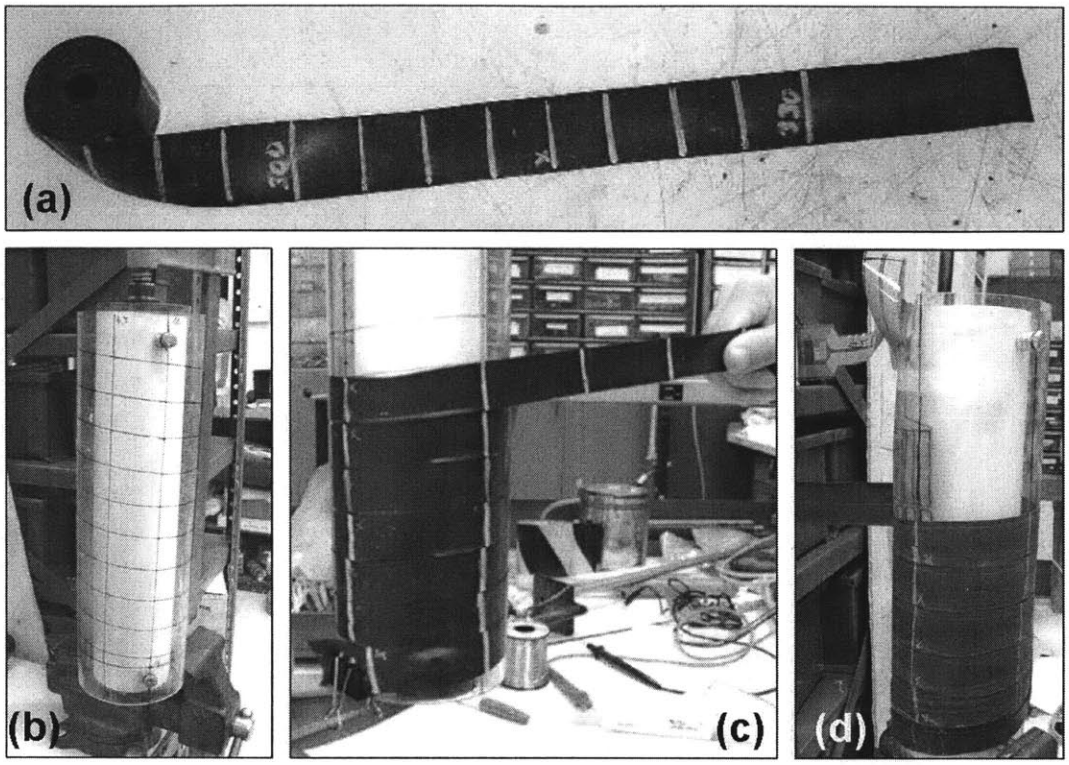

Figure 4-4: (a) Neoprene rubber elastic bindings showing custom-measured alignment marks. (b) The 100mm-diameter rigid plastic cylinder used as an idealized model of a human leg, showing both longitudinal alignment lines (eight total, spaced 45° apart) and alignment spirals. The longitudinal lines align with the marks drawn on the bindings in (a) while the spirals guide the edges of the bindings as they are wrapped around the cylinder. (c) Binding being wrapped around the test cylinder, guided by both the alignment lines and spirals. In these experiments the required binding strain was typically 100%, as illustrated, to achieve the desired 26.7kPa (200mmHg) pressure on the 100mm diameter cylinder. (d) Tekscan I-Scan sensors were placed on the cylinder to measure the pressure distribution generated by the bindings on the cylinder.

advantage of the double-layer concept would be that a higher MCP could be achieved with two layers rather than one. However, the primary disadvantage would be an increase in donning time since a a greater number of turns (and a longer binding) would be required to cover a given area compared to a "single-wrapped" binding following the alignment lines and spirals.

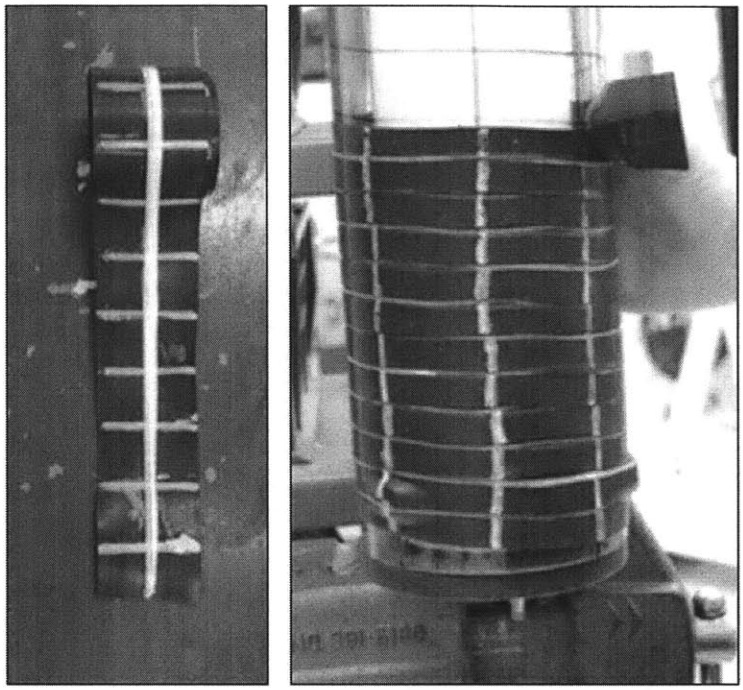

Figure 4-5: (a) Elastic binding marked with centerline for use in a double-wrapped cylinder. (b) Binding being "double-wrapped" around the cylinder. Each wrap is guided by the centerline on the binding rather than the alignment spiral on the cylinder.

In summary, the most time-consuming aspect of the new methods described in this section was the necessity to individually characterize each binding before use. This was important even if the bindings had the same dimensions, were made of the same material and were sourced from the same manufacturer, as the strain curves for such "identical" bindings differed by up to a few percent. The individuality of each binding also required its alignment marks, and corresponding alignment spirals on the cylinder, to be individually drawn for each binding.

However, the primary advantage was that the actual wrapping process was faster

than the Phase I method (approximately 3 minutes for the test cylinder in Figure 4-4(b)) and eliminated the use of the cumbersome spring scale. The next section presents the pressure distribution that the bindings generated using this method.

4.4.4 Testing – Methods and Materials

Previously, only one pressure measurement was made as an approximate "snapshot" of the pressure distribution that the detached bindings and Phase I elastic bindings could potentially achieve. Much of the Phase II effort was devoted improving the uniformity of the pressure distribution; as such, multiple pressure measurements were taken in order to determine the repeatability, as well as the uniformity, of the pressure that the Phase II bindings could provide.

The test cylinder consisted of a 100mm diameter, 350mm long PVC cylinder (Figure 4-4(b)). As mentioned in Section 3.3.3, the cylinder diameter was chosen to match the diameter of a relatively small female calf while the material was chosen not only for its rigidity but also because its surface finish is smooth, thus minimizing the possibility that the I-Scan pressure sensors would record false pressure spikes that may occur when in the sensors are in contact with rough, unfinished surfaces. An I-Scan 9801 sensor was then calibrated on the surface of the test cylinder, as per the methods and reasoning described in Chapter 3, before being attached onto the cylinder in preparation for testing.

Three series of tests were performed:

1. Four alignment lines on the cylinder, spaced 90° apart; target pressure 26.7kPa (200mmHg).

2. Eight alignment lines plus alignment spirals on the cylinder, again with 26.7kPa target pressure.

3. As with item 2, but using the double wrap concept. For consistency, the alignment marks from item 2 were unchanged; the target pressure was therefore doubled to 53.3kPa (400mmHg).

In each series the binding was donned and doffed from the cylinder ten times, and the pressure distribution recorded for each. These measurements were taken at least two minutes after the donning process was complete to allow for hysteresis and creep (Section 3.4).

4.4.5 Testing – Results

For each series, ten pressure distribution measurements (or "snapshots") were recorded; each snapshot in turn consisted of 96 individual pressure readings, one from each sensel, as described in Section 3.3.2. Therefore, to describe the method in which the results were analyzed, let $P_{(i,j)}$ be the jth sensel reading ($j = 1 \ldots 96$) of the ith snapshot measurement ($i = 1 \ldots 10$). Also let $\overline{P}_i$ be the average of $P_{(i,1)}, P_{(i,2)}, \ldots, P_{(i,96)}$. Finally, let the average pressure $\overline{P}$ and the standard deviation S of the *series* (not the snapshot) be be the average and standard deviation of $\overline{P}_1, \overline{P}_2, \ldots, \overline{P}_{10}$ respectively.

The pressure distribution generated by the bindings should repeatably match the target (or design) pressure P_t. In other words, $\overline{P}$ should be as close to P_t, and S as close to zero, as possible. Figure 4-6 shows $\overline{P}$ and S generated by the Phase II elastic bindings on the test cylinder, and compares these to the results from the detached bands and Phase I elastic bindings.

The other crucial metric for evaluating the pressure distribution generated by the bindings is its uniformity. An ideal binding would generate a perfectly uniform distribution, meaning that the individual sensel readings $P_{(i,1)}, P_{(i,2)}, \ldots, P_{(i,96)}$ would all be identical. For each snapshot, define s_i ($i = 1 \ldots 10$) to be the standard deviation of $P_{(i,1)}, P_{(i,2)}, \ldots, P_{(i,96)}$ and $\overline{s}$ to be the average of $s_1, s_2, \ldots, s_{10}$. $\overline{s}$ will hereafter be loosely termed the "non-uniformity" of the pressure distribution generated by the bindings; in an ideal binding $\overline{s} = 0$. Figure 4-7 shows $\overline{s}$ generated by the Phase II elastic bindings on the test cylinder, and compares these to the results from the detached bands and Phase I elastic bindings.

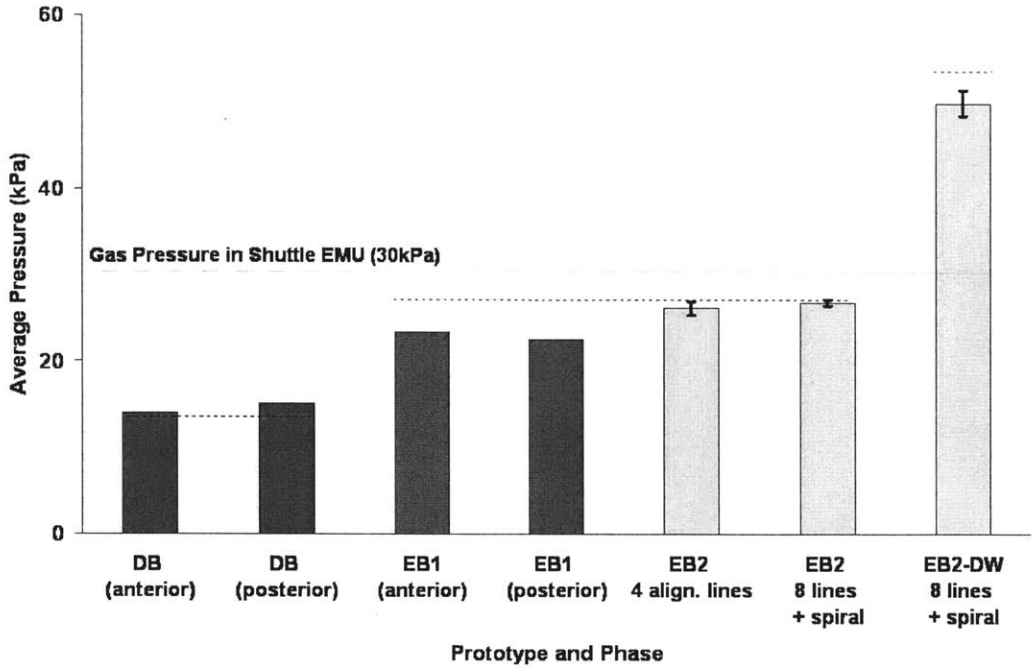

Figure 4-6: Series average pressure $\overline{P}$ generated by various MCP prototypes on the test cylinder, except where 'anterior' or 'posterior' are stated, in which case the test object is the anterior or posterior of a human calf, as described in the text. 'DB' = detached bands; 'EB1' and 'EB2' = elastic bindings phases 1 and 2 respectively; 'DW' = double wrap. 'Lines' refers to the longitudinal alignment lines and 'spiral' refers to the alignment spirals (Figure 4-4(b)). Dotted lines indicate the target pressure P_t for that prototype. Error bars show standard deviation S of of the average pressure; these bars are not available for DB and EB1 as only one snapshot, not ten, was measured for these prototypes.

4.4.6 Discussion

Average pressure and repeatability

At first glance, Figure 4-6 suggests that the methods and materials developed in Phase II were successful in improving the performance of the elastic bindings. The series average pressure $\overline{P}$ of the Phase II bindings ('EB2' in Figure 4-6) was far closer to its 26.7kPa (200mmHg) target pressure than the other prototypes (the Phase II double-wrapped binding ('EB2-DW'), whose target was 53.3kPa, which is discussed later). Furthermore, the standard deviation S of the average snapshot pressure in the

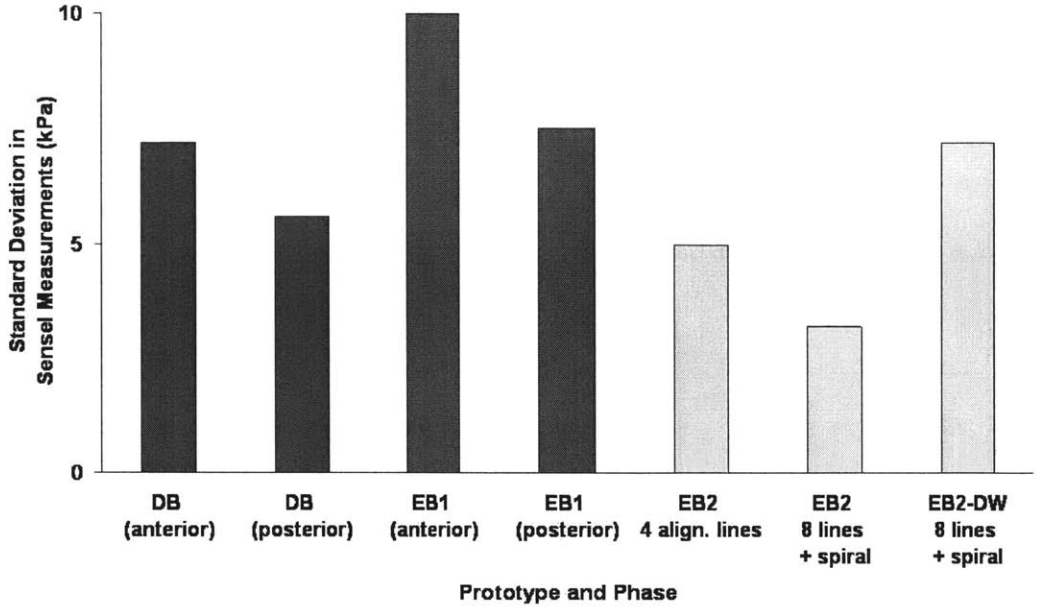

Figure 4-7: Non-uniformity $\overline{s}$ in the pressure distribution generated by the elastic bindings and other MCP prototypes. The labels 'DB', 'EB1' etc are defined in Figure 4-6. Note that the data for DB and EB1 are for one snapshot only, not ten.

Phase II bindings decreased from 0.79kPa (6mmHg) to 0.35kPa (2.6mmHg) when the number of alignment lines increases from four to eight and the alignment spiral was included.

However, these positive results must be interpreted with some caution. First, the pressure measurements for Phase II were performed on a rigid cylinder, rather than on a human calf that the Phase I elastic bindings and detached bands were tested upon. It is almost undoubtedly easier to achieve better performance on a cylinder than a calf because the former has a much simpler shape: the tension necessary in the binding to achieve a uniform pressure distribution on a cylinder is constant, whereas the tension in a binding wrapped on the limb varies proportionately with limb circumference.

It is also difficult to isolate the amount which each of the improvements – improved binding material, use of alignment lines, and the alignment spiral – contributed to the perceived performance improvement, and whether these contributions were additive, multiplicative or otherwise. Quantifying the contributions from each improvement

would require significantly more experimental effort than was possible for this thesis. Despite these concerns, however, the initial Phase II results appear promising, as both $\overline{P}$ and S were almost ideal for the Phase II binding whose target pressure P was 200mmHg.

The target pressure P_t for this Phase was set at 200mmHg only because it was an integer multiple of the 100mmHg target used in the detached bindings development (Section 4.2). In hindsight, P_t should have been increased to the operational 222mmHg target discussed in Section 2.1.2 – as was rectified in the experiments of Chapter 6.

The performance of the double-wrapped Phase II binding ('EB-DW') did not appear to be as impressive, with $\overline{P}$ being 49.9kPa (374mmHg), short of the 53.3kPa (400mmHg) target, and S being 1.48kPa (11.1mmHg), far higher than that of the same binding guided with alignment lines and spirals. However, these results may well have been clouded by poor Tekscan performance since the Tekscan is calibrated to a maximum of 300mmHg (Appendix B). The calibration procedure for the double-wrapped binding used the Appendix B procedure for consistency with the other bindings; the sensor's output beyond 300mmHg applied pressure may therefore not have been accurate.

In light of this, the results of the double-wrapped binding were not as poor as they first appeared as the pressure they generated was nearly double that of the normal "single-wrapped" (alignment lines + spiral, no overlap) bindings, as one would expect. The double-wrapping concept would therefore be potentially useful for situations where it is difficult to generate sufficient pressure using a single wrap – for example, on the largest section of a male thigh, which would otherwise require a very high tension to generate the necessary pressure. It must be remembered, however, that double-wrapping requires a longer donning time than the single wrap and should therefore be employed sparingly.

Uniformity

Figure 4-7 shows that the uniformity of the Phase II bindings was considerably better than that of the Phase I bindings and detached bands. It is particularly encouraging that the Phase II bindings achieved better uniformity than the detached bands, despite the former having a higher target pressure (200mmHg vs 100mmHg for the bands) since, all other things being equal, higher P_t generally results in higher $\overline{s}$. However, these results should again be interpreted with caution because the improved uniformity was achieved on a simple cylinder rather than an irregular calf. Similarly, it is impossible to ascertain the contributions of individual factors that may have caused these improvements (better binding materials, alignment lines, alignment spirals or otherwise).

Despite these caveats, the results are encouraging because $\overline{s}$ for the Phase II bindings was as low as 3.2kPa (24mmHg), far closer to the 1.6kPa (12mmHg) limit of Section 2.1.2 than other prototypes. Furthermore, some proportion of $\overline{s}$ was caused by individual sensel fluctuations, which could be as high as 7% (Section 3.4) – i.e. approximately 15mmHg when the applied pressure is 200mmHg[7] – meaning that the uniformity of the pressure generated by the elastic bindings could very well have been within the 12mmHg limit[8]. These positive results are not dampened by the seemingly poor uniformity of the double-wrapped binding (7.2kPa, 54mmHg) since the latter results should again be interpreted with caution in light of the sensor calibration issues described previously.

Finally, the binding techniques described in this section were developed for use on a simple cylinder – particularly the alignment lines and spirals. Some further work was therefore required to adapt these techniques for the irregular geometry of a human leg, as described in the next section.

[7]Some experiments have provided preliminary evidence to support this estimate [44].

[8]A potential method for accounting for fluctuations in sensel noise could be to measure the deviation $\overline{s}_{uniform}$ produced by a uniform load equal to P_t, as could be done using the calibration rigs of Figures 3-2 and 3-3, and use this to scale the deviation $\overline{s}$ of the test measurement. However, it is not clear what this scaling should be – it is unlikely to be as simple as $\overline{s}_{test} - \overline{s}_{uniform}$ or $\overline{s}_{test}/\overline{s}_{uniform}$.

4.4.7 Adapting the Phase II Elastic Bindings for a Human Leg

Three steps were performed to adapt the binding techniques of Section 4.4.3 to a human calf for the experiments of Chapter 6; for future work these can also be used on the thigh with no modification. The first step involved measuring alignment lines on the irregular leg surface. First, a reference line was drawn on the inner surface of the calf from ankle to knee (Figure 4-8(a)).[9] The calf circumference was then measured at 50mm intervals from the ankle to knee. At each interval, four or eight equidistant points (one for each alignment line used) were marked around the circumference starting from the reference line. Finally, the corresponding points at each interval were joined with a smooth curve (Figure 4-8). As expected, these lines are curved, not straight as the lines on a cylinder would be, because calf cross sections are generally not circular.

In the second step, alignment marks were drawn on the binding as per Section 4.4.3. This time, however, the marks were not equidistant along the entire binding due to the changing leg circumference; as such, the tension F throughout the binding and width b of the stretched binding would also not be constant (Figure 4-9). The changing width implied that the pitch of the alignment spiral would also be non-uniform; however, this change was found to be less than 10% along the length of the calf for all subjects[10]. For the sake of simplicity, the binding width was thus assumed to be constant, making the alignment spiral pitch constant.

The third step was to use standard pantyhose as a "tracing image" to quickly replicate the alignment lines and spirals on the test subject's leg without needing to repeat the tedious measurements of the first two steps (Figure 4-10). After the markings were first measured and drawn on the subject's leg, the pantyhose were donned and the markings traced over. On subsequent experiments, the stockings were re-donned and the marks on the stockings traced over again; the permeability of

[9]The choice to use the inner surface was arbitrary; the reference line could have been drawn along any surface between ankle and thigh.

[10]See the final column of Figure 4-9 as an example for one subject.

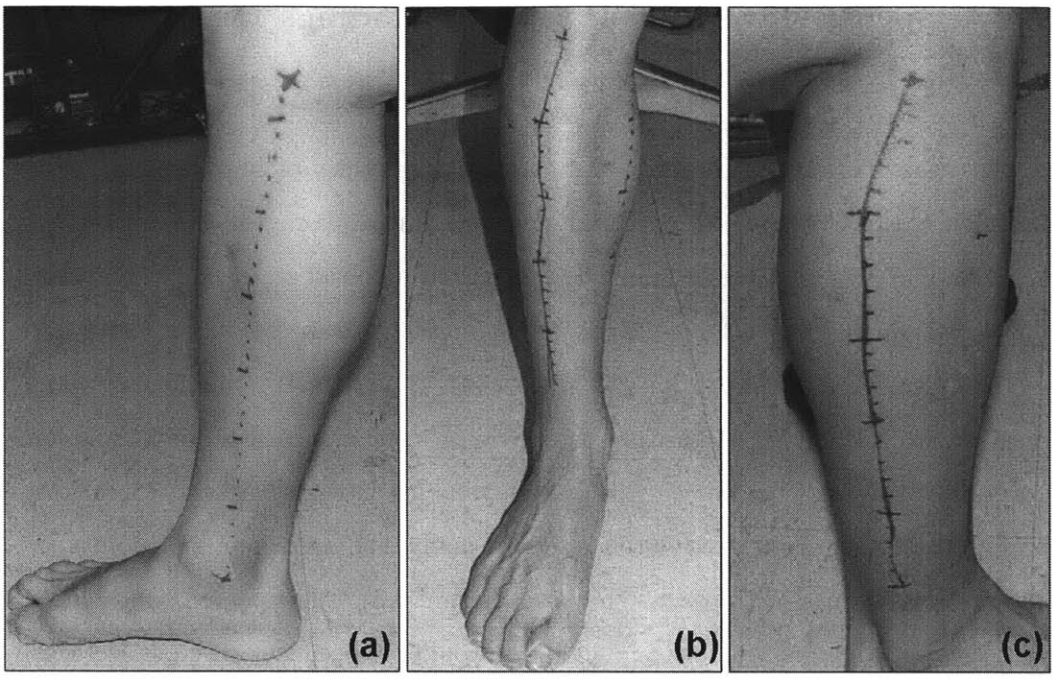

Figure 4-8: (a) Reference line from ankle to knee on inner surface of right calf. (b) and (c) Alignment lines on the front and outer calf surface (see text for full description).

nylon allowed the ink to penetrate easily to the skin. Rather than drawing complete alignment lines and spirals, which would have been inconvenient for the subject to remove after the experiment, a series of dots was drawn in which each dot indicated the intersection between an alignment line and spiral (Figure 4-10). These dots could be used as easily as complete lines/spirals to guide the binding as it was wrapped along the leg.

4.4.8 Summary

The elastic bindings concept fulfilled their objective of achieving faster donning time and increased comfort compared to the detached bands. Furthermore, the Phase II bindings generated a pressure distribution on a test cylinder that was closer to the target pressure, more repeatable and more uniform than that of previous prototypes (detached bands, Phase I bindings) that were tested on the calf. The Phase II bindings were therefore chosen for use in human experiments that measured the phys-

Height above ankle (mm)	Circum-ference (mm)	Required strain (%)	Alignment mark separation (mm)	Binding width (mm)
0	235	70.9	17	29.6
10	230	69.4	17	29.8
20	220	66.3	17	30.1
30	215	64.8	16	30.2
40	210	63.2	16	30.4
50	205	61.7	16	30.5
60	210	63.2	16	30.4
70	215	64.8	16	30.2
80	215	64.8	16	30.2
90	215	64.8	16	30.2
100	220	66.3	17	30.1
110	230	69.4	17	29.8
120	240	72.4	17	29.5

Figure 4-9: Sample spreadsheet used to calculate alignment mark spacing and width changes for elastic bindings. The strain, alignment mark separation and width columns are dependent on the test subject's calf circumference (second column from left) as well as the material properties of the binding (not shown).

iological effects of wearing MCP garments in a low-pressure environment (Chapter 6). The pressure distribution that these bindings generated on the calves of human test subjects (n = 5), rather than test cylinders, is also discussed in Chapter 6. Attempts were made to predict the applicability of the results of this Chapter on the Chapter 6 results by measuring the pressure distribution generated on a soft (foam-filled) cylinder – an "intermediate step" between a rigid cylinder and fleshy calf. However, the calibration procedure for these tests proved difficult, as described in Appendix A, and were therefore discontinued.

Notwithstanding the lack of conclusive results from these soft cylinder tests, the concepts underlying the bindings design are limited by certain assumptions that are likely to affect their performance on a human leg. First, the design assumes that the leg has circular cross sections (Equation 4.2); it does not account for the fact that some areas of the leg are concave (e.g. along the shin) whilst others are sharply

Figure 4-10: Pantyhose used to rapidly replicate the alignment lines and spirals on the leg. Here the subject is preparing for an experiment in the low pressure chamber (Chapter 6) as evidenced by the Tekscan sensor and black-colored chamber seal on the knee.

convex (e.g. along the edge of a flexed calf muscle). Unfortunately, a binding that accounts for these local variations in body curvature would be challenging to design, not only because the alignment marks on the leg and binding would be more complex but also because the leg geometry would have to be mapped with great accuracy even before the bindings are fabricated.

Second, the bindings are passive and do not account for dynamic changes in leg shape that naturally occur with leg movement. There is potential for using active materials to rectify this [13, 4, 10] but these are still in the very earliest stages of development. In November 2005 the MIT Man Vehicle Laboratory received a NASA

Phase 1 Small Business Technology Transfer (STTR) Award to pursue the use of active materials for mechanical counterpressure spacesuits [45], but the research had not begun as of January 2006 and is therefore beyond the scope of this thesis.

Finally, the bindings may cause some discomfort when donned for an extended duration (which was not attempted in the experiments of this Chapter.) The neoprene rubber from which the bindings are made is relatively impermeable and may not allow the wearer's perspiration to be wicked away efficiently. The friction of the bindings against the skin may also be uncomfortable, especially if there is a significant amount of body hair. These discomforts were all observed to varying degrees in the initial calf experiments of this Chapter. The extent to which these limitations cause adverse physiological effects and long-term discomfort is quantified in the human experiments of Chapter 6.

4.5 Hybrid Foot Garment

As described in Section 2.2, hybrid MCP garments have been developed for the hand [2], calf [14] and entire leg [3] with varying degrees of success. Since the fluid pressure within the bladder is uniform and forces the bladder to conform to the shape of the surface against which it is pressed, hybrids are a relatively straightforward means of producing a uniform MCP across complex surfaces such as the hand[11]. Like gas pressure suits, however, the the hybrid must remain as isovolumetric as possible to maximize mobility [3], especially in areas such as the limb where a large range of motion is required. The difficulty in achieving this is the chief reason that the mobility in current and previous gas pressure spacesuits is limited [3].

The elastic-only concepts described in Sections 4.2-4.4 rely on the fact that the limbs are "approximately" cylindrical; they were thus deemed to be inherently too difficult to adapt to the complex geometry of the foot and lower ankle. A hybrid foot garment was therefore developed as a simple, effective means of providing MCP to the

[11] Of course, similar arguments could be made for traditional gas-pressure suits, whose pressure distribution is even more uniform since there is no bladder between the fluid and body surface. This is discussed in more detail in Chapter 2.

foot for the physiological experiments of Chapter 6. Since the foot's range of motion is not as large as that of the knee, pressure-volume work due to foot flexion was predicted to be far less problematic for a hybrid foot than for hybrid limb garments.

Numerous materials and methods were attempted during the development process; the following text describes only the most successful design that was used for all physiological experiments in this thesis.

The garment consists of an inflatable bladder (Figure 4-11(a)) whose outward inflation is restricted by a standard athletic shoe (Figure 4-11(b)). The bladder consists of two XL-size Sealskinz Water Blocker^{TM}socks (Danalco Inc, Duarte CA), one inside the other. These socks are ideal for use as a foot bladder for several reasons. First, their shape naturally conforms to the foot very well; we discovered that the one XL size was suitable for subjects of all foot sizes. Second, the socks are air pressure-tested to more than 1atm (101.3kPa, 760mmHg) overpressure before being released for sale to check for leaks and verify waterproofing. Finally, the sock contains a waterproof membrane seal between ankle and calf; when the membranes of the two socks are sealed together, as described below, the resulting seam is far more air- and water-tight than any other foot bladder fabricated for this project. Note that the inner sock is turned inside-out to allow the two membranes to be sealed together.

A bulkhead fitting (Part No. 5454K85, McMaster-Carr, New Brunswick NJ) is attached to the outer sock (Figure 4-11(a)), just below blue line) and sealed on both sides using flexible Marine Goop sealant (Eclectic Products, Lineville LA) that has sufficient strength and flexibility to maintain an airtight seal despite being repeatedly stretched when the sock is donned or doffed. Finally, the waterproof membranes of the two socks are glued together using Marine Goop. The space between the inner and outer sock thus forms an inflatable bladder.

The bladder is inflated by connecting the bulkhead to an air tube (Figure 4-11(b)) that is open to the atmosphere when the foot garment is used inside the low-pressure chamber (Figure 4-11(c)). Since the bladder is connected directly to atmosphere, the MCP generated by the foot garment is theoretically equal to the (absolute) level of underpressure inside the chamber, as long as the bladder pressure is completely

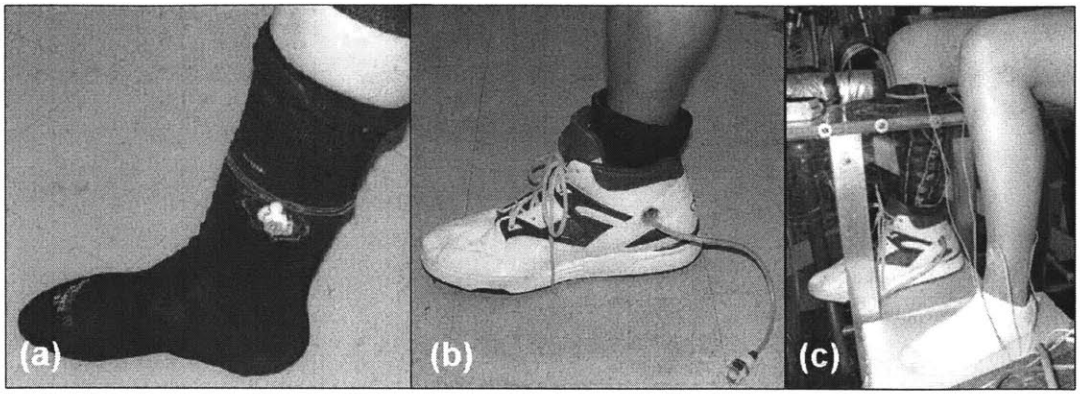

Figure 4-11: (a) Bladder layer of hybrid foot garment with bulkhead fitting immediately below the ankle-height blue line. (b) The bladder layer inside a standard athletic shoe, which acts as the restraint layer. The shoe prevents the bladder from expanding outwards, thus directing the inflation inwards onto the wearer's foot. (c) Hybrid foot garment providing MCP on a test subject's foot during low pressure leg chamber experiments described in Chapter 6 (reproduced from Figure 4-3).

transmitted to the foot, rather than being supported by elastic tension in the bladder walls.

The performance of the foot garment is discussed in Section 6.4.4.

Chapter 5

Review of the Physiological Effects of Spatial Pressure Variations on the Body Surface

5.1 Introduction

As discussed in previous chapters, the pressure applied by MCP garments is unlikely to be uniform across the entire body surface. These spatial pressure variations may cause adverse physiological effects if their magnitude and duration are sufficient. Overpressure may occlude perfusion (blood flow) leading to pressure sores, compartment syndrome and similar effects [42]. On the other hand, the increased perfusion caused by excessive underpressure may result in edema, swelling and blistering. As well as the magnitude and duration of the pressure variation, the type and level of physiological response is also influenced by factors such as the anatomical area, humidity and temperature conditions and the activity of the subject.

This chapter reviews the spatial pressure variations necessary to produce these adverse effects, as well as the mechanisms driving them. The approach of this chapter is somewhat different to previous studies of the physiological effects of MCP suits [12, 1, 6, 7, 46, 8, 9]. that, along with many other studies in the more general field of

lower body negative / positive pressure (LBNP/LBPP) have focused on the effects of over- or under-pressure applied to relatively "large" sections of the body, ranging from a hand or arm to the entire lower body[1].

However, there are no known reports in the literature regarding more *localized* effects within small anatomical areas (e.g. different areas of the hand or calf) caused by spatial variations generated by an MCP garment. Some MCP studies have reported qualitative observations about adverse effects of such localized variations, including swelling and petechiae [1, 5, 7]. However, the magnitude, duration and other factors that influence the occurrence of these effects has not been investigated in detail.

This chapter provides a preliminary review of these localized effects by drawing on medical studies unrelated to spaceflight regarding the effects of localized pressure variations. Both localized overpressure (Section 5.2) and underpressure (Section 5.3) are of medical interest: overpressure because it is a common occurrence in daily life, e.g. for bedridden patients who develop pressure sores; underpressure because it is a useful method for investigating circulatory system mechanisms.

It is important to note, however, the test durations in most of these studies – like many of the aforementioned MCP studies – were too short (less than 10 minutes) to reveal the physiological effects that are likely to occur with longer exposures to pressure variations that an astronaut on a typical multi-hour EVA would experience.

5.2 Localized Overpressure

Introductory reviews [48, 49, 50] state that positive pressures in excess of capillary pressure (12-33mmHg as measured by Landis in 1930 [48]) applied over a sufficient period of time will produce ischemia followed by edema, inflammation, and small vessel thrombosis, followed by necrosis and pressure sores. Even if pressure is initially applied for a time insufficient to produce pressure sores, the capillary dilatation and inflammatory response that it causes make the tissue more susceptible to future

[1]Many of LBNP studies were motivated by the intense interest in using LBNP for spaceflight applications in the 1970s and early 1980s; see [47] for a review.

ulceration from lower pressures.

The most common situation in which these effects occur is in bedridden patients whose points of contact with the bed must support their body weight for days or even weeks at a time. However, the sores can also develop in shorter time periods with the application of sufficient force. There is an inverse relationship between the amount of pressure applied and the length of time of application in the production of pressure sores, although a low pressure maintained for a long period of time generally produces a greater damage than high pressure applied for a short period.

Shear forces and friction against the skin are also important cofactors as they help to diminish or eliminate perfusion; in fact, the degree of pressure necessary to reduce perfusion could be almost halved when accompanied by a sufficiently high level of shear. Humidity and lack of evaporation are also factors that increase predisposition to the adverse effects of overpressure. It is important to note that these factors were observed to various degrees in the elastic bindings experiments of Section 4.4.8 as well as Chapter 6.

The following studies provide more detailed insight into the mechanisms of localized overpressure; however, most do not apply pressure for a sufficient time to produce adverse effects such as pressure sores. The pressure regimes applied by these studies is summarized in Table 5.1.

Patel et al [49] examined the effect of temperature and pressure increases in the skin perfusion of rats. They found that at constant temperature, skin perfusion *increases* at <18mmHg overpressure[2] but decreases to zero at 73mmHg, while perfusion increases with temperature below 73mmHg. This is significant for MCP garment design because it suggests temperature control could be used to increase perfusion on areas of local overpressure to delay the onset of pressure sores. However, this beneficial effect must be balanced against the increasing nutritional requirements of the underlying tissue, as discussed in the paper.

Nola and Vistnes [48] investigated the differences in pressure regimes necessary to develop pressure sores on skin and muscle by applying up to 110mmHg overpressure

[2]This may be partially due to sensor noise [53].

Authors	Research Topic	Over-pressure (mmHg)	Duration (min)
Patel et al (1999) [49]	Temperature and pressure effects on skin perfusion in rats	73	3
Nola and Vistnes (1980) [48]	Differential response of skin and muscle in pressure sore development	110	6hr/day for 4 days
Stolk et al (2004) [51]	Changes in MCP produced by medical compression stockings during walking	30*	(Not specified)
Mann et al (1997) [26]	Glove and sleeve pressure garments	8-35	0.5
Hooper and Jones [52]	Interface pressure at shoulder of men carrying rucksacks	75	3
Schubert and Fagrell (1989) [50]	Effect of local pressure on skin microcirculation at the sacrum and gluteus muscles	110	0.5**

Table 5.1: Summary of overpressure studies reviewed in this section. *Note: Garments are designed to provide 30mmHg; actual pressure not measured **With 5 minutes of pressure ramp-up and ramp-down.

on small "bony" and "fleshy" areas of skin on rats. They found that pressure regimens that consistently produce ulcers over bony pressure points produce considerably less ulceration if a muscle flap lies between skin and bone. All else being equal, it is therefore more important to minimize the pressure variations produced by an MCP garment on bony areas such as the shin, than on fleshy areas such as the calf posterior.

Stolk et al [51] measured the changes in MCP produced by medical compression stockings during walking. They noted a considerable difference between the pressure of medical compression stockings at rest and walking in areas where muscle movements occur. For example, a muscular region such as the upper calf that experiences 30mmHg static pressure at rest could be subject to 10-50mmHg when walking. This confirms the prediction of Section 4.4.8 that an MCP suit would need to actively change its shape or material properties to provide uniform MCP while the user is walking or performing other activities that utilize large muscle groups.

Mann et al [26] used I-Scan sensors to measure the pressure distribution generated by glove and sleeve pressure garments used on burn victims. They discovered that

local pressures in garments whose design pressure is between 20 and 30mmHg deviate up to ±33% (±10mmHg) from the design pressure. According to Carr [53], such small absolute variations may be acceptable as the variations are within the capillary oncotic pressure; however, 33% variations in an MCP garment at the operational pressure of 222mmHg (Section 2.1.2) are likely to cause physiological effects if applied for multi-hour durations, as in a typical EVA.

Hooper and Jones [52] used also used I-Scan sensors to measure the interface pressure on the shoulder of men carrying heavy army rucksacks. They stated, but did not demonstrate, that a continuous 100mmHg applied to the shoulder when carrying a rucksack for sustained periods may cause tissue damage at the shoulder. Based on the other aforementioned studies, this appears to be an obvious conclusion from a paper whose methods and results were unrigorous.

Finally, Schubert and Fagrell [50] measured the effect of local pressure on skin microcirculation at the sacrum and gluteus muscles. They found that perfusion increases over the sacrum at 12-50mmHg but decreases to 43% below initial value at 110mmHg. Perfusion is more stable in gluteus section and is at a maximum at 13-60mmHg. Furthermore, skin temperature increased by 3° C during the overpressure regimen.

The results concur with those of Patel et al [49] which demonstrated low levels of overpressure counterintuitively increase blood flow, and with Nola and Vistnes [48] which demonstrated that it is easier to produce pressure sores on bony areas than muscular areas. The implications of this study for MCP garment design are therefore identical to [49] and [48], as described above.

5.3 Localized Underpressure

There are comparatively few studies regarding the physiological effects of localized underpressure because, unlike localized overpressure, it rarely occurs in everyday life. The motivation for most underpressure studies has been to use it to study the circulatory system by altering the local vascular transmural pressure without

significantly affecting the remainder of the circulatory system [54].

Wolthuis et al [55] note that low levels of localized underpressure actually reduce perfusion because the initial arterial dilation (and thus increased bloodflow) caused by the pressure decrease is compensated by a local sympathetic reflex that constricts the arteries; however, the mechanism behind this constriction is still uncertain [7]. At higher levels of underpressure perfusion increases above baseline levels because the arterial walls are unable to overcome the dilatation caused by the underpressure.

The pressures at which these responses occur depends on both the underpressure level and the anatomical area. In particular, the blood vessels in the legs are able to compensate for the dilatory effects of underpressure more readily than in other parts of the body, perhaps because their length and vertical distance from the heart naturally conditions them to withstand pressure variations [53]. This is important for MCP garment development because it suggests that pressure variations that can be tolerated by the leg may not necessarily be tolerated on other parts of the body.

The following studies provide more detailed insight into the mechanisms of localized underpressure; again, most do not apply pressure for a sufficient time to produce adverse effects. The underpressure regimes applied by these studies are shown in Table 5.2.

Authors	**Research Topic**	**Under-pressure (mmHg)**	**Duration (min)**
Lundvall and Lanne (1989) [54]	Transmission of negative skin pressure into underlying upper arm tissues	-50	<0.5
Skagen and Hendriksen (1982) [56]	Changes in perfusion due to localized underpressure on healthy patients	-250	6-10
Lasheen et al (2004) [57]	Human burn victims – pre-operative tissue expansion using negative pressure	-150	10hr a day*

Table 5.2: Summary of underpressure studies reviewed in this section. *For 2-3 weeks prior to surgery.

Lundvall and Lanne [54] studied the transmission of negative skin pressure into underlying upper arm tissues, finding that negative skin pressure is transmitted al-

most entirely into the underlying tissue regardless of position, tissue depth or pressure level. That is, reduction in atmospheric pressure leads to similar alteration of vascular transmural pressure. This provides a strong incentive to minimize the occurrence of underpressure in an MCP suit because underpressure may have adverse effects not only near the skin but also in internal tissue.

Skagen and Hendriksen [56] used a 40mm diameter "sucking glass" to measure changes in perfusion due to localized underpressure on the forearm of healthy patients. They found that transmural resistance increases up to 85% and blood flow decreases by 43% at -40mmHg underpressure but does not significantly increase between 40-250mmHg. This is surprising because it suggests that -250mmHg localized underpressure in an MCP garment is no worse than -40mmHg – which strongly defies expectations. Further investigation is required to verify these results and confirm their relevance to MCP garment design requirements.

Lasheen et al [57] demonstrated the use of negative pressure "suction cups" on the wounds of burn victims prior to surgery, applying a extremely strong level of underpressure for lengthy periods (-150mmHg, 10 hours a day for 2-3 weeks prior to surgery). In doing so, they discovered that the negative pressure considerably expanded tissue and improved wound closure prior to burn wound excision surgery but does not eliminate the need for Z-plasty. Some blisters occurred at higher negative pressures, as well as bruising around the seal site. At first glance, the relevance of this paper to MCP garments seems questionable as one would never expect such a regimen to occur in an MCP suit, unintentionally or otherwise; additionally, the findings apply to burn wounds rather than healthy skin. However, the paper provides strong evidence that exposures to underpressure can cause significant changes in local body shape and composition, which may not necessarily be a disadvantage in an MCP suit: the underpressurized area may swell against the suit and thus increase the applied MCP until the underpressure disappears [53]. Even so, excessive underpressure will cause blister and bruising, as described in the paper.

5.4 Discussion

These medical studies provide some insight into the mechanisms behind the physiological effects of spatial pressure variations. However, they do not provide sufficient data to develop a quantitative model to describe the magnitude and duration of the pressure regimens necessary to induce adverse physiological effects in MCP suits used in planetary EVA. The magnitude and duration of applied pressure for some studies was so great – far higher than would be expected in any operational MCP garment – that adverse effects were inevitable [48, 57]. On the other hand, the duration of most other studies was short – less than 15 minutes – so that no *adverse* physiological effects were noted: all studies induced some physiological effects, but these were not maintained for sufficient duration to be detrimental. Had the over-pressure regimens of Patel et al [49] or Schubert and Fagrell [50], for example, been maintained, adverse effects such as pressure sores are likely to have resulted.

It is thus difficult to directly utilize the results of these studies to define acceptable limits for the magnitude and duration of the localized pressure variation in an MCP garment. To rectify this, experiments in which spatial pressure variations typical in an MCP garment (perhaps up to $\pm$100mmHg, based on the initial work of Chapter 4) are applied to localized body areas (e.g. a small 40mm diameter patch, as done by Skagen et al [56]) for various durations up to several hours, the duration of a typical EVA. The ultimate result from such experiments would be curves that quantify the relationship between the time and duration necessary to develop adverse effects such as pressure sores or edema. Factors such as friction, humidity, skin temperature and so on would have to be carefully controlled. Unfortunately, the complexity of such experiments are well beyond the scope of this thesis.

Nevertheless, the next chapter qualitatively confirms some of the results of this review, and provides rough first-order *experimental* estimates regarding acceptable limits for pressure variations in an MCP garment.

Chapter 6

Physiological Experiments

6.1 Introduction and Motivation

The elastic bindings described in Chapter 4 demonstrated rapid donning time, increased comfort and evidence of a more uniform pressure distribution than other Bio-Suit leg prototypes. Their performance was thus deemed sufficient to be tested on human subjects – not only to determine their comfort and pressure distribution, as done in Sections 4.2 and 4.3, but also to ascertain whether the bindings could fulfill their primary objective of protecting the wearer's leg from the effects of underpressure[1] that would otherwise occur during an EVA performed by an unsuited astronaut.

This chapter therefore describes experiments in which five subjects wore the elastic bindings on one calf, and exposed the calf to underpressure in a low pressure leg chamber for more than one hour[2]. Following the methodology of Tanaka et al [9, 7] and Tourbier et al [6], two phases of experiments were performed. The first phase measured the physiological effects induced by exposing *unsuited* (unprotected) calves to underpressure . The results were then used as a base from which to compare the results of the second phase, in which *suited* (protected) calves were exposed to underpressure. All experiments were approved by the MIT Committee on the Use of

[1] In this context "underpressure" refers to the vacuum of space or the lunar surface, or the near-vacuum environment of Mars, rather than the spatial pressure variations discussed in Section 5.3.

[2] For this thesis there was insufficient time to extend the experiments to the entire leg.

Humans as Experimental Subjects (COUHES).

6.2 Methods and Materials

6.2.1 Subjects

Three male and two female subjects were employed (Table 6.1). Subjects who smoked or who had any history of systemic disease or injury in their leg were excluded. In accordance with COUHES, informed consent was obtained from all subjects prior to participation.

Subject	Gender	Height (cm)	Calf length (cm)	Calf Circ* (cm)	Weight (kg)
0	M	170	38	35	63
1	M	183	41	44	86
2	F	157	36	35	52
3	F	169	39	35	60
4	M	188	40	37	80

Table 6.1: Subject characteristics. *Calf circumference in ambient conditions.

6.2.2 Phase I – Unsuited Calf

First, the subject donned a heart rate monitor (Acumen TZ-Max100, Sterling, VA), a blood pressure cuff (Omron HEM-711, Bannockburn, IL) on the left upper arm, and four skin temperature sensors (Pasco PS-2135 Fast Reponse Temperature Probes, Roseville, CA) – one on the shin (anterior) and one on the posterior of each calf (Figure 6-1).The subject wore the hybrid foot garment (Section 4.5) to provide MCP on the right foot[3].

The subject than sat with his/her right calf[4] in a custom-built low pressure leg chamber (Figure 6-1 and Appendix I of [3]). Foam blocks were placed under the

[3]As discussed in Section 6.1, the main purpose of this study was to ascertain the capability of the elastic bindings in protecting the calf from the effects of underpressure. Since the bindings do not cover the foot, the subject wore the hybrid foot garment to remove the potential effects of underpressure on the foot in both unsuited calf and suited calf phases.

[4]The choice to place the right, rather than lef, calf inside the chamber throughout the experiments of this chapter was arbitrary.

subject's feet to ensure a comfortable sitting position and to maintain both feet at an equal height.

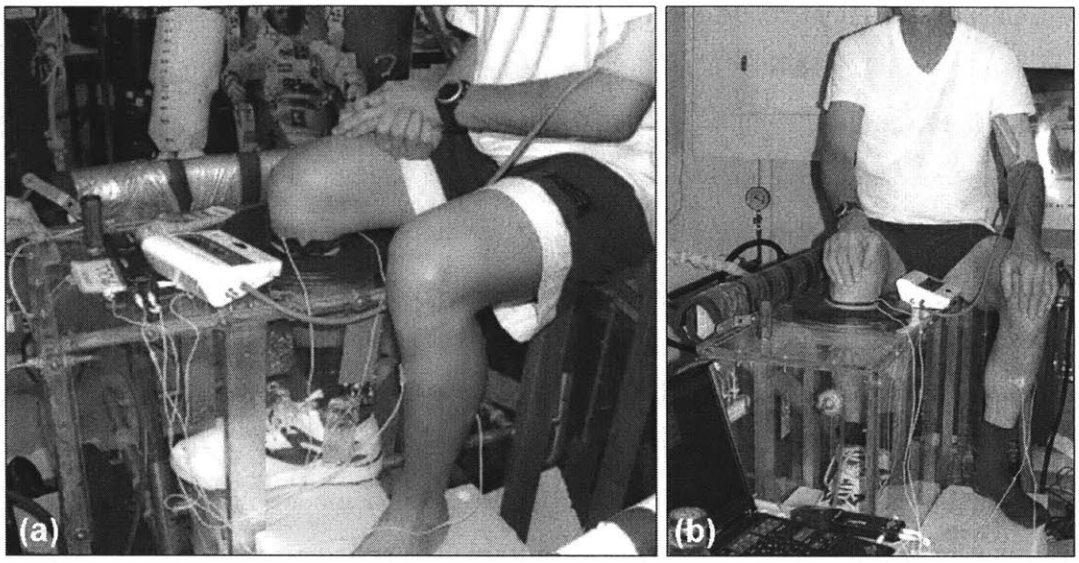

Figure 6-1: (a) Side view of subject with unsuited right calf exposed to underpressure inside the low pressure leg chamber. The subject is wearing a blood pressure cuff (left arm), heart rate monitor (with data-logging watch on left wrist), temperature sensors on the front and back of the calf on both lefts (white wires) and the hybrid foot garment, as described in the text. (b) Front view of the setup shown in (a).

After the subject was settled, six minutes of baseline physiological measurements were recorded with the chamber at ambient pressure. Heart rate and skin temperature were recorded once every five seconds; blood pressure and subject discomfort every two minutes. The discomfort was measured on a subjective scale of 0-5, with 0 being the (lack of) discomfort at ambient conditions and 5 being discomfort sufficiently high for the subject to terminate the test. The subject was instructed to speak as little as possible, especially during blood pressure measurements to minimize confounding fluctuations in the physiological response; as such, the subject did not announce discomfort every two minutes but only announced any changes in discomfort, based on the 0-5 scale, as the changes occurred.

After the six minute baseline measurement at ambient pressure, the chamber pressure was lowered in -25mmHg steps every six minutes (Figure 6-2.) These steps were small compared to the 50-150mmHg increments used by Tanaka et al [9, 7]

and Tourbier et al [6] and was intended to minimize any potential "shock effects" caused by suddenly applying large pressure changes[5]. Physiological and subjective measurements continued to be recorded at the previous sampling rates. The test concluded either at the subject's request or at the discretion of the test observers by immediately returning the chamber to ambient pressure.

Physiological data was analyzed using SYSTAT 11 (Point Richmond, CA) for significance in a linear regression model with the chamber pressure being the most important independent variable. Regression, rather than repeated measures ANOVA, was chosen because the number of data points per cell varied considerably[6] [58] and also because the data generally did not satisfy the homoscedasticity and normality conditions necessary for ANOVA. Significance was set at $p < 0.05$.

Both single-variable ("single") and multiple regression models were calculated, the latter using the subject characteristics of Table 6.1 as independent variables in addition to chamber pressure. However, the main objective of this study was to quantify the effect of chamber pressure on the physiological response; furthermore, the number of subjects was insufficient to yield meaningful multiple regression results. As such, the multiple regressions were largely used to verify the results of the single regressions.

6.2.3 Phase II – Suited Calf

An elastic binding designed to generate 30kPa (225mmHg) counterpressure – the gas pressure inside the Space Shuttle EMU (Section 2.1.2) – was custom-made for the subject according to the methods of Section 4.4.7. The subject donned a heart rate monitor, blood pressure cuff, four temperature sensors and the hybrid foot garment as before. Before entering the chamber, six minutes of baseline physiological measurements were recorded at ambient conditions with the subject in a normal sitting position identical to that used for the low pressure chamber (Figure 6-1).

[5] Anecdotal experience with the low pressure chamber suggested that subjects could tolerate a larger magnitude of underpressure if applied gradually rather than suddenly.

[6] Each subject chose to end the test at different pressure levels; the number of data points therefore varied between subjects.

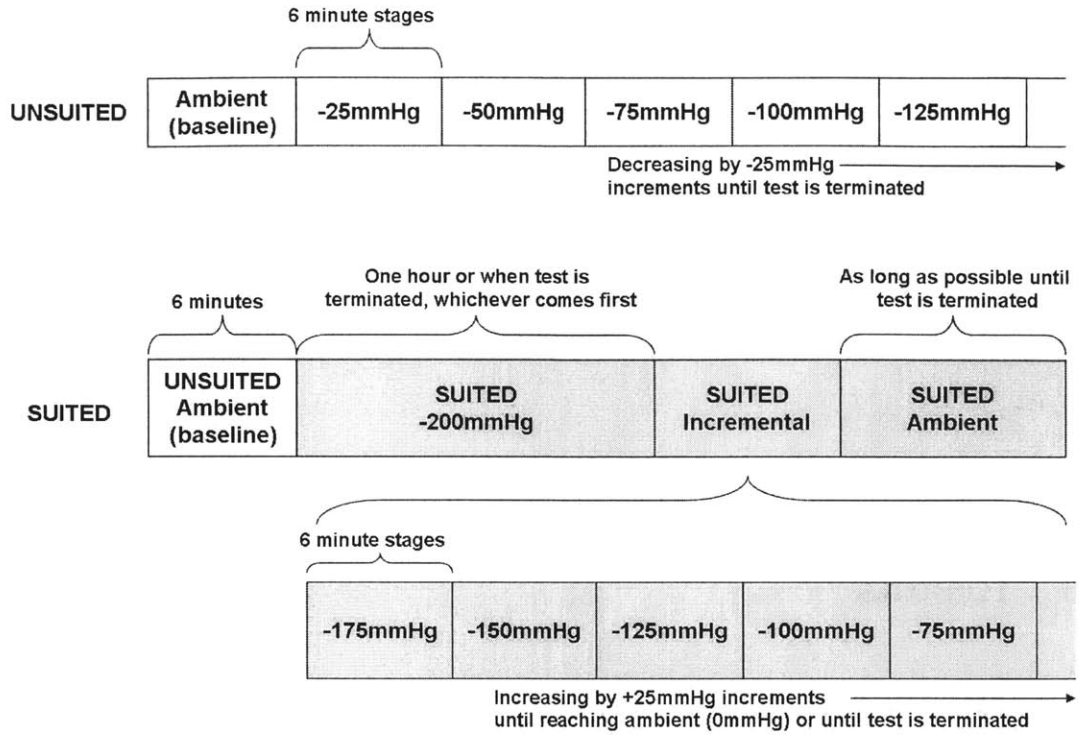

Figure 6-2: Protocol for the unsuited and suited experiments described in this chapter.

A Tekscan I-Scan 9801 sensor was then attached to the subject's calf anterior, as done in Sections 4.2 and 4.3. The subject donned the elastic bindings and placed his/her calf in the low-pressure leg chamber as before (Figure 4-3(b) in Chapter 4). The chamber pressure was immediately lowered to -225mmHg, the MCP the bindings were designed to produce, to minimize the time that the subject had to endure with overpressure on the bound calf.

Once the chamber pressure reached -225mmHg and subject was settled, physiological measurements and subjective discomfort began to be recorded as before. I-Scan pressure measurements were also recorded every 20 minutes[7]. This state, in which the chamber underpressure matched the design MCP of the elastic bindings, was maintained for up to one hour unless terminated at the request of the subject or discretion of the test observers (Figure 6-2).

[7]Since the in-chamber calf was stationary, the pressure distribution generated by the bindings was assumed to be relatively stable and was therefore not recorded with the same frequency as the other measurements.

After this first hour, the chamber pressure was increased in +25mmHg steps every six minute intervals, the purpose being to investigate the effects of *over*pressure (since the MCP generated by the bindings should then be higher than the chamber underpressure). As before, small (+25mmHg) pressure increments were employed to minimize shock effects. The test concluded either at the subject's request or at the discretion of the test observer. As before, data was analyzed using SYSTAT 11 for significance in single and multiple linear regression models with significance set at $p < 0.05$.

6.3 Results

6.3.1 Test Duration and Subject Discomfort

Figure 6-3 shows the duration of the unsuited and suited tests performed according to the protocol of Figure 6-2. Subjects spent up to 57 minutes and experienced up to -225mmHg with their unsuited calf in the chamber (Figure 6-4) while the suited tests extended as long as 92 minutes with the subjects experiencing a range of pressure levels from -225mmHg, the MCP that the bindings were designed to generate, to -13.3kPa (-100mmHg, Figure 6-5).

6.3.2 MCP generated by Bindings on the Calf Anterior

Following the notation of Section 4.4.5, Figure 6-6 shows the series average pressure $\overline{P}$, standard deviation of the average pressure S and the "non-uniformity" $\overline{s}$ for the pressure distribution generated by the bindings on the calf anterior during the suited tests described in this chapter. Across all subjects, the bindings generated an average pressure $\overline{P}$ of 23.8kPa (179mmHg) with S being as high as 5.4kPa (41mmHg). The average $\overline{s}$ across all subjects was was 8.7kPa (65mmHg).

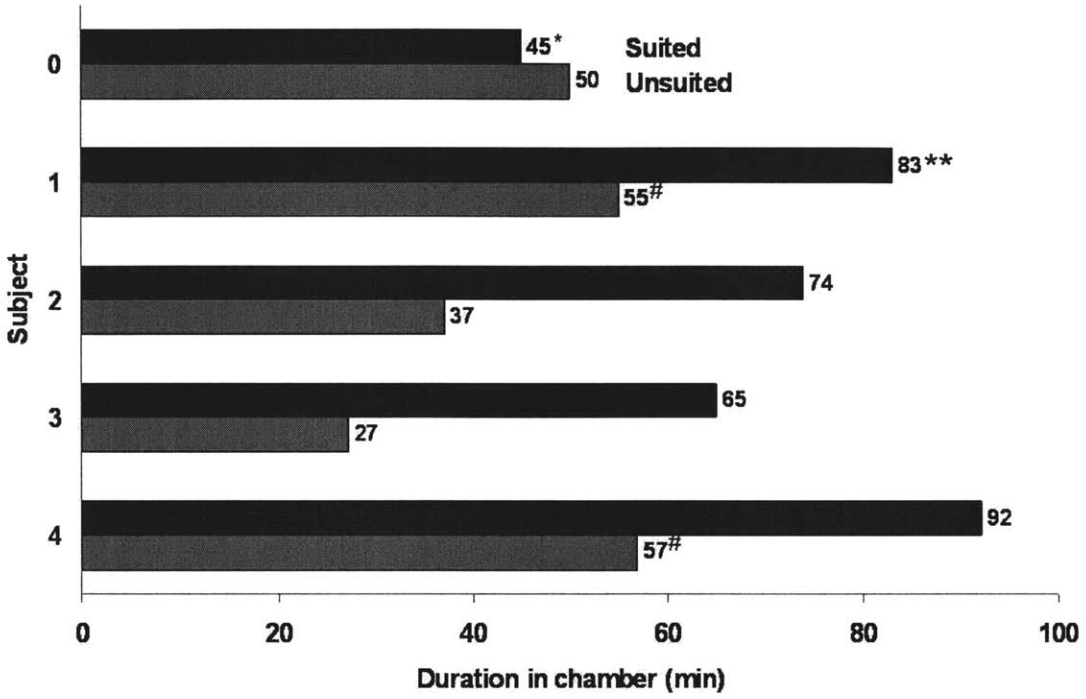

Figure 6-3: Test duration by subject and phase. All tests were terminated at the subject's request unless stated. *Subject terminated test early due to gradual loss of pressure in MCP foot garment. **Observer terminated test due to uncertainty regarding the condition of the suited calf. It was feared that since the subject had a very high pain threshold, he might not report any feelings of discomfort sufficiently early to prevent potential adverse effects. In this suited experiment, the calf could not be observed as it was concealed from view under the elastic bindings; the test observer therefore terminated the test as a precautionary measure, despite the subject's insistence that he felt fine (as indicated by the low level of discomfort). #Test observer terminated test after observing swelling or slight blistering on the calf inside the chamber.

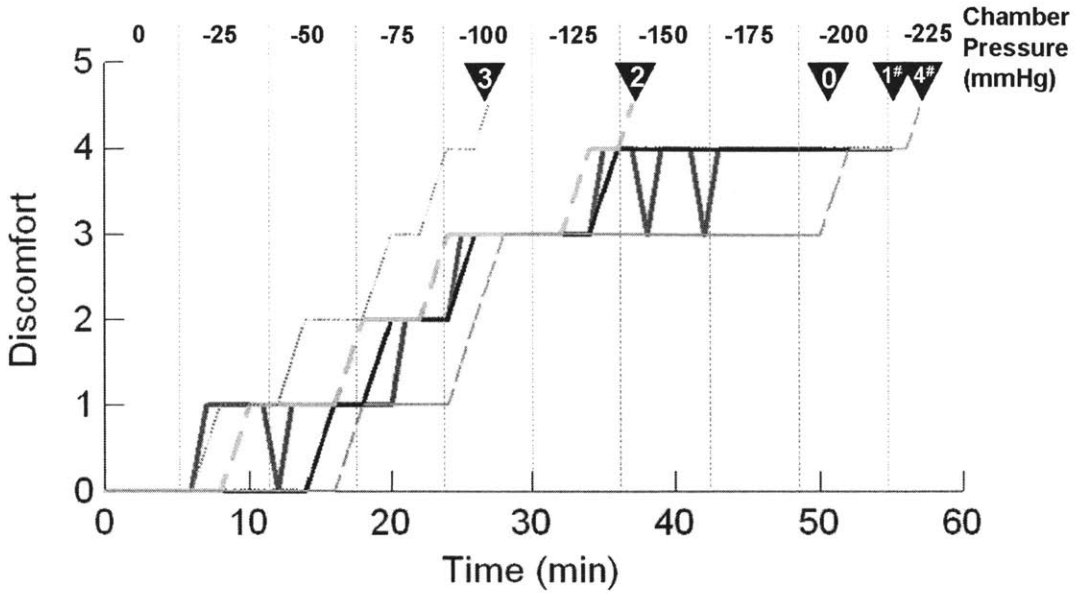

Figure 6-4: Subjective discomfort in **unsuited** tests. Black triangles marked with subject number (0-4) indicate the point at which that subject's test terminated. All tests were terminated at the subject's request unless stated. #See note in Figure 6-3.

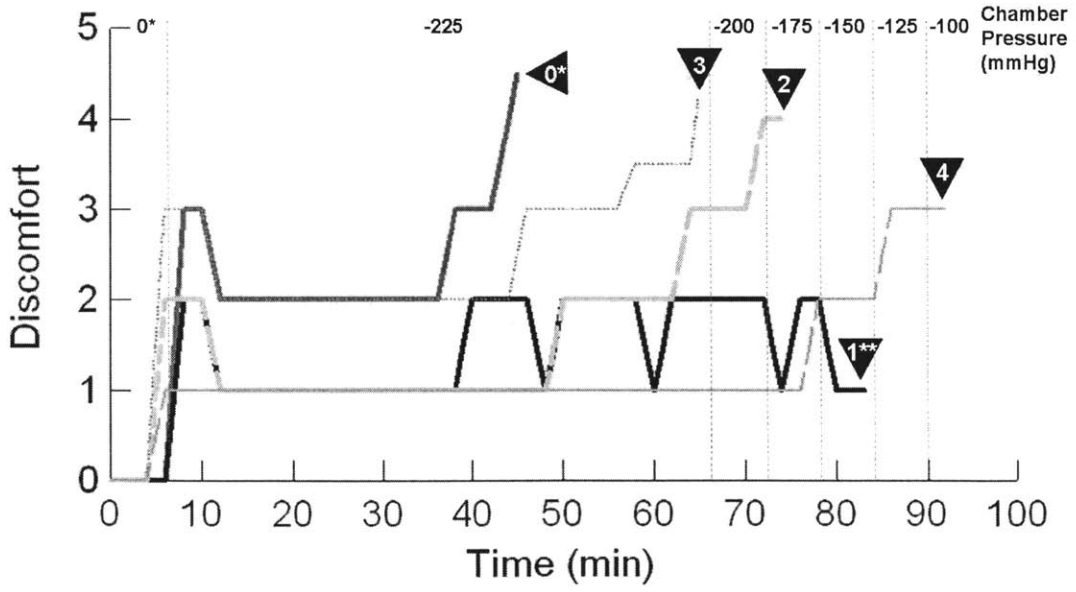

Figure 6-5: Subjective discomfort in **suited** (Phase II) tests. Black triangles marked with subject number (0-4) indicate the point at which that subject's test terminated. *See note in Figure 6-3. **See note in Figure 6-3.

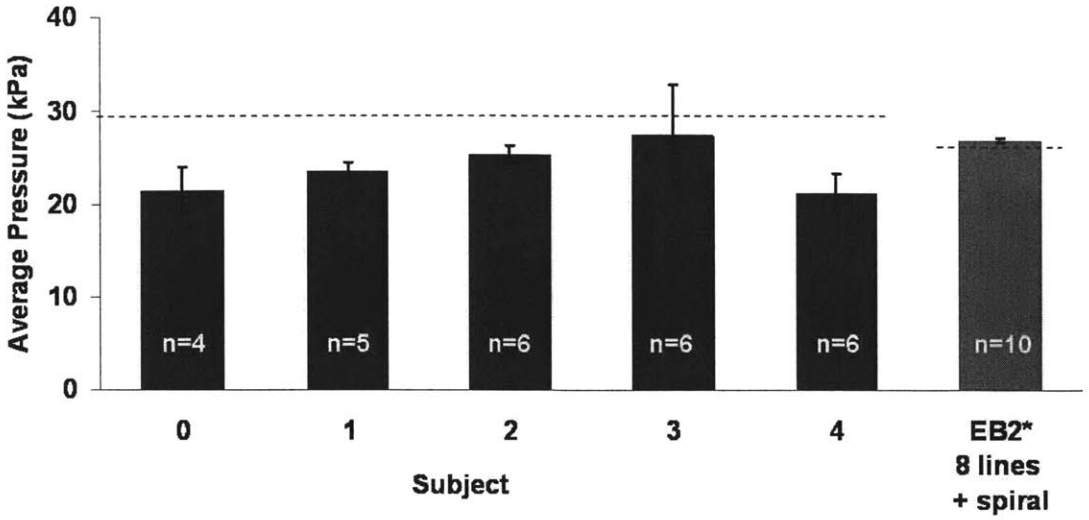

Figure 6-6: Series average pressure $\overline{P}$ generated by elastic bindings on the calf anterior during suited tests, by subject (blue bars). The pressure generated by the bindings on rigid test cylinders is reproduced from Figure 4-6 for comparison (red bars). Error bars show standard deviation S of of the average pressure. Numbers within bars show the number of pressure snapshot measurements used to calculate $\overline{P}$ and S. Dotted lines indicate the target MCP P_t to which the bindings were designed; the 30kPa (225mmHg) target for the bindings used by the test subjects is equal to the gas pressure inside the Space Shuttle EMU.

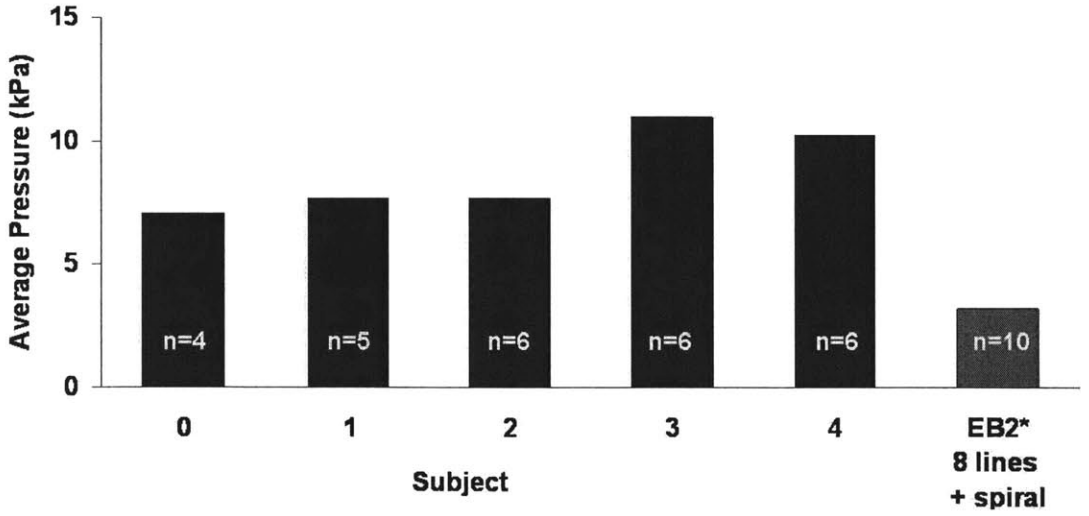

Figure 6-7: Series standard deviation $\overline{s}$ in the pressure distribution generated by elastic bindings on the calf anterior during the suited tests, by subject (blue bars). $\overline{s}$ for the pressure generated by the bindings on rigid test cylinders is reproduced from Figure 4-7 for comparison (red bars). Numbers within bars show the number of pressure snapshot measurements used to calculate $\overline{s}$.

6.3.3 Physiological Measurements

Figures 6-8 to 6-17 show the changes in heart rate, blood pressure and skin temperature during the unsuited and suited tests respectively, normalized or zeroed to the baseline measurements at ambient conditions (0mmHg chamber pressure) during the first six minutes of each test (as described in Figure 6-2.) All figures show the average $\pm$ standard error of five subjects.

The statistical significance results quoted below are the *effect of chamber pressure on the parameter of interest.* The results of the single regression were verified using multiple regression models, as discussed in Section 6.2.2. At no point did the single regression results contradict those of the multiple regressions.

It is extremely important to emphasize that these figures only show the average response of the five subjects – for some parameters, particularly skin temperature, *the response of individual subjects differed considerably from the average.* In some cases, this difference was so great that the exclusion of a single subject from the data set affected the statistical significance. These results in this section should therefore be interpreted with caution. All known cases in which the exclusion of a single subject affected statistical significance are described.

Heart rate

There was no significant change in heart rate during any unsuited or suited experiments (Figures 6-8 and 6-9).

Blood pressure

There was a significant increase in both systolic and diastolic blood pressure during unsuited exposure to underpressure ($p < 0.05$, Figures 6-10 and 6-12 respectively) but no change during suited exposure (Figures 6-11 and 6-13 respectively). In this non-significant result the diastolic pressure of Subject 1 during the suited test was deliberately excluded from the regression model [58] as it appeared considerably different from that of other subjects (Figure 6-14) – so much so that the diastolic pressure

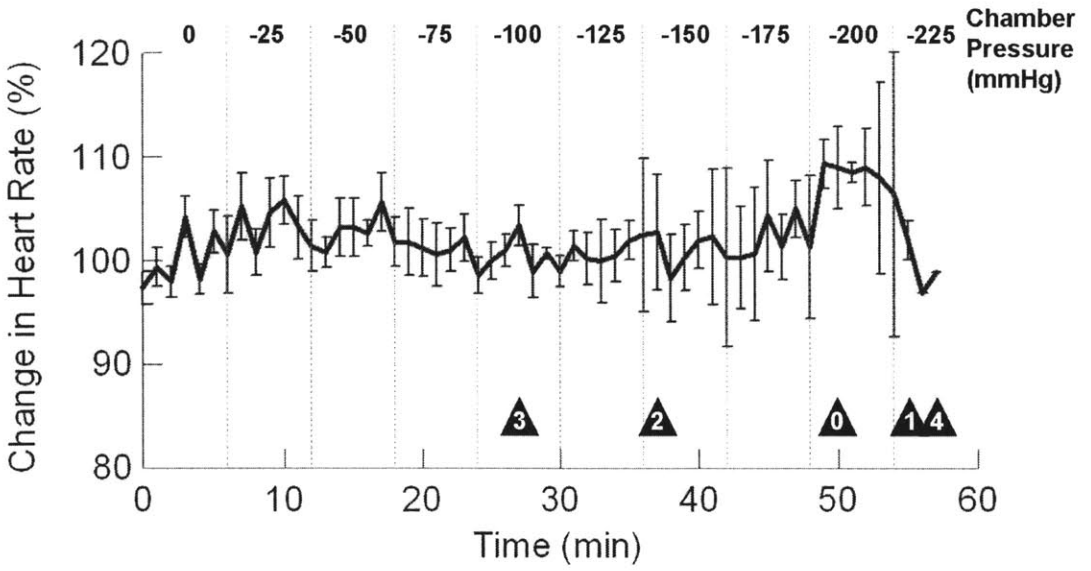

Figure 6-8: Change in heart rate during **unsuited** tests, normalized to baseline heart rate during ambient conditions. Black triangles indicate test termination point for the individual subject, as before.

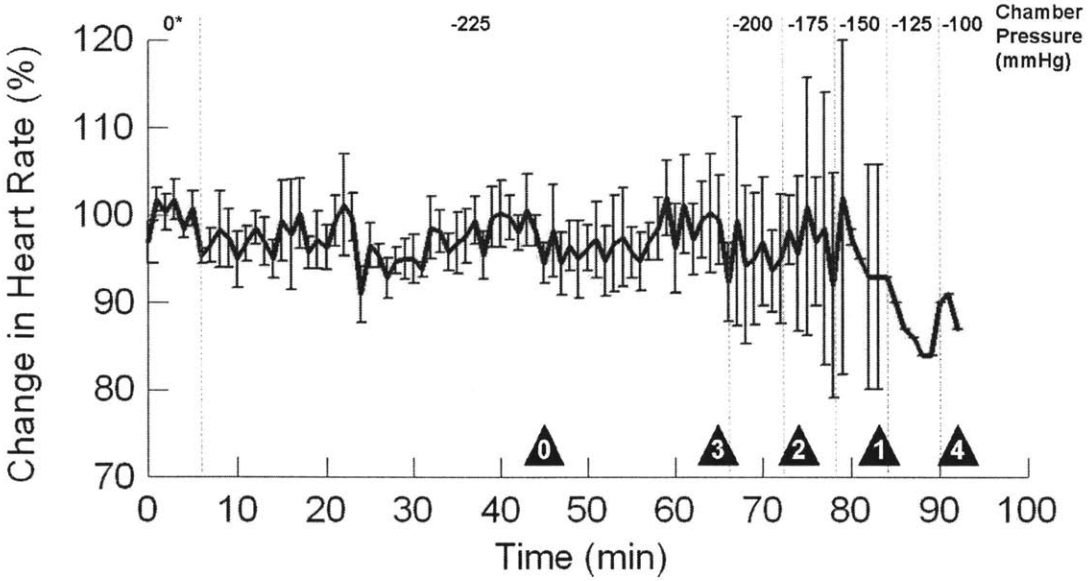

Figure 6-9: Change in heart rate during **suited** tests, normalized to baseline heart rate during ambient conditions. Black triangles indicate test termination point for the individual subject, as before. *Baseline measured on *unsuited* subject, as discussed in text.

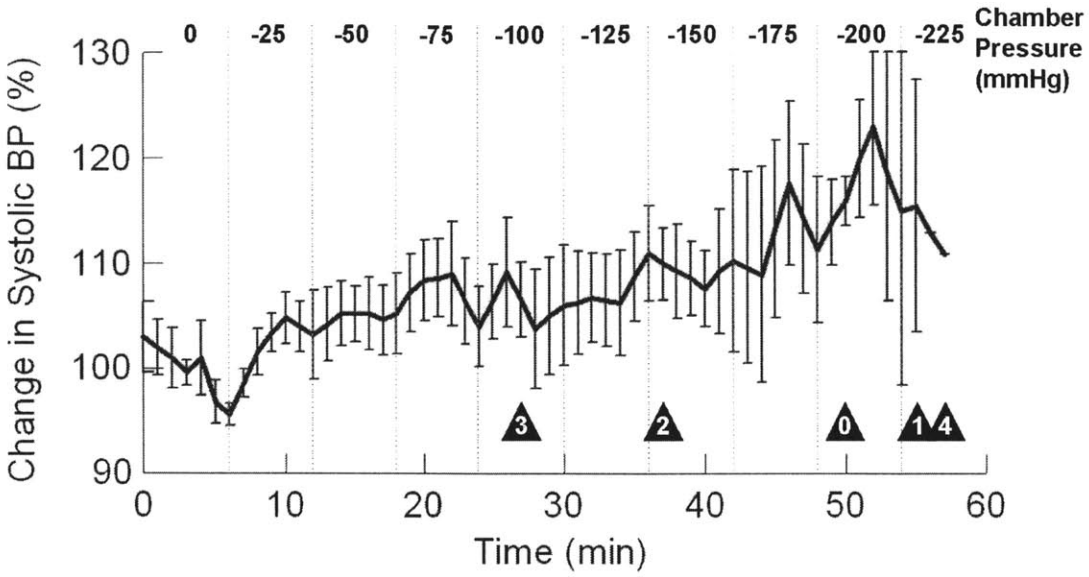

Figure 6-10: Change in systolic blood pressure during **unsuited** tests, normalized to baseline pressure during ambient conditions. Black triangles indicate test termination point for the individual subject, as before.

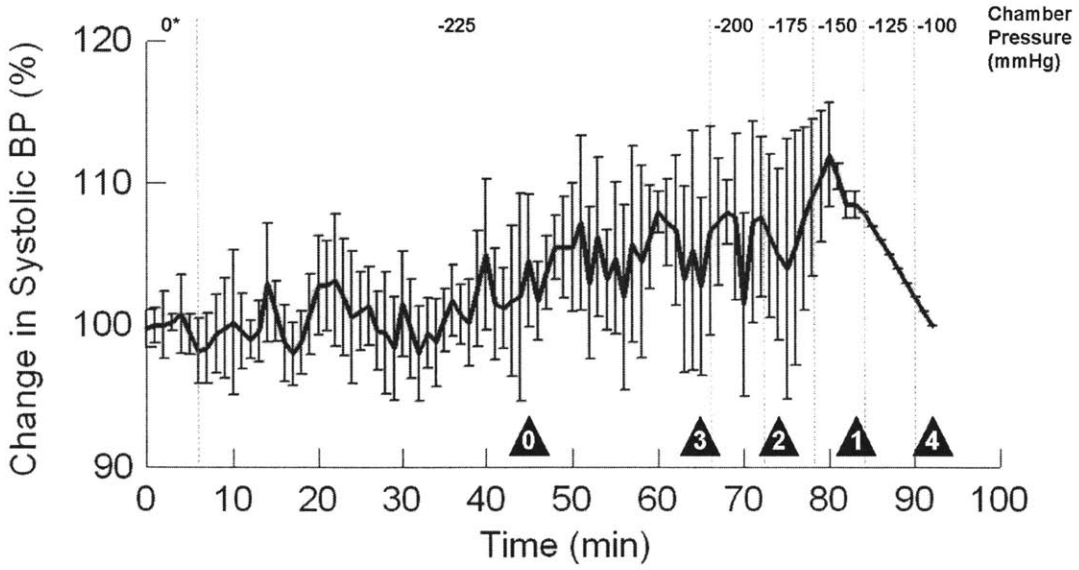

Figure 6-11: Change in systolic blood pressure during **suited** tests, normalized to baseline pressure during ambient conditions. Black triangles indicate test termination point for the individual subject, as before. *Baseline measured on *unsuited* subject, as discussed in text.

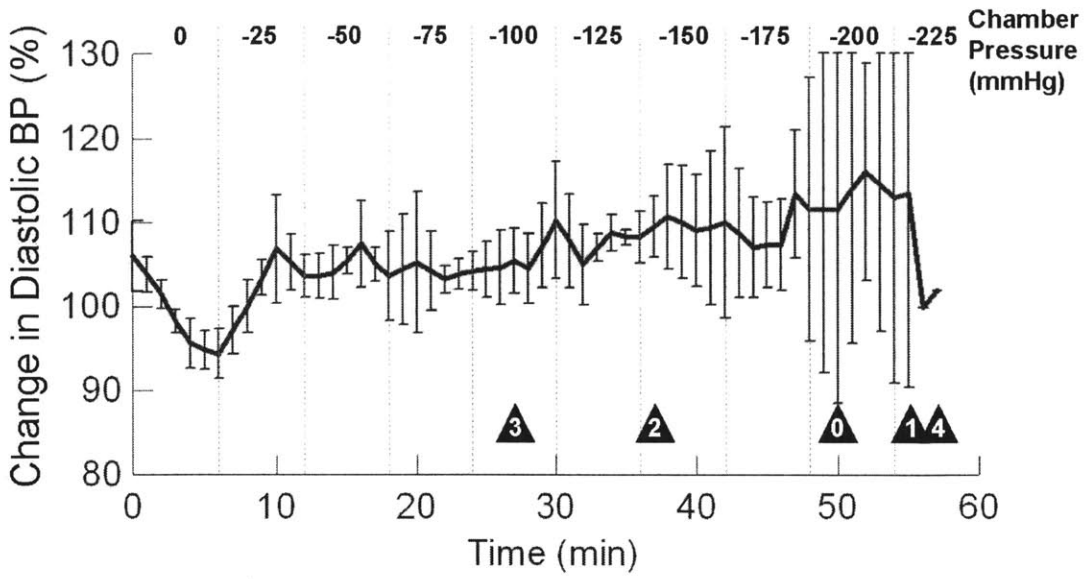

Figure 6-12: Change in diastolic blood pressure during **unsuited** tests, normalized to baseline pressure during ambient conditions. Black triangles indicate test termination point for the individual subject, as before.

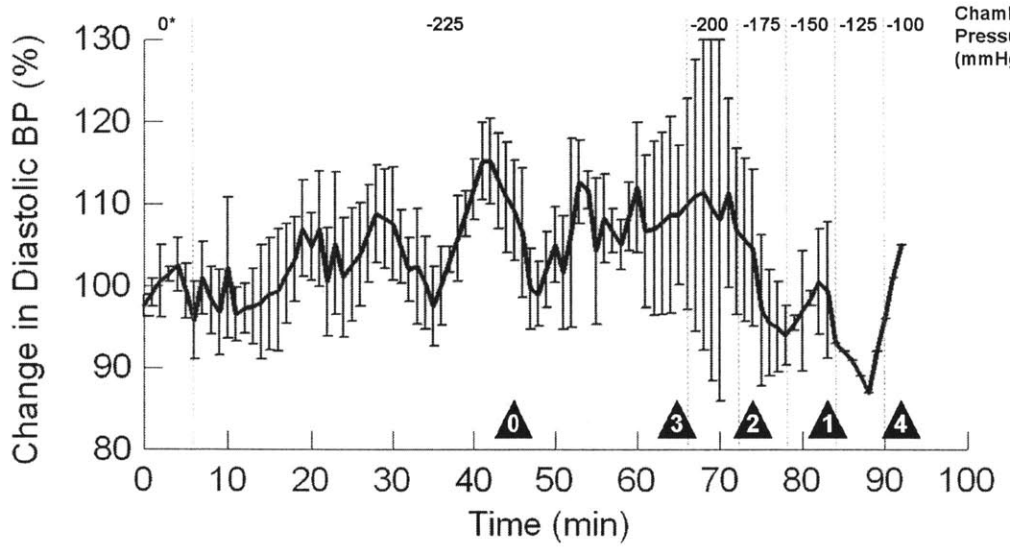

Figure 6-13: Change in diastolic blood pressure during **suited** tests, normalized to baseline pressure during ambient conditions. Black triangles indicate test termination point for the individual subject, as before. *Baseline measured on *unsuited* subject, as discussed in text.

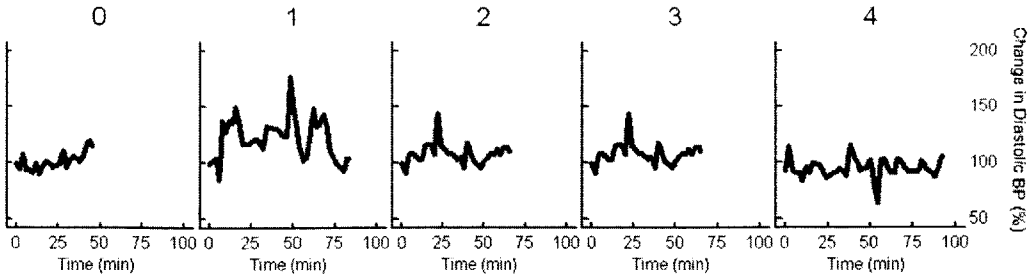

Figure 6-14: Data of Figure 6-13 by subject.

did significantly increase when the data of Subject 1 was included.

Skin temperature

Figure 6-15 shows the changes in skin temperature on the calf during unsuited exposure to underpressure. Temperature decreased significantly on both the anterior and posterior of the left (out-of-chamber) calf. Temperature also decreased significantly on the posterior of the right (in-chamber) calf despite a sharp increase beyond -175mmHg as this was caused by only one subject (Subject 1, Figure 6-16(a)). No conclusions could be made regarding the change in temperature on the anterior of the in-chamber calf as the linear regression model could not be fit to the curve, as the temperature increase beyond -175mmHg was observed in two subjects (Subjects 0 and 1, Figure 6-16(b)). Note that the in-chamber calf data excludes Subject 4 as the temperature sensors on this subject's calf became loose and could not be reattached during the test while the calf was inside the low-pressure chamber.

Figure 6-15 shows the changes in skin temperature on the calf during suited exposure to underpressure. Unfortunately, no meaningful conclusions should be made from this data as the responses of individual subjects were considerably different from each other (Figure 6-18) and from the averaged data of Figure 6-15. Subject 2 clearly had the greatest effect on the averaged data of Figure 6-15 as shown by the step change at -175mmHg when Subject 2 terminated the test; removing Subject 2, however, did not eliminate the considerable differences between the individual and averaged data.

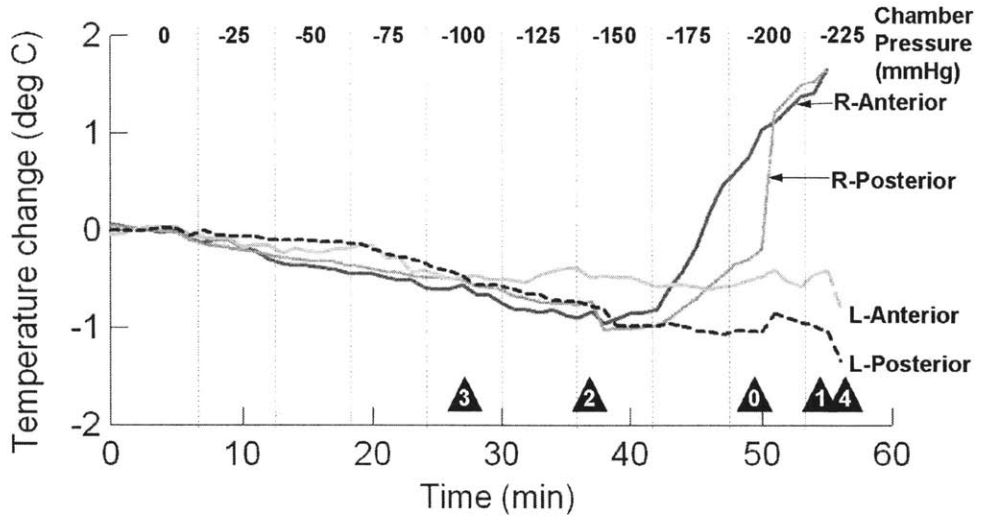

Figure 6-15: Change in skin temperature during **unsuited** tests, with 0 being the average baseline temperature during ambient conditions. 'L' and 'R' refer to left (out-of-chamber) and right (in-chamber) calves respectively. Figure excludes temperature data for the right calf of Subject 4 as the temperature sensors on this calf became loose, as explained in text. Error bars have been removed for visual clarity. Black triangles indicate test termination point for the individual subject, as before.

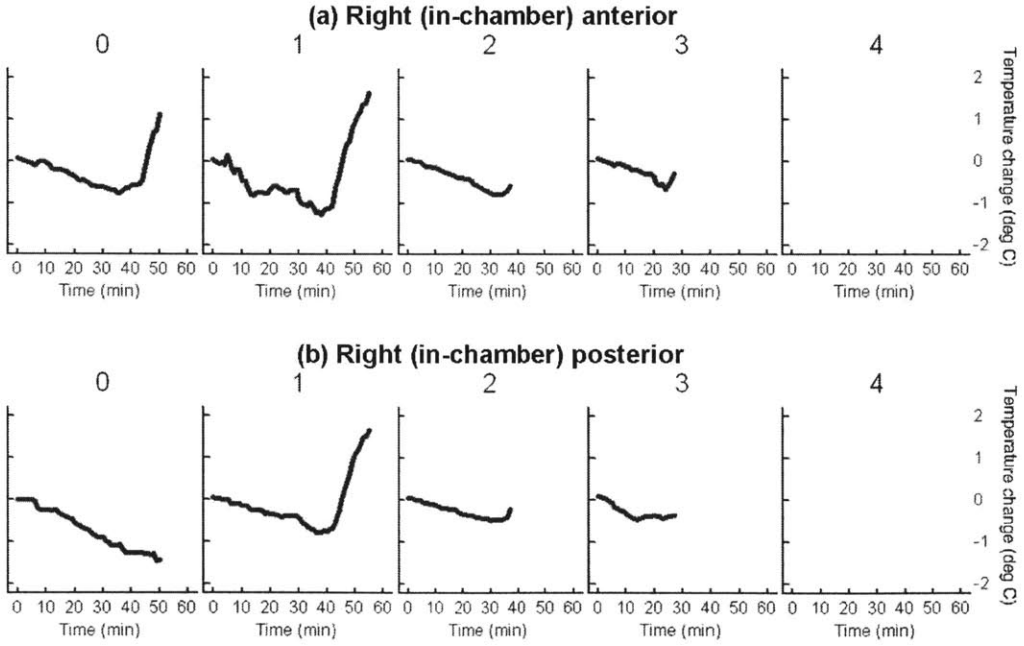

Figure 6-16: Data for right (in-chamber) calf of Figure 6-15 by subject.

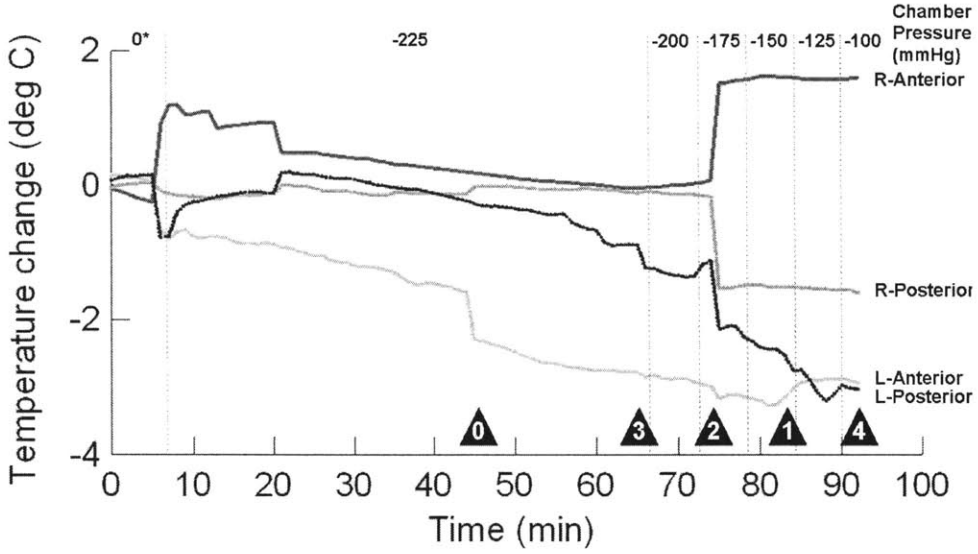

Figure 6-17: Change in skin temperature during **suited** tests, with 0 being the average baseline temperature during ambient conditions (0mmHg chamber pressure). 'L' and 'R' refer to left (out-of-chamber, unsuited) and right (in-chamber, suited) calves respectively. Figure excludes majority of temperature data from Subject 1 (see Figure 6-18)that was lost during a computer crash at the conclusion of the test. Error bars have been removed for visual clarity. Black triangles indicate test termination point for the individual subject, as before. *Baseline measured with *unsuited* subject, as discussed in text.

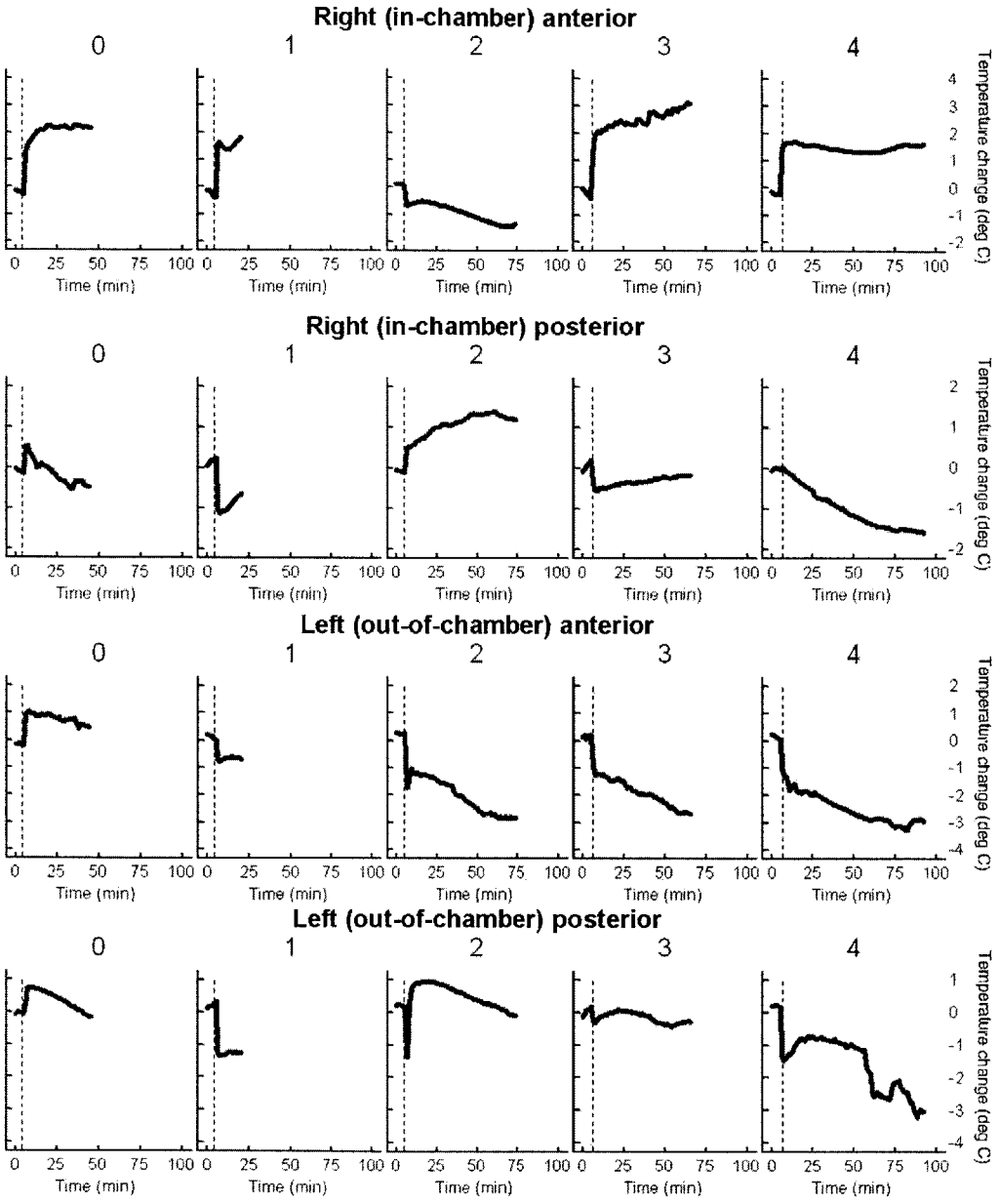

Figure 6-18: Data of Figure 6-17 by subject. The majority of temperature data from Subject 1 was lost during a computer crash at the conclusion of the test. Dotted line indicates end of unsuited baseline measurement at 6 minutes.

6.4 Discussion

6.4.1 Effectiveness of Bindings in Protecting against Underpressure

The experiments described in this chapter have demonstrated the use of an elastic-only mechanical counterpressure garment at higher[8] levels of underpressure (-30kPa, -225mmHg) and longer duration (over an hour) than previous MCP garments (Table 2.2). The glove and sleeve of Tanaka et al [9] was worn for up to five minutes at -150mmHg[9]; the Clapp "skinsuit" glove [5] for up to 30 minutes at -180mmHg; and the Space Activity Suit of Annis and Webb for up to 20 minutes in an altitude chamber with the subject breathing up to 200mmHg positive pressure[10].

A comparison of the unsuited and suited test durations (Figures 6-4 and 6-5) confirms that the elastic bindings were effective in protecting the calf against exposure to underpressure. Without the bindings, no subject was willing to tolerate -225mmHg (the MCP garment design pressure, as discussed in Section 2.1.2) for more than a minute; the two female subjects were not willing to tolerate more than -150mmHg. With the bindings, four of five subjects – including the two female subjects – spent an hour or more at -225mmHg with no significant adverse effects, as discussed in more detail below. The fifth subject did not complete the hour-long regimen only because of a loss of pressure in the MCP foot garment, as discussed further in Section 6.4.4.

To be fair, the success of these experiments may be attributed not only to the bindings per se – the fact that the bindings were demonstrated on the calf, rather than another anatomical region, may also be a contributing factor. The subjects in this experiment were willing to endure a high level of underpressure on their *unsuited* calf – up to -225mmHg (Figure 6-4). By contrast, the subjects of Tanaka et al [9] were not willing to tolerate underpressures of more than -100mmHg on their unsuited arm and hand; in lower body negative pressure (LBNP) experiments, in which the entire

[8] In this context "higher" means "more severe", not numerically greater.

[9] In development trials the glove, but not the sleeve, was worn at -218mmHg for up to an hour, according to *unpublished* data cited in Waldie et al [42].

[10] Excludes considerable pressure ramp-down and ramp-up times in the altitude chamber.

body below the abdomen is subjected to negative pressure, -70mmHg is typically sufficient to induce presyncope [47].

This may be because the leg has a greater capacity to tolerate blood pressure differentials than the arms in order to cope with the blood pressure gradient in a standing human being [16, 53]. Furthermore, the subjects were in a seated position, which significantly reduced the initial pressure gradient to be supported by the calf. Finally, only one calf of one leg, a small area compared to the whole lower abdomen, was exposed to underpressure. Had the bindings been tested on anatomical areas other than the calf, subjects may not have been willing to tolerate underpressure levels as high as -225mmHg. In light of these considerations, the effectiveness of the bindings requires further verification through testing not only on the calf, but on other "cylindrical" anatomical areas, particularly the entire leg and the arms.

6.4.2 Pressure Distribution Generated by the Bindings

Average pressure

The bindings generated an average $\overline{P}$ of 23.8kPa (179mmHg) on the calf anterior, considerably less than 30kPa (225mmHg) target pressure. At first glance this appears to be a poor result; if the bindings had generated only an average of 179mmHg across the entire calf to compensate for the -225mmHg chamber pressure, the 55mmHg pressure differential would, according to the review of Chapter 5, cause adverse physiological effects since it was applied for a relatively long time (an hour or more)[11]. For most subjects, the suited calf appeared slightly swollen after an hour of exposure to underpressure (Figure 6-19), providing further evidence that the bindings did not generate sufficient pressure to completely compensate for the -225mmHg chamber pressure.

However, the pressure sensor was deliberately located on the calf anterior to to

[11]It is true that in Waldie et al [42] the palm of the hand displayed little pathologic response (edema, swelling etc) when an the MCP glove was worn for up to 60 minutes with the difference between the chamber pressure and MCP applied on the concave palm area appeared to be as much as 100mmHg. Waldie et al attributed this to the relatively high elastic strength and thickness of the skin on the palm. The calf, whose skin is not as strong as that of the palm, is unlikely to withstand magnitudes and durations of underpressure as high as the palm without adverse effects [9].

measure the pressure on the flat or concave shin area (Figure 4-1(b)). Equation 4.2 shows that the MCP produced for a given elastic tension decreases with increasing radius of curvature. As such, the MCP on a flat or concave area should theoretically be zero. Nearly all previous elastic-only MCP designs have noted the difficulty in pressurizing flat or concave areas without inserts to compensate for the concavity [1, 5, 42, 9]. The fact that the bindings were able to generate an average of 179mmHg across the shin suggests that the average pressure on convex regions away from the shin was higher than 179mmHg, possibly explaining why subjects were able to tolerate over an hour at -225mmHg despite the insufficient MCP applied to the shin[12].

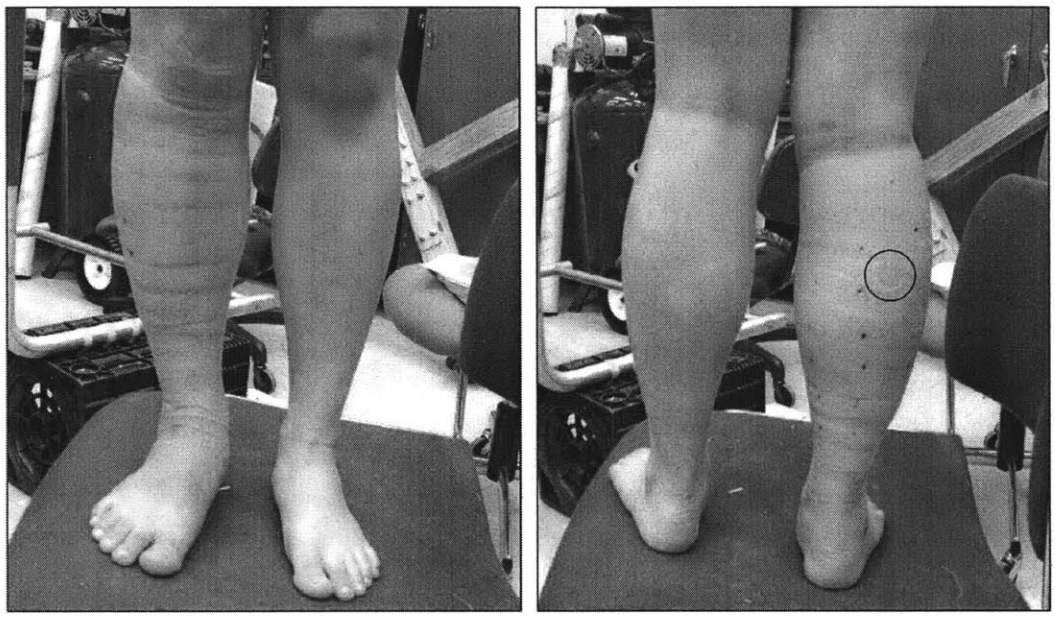

Figure 6-19: Typical front and back views of the calves after a suited chamber test. The right calf that was suited during the chamber test appears slightly swollen compared to the left calf. The horizontal indentations on the suited calf are areas where bindings unintentionally overlapped to produce excessive MCP – very similar to foot and ankle indentations that naturally occur when socks are worn for several hours. The circular indentation on the calf posterior (black circle, right) was made by the skin temperature sensor. All these observable effects were temporary and naturally disappeared within several hours after the conclusion of the test.

[12]It also suggests that 4.2 is too simple a model to describe the pressure generated by the bindings [59].

Uniformity

The elastic bindings did not generate as uniform a pressure distribution on the calves as they did on the test cylinder in Section 4.4.5: $\overline{s}$ was 8.7kPa (65mmHg), considerably higher than the 3.2kPa (24mmHg) on the cylinder[13] and the 1.6kPa (12mmHg) limit of Section 2.1.2. The lack of uniformity is likely to have been caused several factors, some of which were already discussed in Section 4.4.8. The most obvious was the aforementioned flat or concave contour of the shin that contradicted the simplistic design assumption that the calf is cylindrical. Additionally, there may have been changes in leg shape due to muscle movement: although the subject sat in a position that inherently prevented them from moving their suited calf, some subjects deliberately flexed the muscles on their suited calf to relieve discomfort. As discussed in Section 4.4.8, it would be extremely challenging to design bindings that could cope with the the non-cylindrical, dynamic shape of the leg to produce a uniform pressure distribution.

Another factor contributing to the lack of uniformity was alignment marks on the binding that were not well aligned with one another and with the alignment lines on the skin. Although the marks were accurately aligned at the start of the test, perspiration may have reduced the friction between skin and binding and allowed the bindings to slip from their original position, particularly on regions where calf circumference changed rapidly as the elastic tension in the bindings covering these regions must vary within a short length of binding to maintain a uniform pressure distribution. It was also difficult to use the alignment spirals to minimize both the overlap and potential gaps between adjacent binding edges, which would result in over- and under-pressure respectively, as discussed in Section 4.4.3. Finally, the inherent inaccuracies in the individual sensel measurements of the Tekscan sensor would have contributed another few percent to the lack of uniformity, as discussed in Chapter 3.

The lack of uniformity caused some observable effects, particularly skin indentations (Figure 6-19). However, *all observed effects were temporary and disappeared*

[13]This is the result for the cylinder using 8 alignment lines and spiral – the same alignment patterns used on the leg for the experiments in this chapter.

within a few hours after the conclusion of the test. No subject experienced any bruising, edema or other adverse effects that required medical treatment. It is likely that these relatively mild effects could be further mitigated by leg movement (as would occur during an EVA) that would increase the speed and uniformity of blood circulation throughout the leg.

In summary, the bindings generated a pressure distribution that was neither sufficiently high to completely compensate for the -225mmHg chamber pressure nor sufficiently uniform to completely avoid mild physiological effects induced by localized pressure differentials. As such, bindings development should continue to focus on improving the magnitude and uniformity of the pressure distribution that the bindings generate *on an irregularly shaped human leg*, rather than the simple test cylinders of Section4.4.4. The next section discusses the physiological measurements in light of the pressure distribution results of this section.

6.4.3 Physiological Results

Heart rate

There was no significant change in heart rate during any suited or unsuited experiments. This is commensurate with the results of Tanaka et al [9, 7] where subjects were exposed to underpressure both with and without an MCP glove and sleeve[14]. In contrast, Reddig et al [8] found that heart rate increased significantly (up to 30%) in subjects exposed to -40mmHg lower body negative pressure (LBNP) with no compensatory MCP. It is likely that the heart rate increase occurred in the LBNP, but not with those involving only a single hand [7], arm [9] or calf (this chapter) because exposure of a larger surface area to negative pressure results in a greater volume of blood shift. The large blood shift activates a sympathetic response that increases heart rate and blood pressure, among other effects [8, 6].

[14]In contrast, Tourbier et al [6] measured a significant 10% increase in heart rate over normal baseline values with MCP-suited hands exposed to -150mmHg. However, the paper's definition of "baseline value" is unclear and, depending on the definition, may change the significance of the result. The results are therefore not considered in this discussion.

Systolic and Diastolic BP

In the present study, unsuited exposure to underpressure resulted in a significant increase in both systolic and diastolic blood pressure. This is again commensurate[15] with Tanaka et al [9] who found an increase in mean arterial pressure[16] with an unsuited arm exposed to -50mmHg[17] Similarly, Reddig et al [8] found a significant increase in arterial pressure at -50mmHg LBNP.

However, subjects suited with the elastic bindings did not experience any significant change in systolic or diastolic blood pressure. *The bindings therefore provided protection from the increase in blood pressure that occurred with unsuited exposure to underpressure.* Furthermore, this result does not contradict Tanaka et al [9, 7] or Tourbier et al [6] who reported an increase in mean arterial pressure for gloved subjects, since the MCP provided by the glove in these studies *overcompensated* for the underpressure inside the test chamber. The overpressure is likely to have been the main cause of the increase in blood pressure in these studies.

Skin temperature

During unsuited tests, the present study found that the skin temperature of the in-chamber calf decreased with exposure to up to -150mmHg underpressure (Figure 6-15), in agreement with the studies of Tanaka et al [9, 7], Reddig et al [8] and Knudsen et al [46] on unsuited hands exposed to underpressure. The decrease is largely driven by enhanced evaporative heat transfer facilitated by the decreasing chamber pressure [6]. The temperature increase observed in Subjects 0 and 1 above

[15]The reader should interpret "commensurate" with caution as the data in the present study was analyzed using multiple linear regression, for reasons explained in Section 6.2.2, rather than the repeated measures ANOVA employed in [9, 7, 8, 6]. Statistical significance in the present study therefore means that the coefficient of the *linear* regression in question is statistically different than zero, whilst significance in the ANOVA of the other studies entails a significant difference in the factor level means that is not necessarily linear. It is therefore possible that a statistically significant ANOVA result would not arise using regression analysis as the latter requires linearity for significance. Any known differences in interpretation between significant regression and ANOVA results is discussed in the main text.

[16]Defined as the diastolic BP plus one third of the systolic BP.

[17]There are no results for higher levels of underpressure as Tanaka's subjects were unwilling to endure the discomfort expected at these pressures, or because the measurements were stopped by a medical monitor due to symptoms such as petechiae.

-175mmHg has not been reported elsewhere as other studies did not expose unsuited subjects to such extreme magnitudes of underpressure. The increase may be a stress response to the subject's increasing discomfort at higher levels of underpressure, as indicated by increased blood pressure. However, the corresponding increase in heart rate and temperature increase on the out-of-chamber calf that would also be induced by this stress response was not observed.

The change in skin temperature during suited tests varied so greatly (Figure 6-17 and 6-18) that no meaningful conclusions could be made regarding the effect of chamber pressure on skin temperature. It would also be meaningless to draw parallels between these results and those from previous MCP studies [9, 7, 6], as the latter deliberately exposed suited hands to *overpressure*, whereas the MCP elastic bindings of the present study were designed to match the -225mmHg chamber pressure sustained through the majority of the experiment.

However, there is strong evidence that skin temperature under an MCP garment exposed to underpressure is influenced not only by the chamber pressure but also by the material properties of the garment [6, 1]. A sufficiently porous MCP garment may lower skin temperature by allowing perspiration to evaporate; in contrast, the elastic bindings of the present study consisted of neoprene rubber, which is relatively impermeable. Skin blood flow also influences skin temperature because internal heat transport is dependent on blood flow; however, skin temperature may change without corresponding changes in blood flow and vice versa. Further theoretical and experimental work is required to quantify the competing effects of these factors on skin temperature underneath an MCP garment.

In summary, the present study was in agreement with previous studies showing that skin temperature in unsuited anatomical areas exposed to underpressure decreased due to enhanced evaporative heat transfer, but no conclusions could be drawn regarding the temperature changes on suited areas due to substantial variations in the response of individual subjects.

6.4.4 Effectiveness of Hybrid Foot Garment

The present study provided strong empirical evidence that the hybrid foot garment was effective in protecting the foot against the effects of underpressure. During unsuited tests, when the foot was the only anatomical region inside the chamber to which MCP was applied, all subjects commented that their foot felt comfortable, especially compared to the discomfort in the unprotected calf exposed to underpressure.

The importance of the foot garment was highlighted in several instances when it did *not* provide adequate pressure to the foot. During the suited test of Subject 0 a leak substantially reduced the MCP generated by the foot garment; the subject ended the test a few minutes later due to the intense discomfort caused by increased blood flow into the foot exacerbated by the tourniquet effect of the calf MCP produced by the elastic bindings. Similarly, a kink in the foot garment's air line prevented the bladder from providing any MCP during the first attempt to conduct the suited test of Subject 3. As such, Subject 3 ended the test even before the low pressure chamber had reached the -225mmHg test pressure, again due to increased blood flow into the foot.

However, a few practical problems arose during the use of the foot garment. Some discomfort was occasionally experienced at the ankle and Achilles tendon where excess bladder material "bunched" together during inflation to produce mild pressure points; in some other areas the bunched material prevented the bladder pressure from being fully transmitted to the skin. Second, the bladder occasionally expanded outwards above the top of the the restraint layer above ankle height, especially if the restraint layer was not tightly laced. Finally, the location of the bulkhead connector made it cumbersome to attach the air tube to the bladder through the restraint layer. It is likely that these practical problems could easily be solved with minor modifications to the bladder and restraint layer design.

6.4.5 Experimental Limitations

This study was constrained by some major limitations. First, several physiological parameters that would have yielded direct insight into the mechanisms of physiological responses to mechanical counterpressure were not measured, particularly perfusion (blood flow rate) and the resulting change in calf circumference. One of the most obvious effects of exposure to underpressure is an increase in blood flow to anatomical areas exposed to underpressure – an increase that the use of a mechanical counterpressure garment can prevent, as all subjects in this study clearly experienced. Laser Doppler flow meters and strain gages have been used in other studies (e.g. [6, 7, 8, 9]) to quantify these changes but were not available for this study.

The parameters measured in this study – heart rate, skin temperature and blood pressure – are somewhat *indirect* measures influenced by the change in perfusion caused by exposure to underpressure (or overpressure, if the MCP generated by the garment is greater than the chamber underpressure). These indirect parameters are affected by many confounding influences such as circadian cycles, diet, air temperature, posture and so on. Considerable effort was made to minimize the effect of these confounds, e.g. by prohibiting subjects from talking during blood pressure measurements and ensuring that every subject had identical posture during all physiological measurements; but could not completely eliminate them. Perfusion and calf circumference are less affected by these confounds and would also provide a more holistic interpretation of the physiological response to MCP than the "parameter-by-parameter" approach (using the "indirect" parameters) employed in Section 6.4.3.

The design of the rubber seal isolating the external atmosphere from the calf inside the chamber (Figure 6-1, just below subject's right knee) requires improvement. Being the weakest barrier between the atmosphere and chamber interior, the seal was occasionally prone to leaks between the seal and calf that momentarily reduced the magnitude of the chamber's negative pressure from the desired level. Rubber bands were therefore used to tighten the seal against the calf (Figure 6-1). However, these bands occasionally induced an unwanted tourniquet effect may have reduced venous

return and therefore confounded the physiological results. An improved method is therefore required for reducing the incidence of seal leakage.

There were major limitations in the Tekscan I-Scan pressure measurement system. In addition to its unsatisfactory measurement accuracy (Chapter 4) the long calibration procedure necessary to achieve even this level of accuracy, as well as cumbersome software, made it difficult to use more than one Model 9801 sensor at a time; as such, pressure distribution measurements were limited to the calf anterior. Previous Bio-Suit studies did use Model 9801 sensors to measure the pressure distribution over the entire calf; doing so, however, required either a single sensor to be repositioned around different calf locations between trials [14] or used a shorter calibration procedure [3] than that used in this thesis (Appendix B). Once the capability to measure the pressure distribution on the entire calf exists, future studies should not only consider pressure magnitude and uniformity but also the *effect of location* on the pressure generated by the bindings – whether there is a significant difference in the MCP generated on different calf areas, e.g. the bony shin vs the fleshy calf posterior, as postulated above.

Finally, the small number of subjects (n=5) severely restricted the power of the statistical analysis. As mentioned in Section 6.3, the trends in some physiological parameters of individual deviated considerably from the overall trend, considerably increasing the standard error in the regression analysis. Additionally, the multiple regression analyses provided preliminary evidence that body dimensions (particularly calf length, calf circumference, height and weight) and gender have an effect on the physiological response to underpressure. Measurements on many more subjects are therefore required to reduce the effect of individual subject deviations and to test the initial hypotheses regarding these body dimension and gender effects.

6.5 Summary and Conclusions

The experiments of this chapter have demonstrated the use of the elastic bindings concept to protect the calf from the effects of -225mmHg underpressure for up to an

hour – a condition that no subject was willing to tolerate for more than two minutes without wearing the bindings. The bindings also mitigated the physiological effects induced by exposure to underpressure. The bindings concept therefore shows promise for further development, particularly when the positive physiological results of this chapter are combined with the rapid don-doff capability and mobility demonstrated in Chapter 4.

Further development should initially focus on improving the uniformity and magnitude of the pressure distribution that the bindings generate. More specifically, the bindings must generate an average of 225mmHg on all calf sections, particularly the flat or concave sections of the shin. The spatial variation from this average pressure should also be reduced as much as possible to avoid the adverse effects of localized pressure variations discussed in Chapter 5. These improvements would improve comfort and allow the bindings to be worn for even longer durations without causing initial symptoms of adverse physiological effects that occasionally arose in this study.

The effectiveness of the bindings should also be tested on other limbs. Initial tests should extend the calf experiments of this chapter to the entire leg as the bindings are more likely to produce a uniform distribution on the thigh rather than than the more irregularly shaped arm [59]. Further techniques are then required to adapt the bindings concept to the arm and other non-cylindrical geometries.

Chapter 7

Conclusions and Future Work

The major contribution of this thesis was the design and implementation of a novel elastic bindings concept for generating mechanical counterpressure (MCP) on the limbs as part of a Bio-Suit EVA system that is envisaged to be lighter, lower profile, safer and more maintainable than current systems. The bindings rely only on elastic tension, not fluid pressure, to generate MCP and thus do not suffer from the numerous disadvantages inherent in hybrid MCP garments and traditional gas-pressure spacesuits. The bindings demonstrated greater mobility and ease of donning than previous MCP garments, and their effectiveness was demonstrated on the lower leg of five subjects in a low pressure chamber at more extreme magnitudes and durations of underpressure than previous MCP experiments.

The bindings concept therefore exhibits many of the fundamental attributes necessary for the pressure layer in an MCP-based EVA system and is thus extremely valuable for studying the engineering and physiological issues associated with using MCP, as was done in this thesis. However, much further work will be necessary before the bindings can be used an operational spacesuit, for several reasons. First, the don-doff and pressure production processes must be decoupled, not only to further improve the ease and rapidity of donning but also to prevent the wearer from enduring overpressure on part of the body whilst other parts of the suit are being donned. Second, the uniformity of the pressure distribution generated by the garment must also be improved considerably to prevent adverse physiological effects of spatial

pressure variations. Finally, the garment must maintain this uniform pressure distribution despite dynamic changes in body shape that occur during movement or muscle flexion. There is potential to achieve all three of these objectives by utilizing active or "smart" materials; doing so, however, will require not only more sophisticated MCP garment design but also a substantial effort in fundamental materials research, as the characteristics of currently available active materials are not sufficiently well understood nor sufficiently controllable for use in an MCP garment.

Further research is also required to understand the physiological implications of using MCP garments: for example, the acceptable limit for spatial pressure variations has been theoretically estimated but appears conservative. The effects of applying MCP for several hours – the duration of a typical EVA – are unclear, as are the potential effects of repeated use over the several months or even years that a typical human expedition to Mars is projected to last.

Extra-vehicular activity is critical for human spaceflight and particularly for human planetary exploration. The MCP-based Bio-Suit System has the potential to maximize and even augment the EVA capabilities of future planetary explorers. Its continued development is therefore a crucial element in the pursuit toward a human mission to other worlds, especially given the tremendous effort and risk that must be invested in such a challenging, inspirational and noble enterprise.

Appendix A

Further Considerations for Pressure Measurement on the Limbs

These are additional to the issues discussed in Chapters 3 and 4, and should be considered in future work that uses Tekscan sensors for measuring MCP on the human body.

A.1 Pressure Measurement on Soft Surfaces

As mentioned in Section 4.4.8, the pressure distribution generated by the Phase II elastic bindings on a soft cylinder was to be measured as a natural extension of the rigid cylinder tests of Section 4.4.5. The cylinder consisted of a rigid PVC cylinder covered with an outer layer of foam (Figure A-1 (left)) to simulate a fleshy human leg with approximately 170mm diameter. However, this cylinder could not be used as a calibration rig because there was no easy way in which to apply a uniform calibration load to an I-Scan sensor on its surface. To rectify this, a soft cylindrical *calibration* rig was designed in a similar style to the rig used in Chapter 3 (Figure 3-2), the difference being a foam layer that was placed in the channel between two concentric cylinders (Figure A-1(right)).

Figure A-1: Soft cylindrical test rigs: (left) test rig intended for use in the elastic bindings tests; (right) calibration rig.

An I-Scan sensor was calibrated using this rig using the method of Section 3.3.1. The results (Figure A-2) show that the pressure measured by the sensors was considerably lower than the applied pressure – i.e. the air pressure inside the inflated bladder – and that, unlike the results of Section 3.3.2, the deviation increased with pressure.

This poor result was attributed to the soft foam being unable to sufficiently restrain the bladder from expanding into the soft foam and away from the sensor; as such, the fluid pressure inside the foam was being partially restrained by the bladder walls and not transmitted to the sensor.

A solution might be to increase the stiffness of the foam (within reason – excessively stiff foam would not be a fair representation of a human leg) or to reduce the gap between the foam and inner rigid cylinder. However, lack of time prevented this from being attempted. Consequently, the intended test of the bindings wrapped on the soft cylinder was not performed.

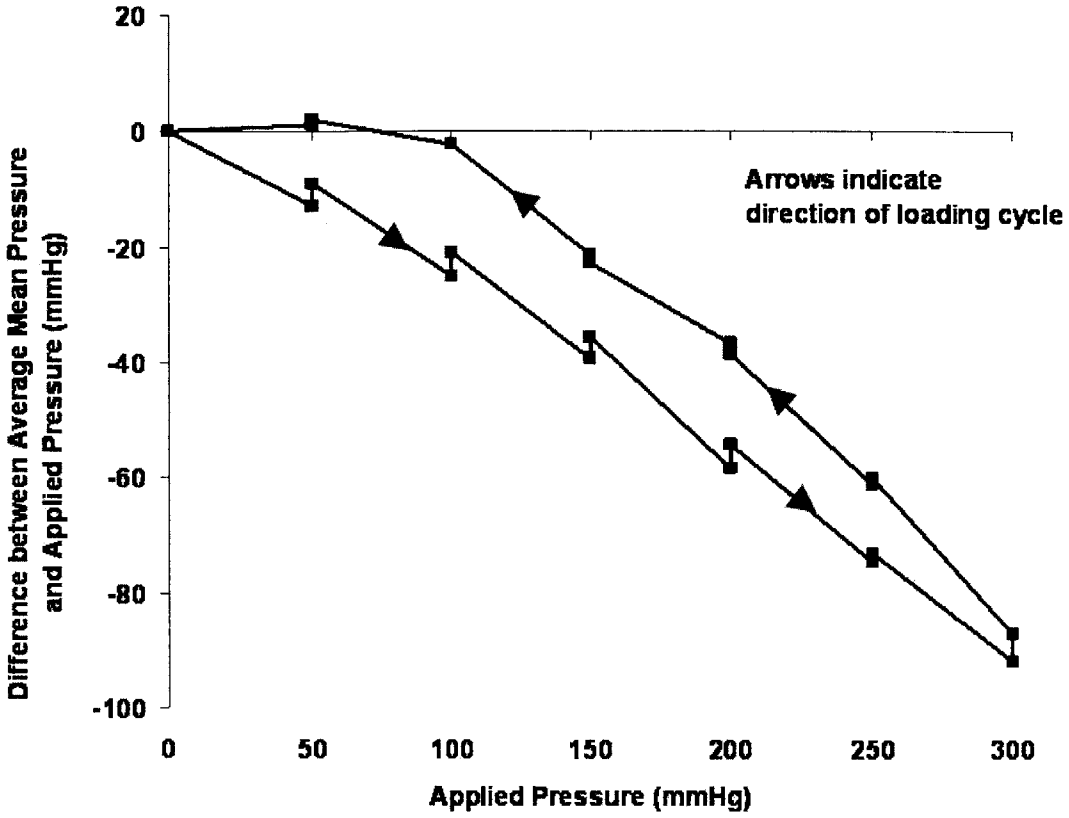

Figure A-2: Difference between average measured pressure and applied pressure for I-Scan in the soft cylindrical calibration rig.

A.2 Definition of Pressure Measurement on Soft Surfaces

A more fundamental problem in using I-Scan sensors – or, for that matter, *any* pressure sensor – to measure the pressure generated by an MCP garment is that it is difficult to physically define the pressure exerted on soft surfaces such as fleshy areas of the limbs. Pressure is the ratio of force over area, and when a force F is applied to a soft, flexible surface such as muscle with area A, both F and A change as the soft surface deforms. Ashruf [32] states: "Up to now, there is no agreed standard for the measurement of interface pressures between soft objects. In other words, it is sometimes questionable what is actually being measured."

This may occur when the elastic bindings are wrapped onto the soft cylinder

described in the previous section: the applied pressure might compress the foam and therefore reduce its surface area. The force applied by the bindings may also change, but it is not clear whether it would increase or decrease because it depends on both the cylinder dimensions as well as the tension in the binding.

This issue requires further investigation.

A.3 Presence of Sensor Interfering with Pressure Garment Dynamics

Wu et al [60] used finite element methods to estimate the effect of using Fuji Pressensor film (a common and cheap precursor / alternative to Tekscan sensors) to measure contact pressures into spherical and cylindrical articular joints. They hypothesized that the mere presence of the sensor in the joint would interfere with the measurement by altering the actual pressure and / or causing the measured pressure to be different from the actual pressure - sometimes known as insertion or interference error. Indeed, the measured contact pressure was up to 26% higher than the actual pressure depending on the loading, joint geometry and joint mechanical properties. Considering this effect on top of the limited accuracy of the film (approx 10%), the total error in the pressure measured by Pressensor film could be up to 28%.

Much of the interference error was attributed to the inherent stiffness of the film (100MPa, much higher than the cartilage stiffness of <1MPa) as well as its thickness (only 0.3mm). The authors suggested that such error is difficult to correct because it depends on many factors, including loading conditions and the material properties and geometry of both the sensor and joint. The most obvious way to reduce the error would be to develop a thinner sensor whose stiffness was closer to that of the joint. For Bio-Suit work this suggests that the sensors must be both thin and extremely pliable to match the inherent "softness" of the skin as well as the pressure garment.

Appendix B

Equilibration and Calibration Procedure for Tekscan I-Scan sensors

This is based on recommendations in [22] and extended, based on experience with the I-Scan sensors, to minimize hysteresis and drift. Refer to [22] for details on how to perform the procedure below.

B.1 Sensor Preparation

- Peel off the protective backing.
- Cut the sensor into strips.
- Use a pin to punch small holes in each sensel to release any air bubbles trapped inside so that the sensels will not expand when used in the low-pressure chamber.
- Encase the sensor inside clear plastic layflat tubing to protect against creasing and other shear effects.

B.2 Preconditioning, Equilibration and Calibration

The experiments in this thesis measured the pressure applied by MCP garments whose design MCP was 150-225mmHg. As such, equilibration was performed at regular intervals between 0-300mmHg, and calibration at 100 and 300mmHg, to make the sensor was as accurate as possible in the 150-225mmHg range.

- Place the sensor in its calibration rig – either flat-plate or cylindrical.
- In the I-Scan software, set the sensor sensitivity to mid-3. This sets the saturation pressure at approximately 500–700mmHg, which maximizes sensitivity whilst minimizing the possibility that the MCP applied by the test garment will exceed this saturation pressure.
- Precondition the sensor before every use by loading it for at least 30s at >400mmHg three or more times.
- Equilibrate the sensor at 50, 100, 150, 200, 250 and 300mmHg. In the I-Scan software, set the equilibration delay timer to 30s to allow the sensor reading to stabilize before its equilibration coefficients are measured by the software.
- Calibrate the sensor at 100 and 300mmHg. In the I-scan software, set the calibration delay timer to 120s for the same reasons described in the previous step.

Appendix C

Acronyms

EMU	Extra-vehicular Mobility Unit
EVA	extra-vehicular activity
MCP	mechanical counterpressure
NASA	National Aeronautics and Space Administration
NIAC	NASA Institute for Advanced Concepts

Bibliography

[1] J. F. Annis and P. Webb. Development of a Space Activity Suit. NASA Contractor Report CR1892, 1971.

[2] F. Korona and D. Akin. Evaluation of a hybrid elastic EVA glove. In *32nd International Conference on Environmental Systems*, San Antonio, TX, 2002.

[3] K. A. Bethke. The second skin approach: Skin strain field analysis and mechanical counter pressure prototyping for advanced spacesuit design. Master's thesis, Massachusetts Institute of Technology, 2005.

[4] J. Hoffman. White paper on the future of advanced EVA research. NASA Request for Information, 2004.

[5] W. M. Clapp. Design and testing of an advanced spacesuit glove. Massachusetts Institute of Technology, 1983.

[6] D. Tourbier et al. Physiological effects of a mechanical counter-pressure glove. In *31st International Conference on Environmental Systems*, Orlando, FL, 2001.

[7] K. Tanaka et al. Skin microvascular flow during hypobaric exposure with and without a mechanical counterpressure space suit glove. *Aviation, Space, and Environmental Medicine*, 73(11):1074–1078, 2002.

[8] M. Reddig et al. Physiological limits of underpressure and overpressure in a study of mechanical counter pressure suits. SAE Paper 2003-01-2444, 2003.

[9] K. Tanaka et al. Mechanical counter pressure on the arm counteracts adverse effects of hypobaric pressures. *Aviation, Space, and Environmental Medicine*, 74(8):827, 2003.

[10] D. J. Newman, K. Bethke, C. E. Carr, J. Hoffman, and G. Trotti. Astronaut Bio-Suit System to enable planetary exploration. In *International Astronautical Conference*, Vancouver, Canada, October 2004.

[11] C. E. Carr. *The Bioenergetics of Walking and Running in Spacesuits.* PhD thesis, Massachusetts Institute of Technology, 2005.

[12] P. Webb. The Space Activity Suit: An elastic leotard for extravehicular activity. *Aerospace Medicine*, pages 376–383, April 1968.

[13] L. Sim et al. Implementation and testing os a mechanical counterpressure Bio-Suit system. In *35th International Conference on Environmental Systems*, Rome, Italy, 2005.

[14] B. M. Pitts. Spacesuit: Spacecraft. Master's thesis, Massachusetts Institute of Technology, 2003.

[15] M. Gernhardt. Bounding the design space for spacecraft internal atmosphere pressure and composition. Briefing to the Office of Biological and Physical Research NASA Headquarters, June 2004.

[16] L. Trevino and C. E. Carr. A first-order design requirement to prevent edema in mechanical counter-pressure space suit garments. Submitted to *Aviation, Space, and Environmental Medicine*, June 2005.

[17] Private communication with P. Webb, Webb Associates, August 2005.

[18] Private communication with V. Koscheyev, University of Minnesota, August 2005.

[19] D. J. Newman et al. Astronaut Bio-Suit System for Exploration Class Missions. NIAC Phase II Final Report, September 2005.

[20] A. S. Iberall. The experimental design of a mobile pressure suit. *Journal of Basic Engineering*, pages 251–264, June 1970.

[21] C. E. Carr and D. J. Newman. New edema assessment technique. Bimonthly Report to NASA Institute for Advanced Concepts (NIAC) for NIAC Contract 070605-003-006, September 2004.

[22] I-Scan Equilibration and Calibration Practical Suggestions Rev A (company publication). Tekscan Inc (South Boston, MA), 10/27/03.

[23] Private communications with Chuck McWilliams, Tekscan representative, June 2005.

[24] D. R. Wilson et al. Accuracy of the I-Scan pressure measurement system. In *44th Annual Meeting of the Orthopedic Research Society*, page 393, New Orleans, LO, March 1998.

[25] S. Matsuda et al. A comparison of pressure sensitive film and digital electronic sensors to measure contact area and contact stress. In *41st Annual Meeting of the Orthopedic Research Society*, page 743, Orlando, FL, February 1995.

[26] K. Mann et al. A new tool to measure pressure under burn garments. *Journal of Burn Care and Rehabilitation*, 18(2):160, 1997.

[27] S. J. Kirstukas. Accuracy of Tekscan I-Scan Force Measurements in Repeated Deforming Use. Unpublished? (supplied by Tekscan Inc to Liang Sim, June 2005).

[28] A. L. DeMarco et al. Measuring contact pressure and contact area in orthopedic applications: Fuji Film vs Tekscan. In *46th Annual Meeting of the Orthopedic Research Society*, Orlando, FL, March 2000.

[29] T. G. McPoil et al. A comparison of two in-shoe plantar pressure measurement systems. *The Lower Extremity*, 2(2):95–103, 1995.

[30] B. J. Fregly and W. G. Sawyer. Estimation of discretization errors in contact pressure measurements. *Journal of Biomechanics*, 36:609–613, 2003.

[31] M. L. Harris et al. An improved method for measuring tibiofemoral contact areas in total knee arthrolasty: a comparison of K-scan sensor and Fuji film. *Journal of Biomechanics*, 32:951–958, 1999.

[32] C. M. A. Ashruf. Thin flexible pressure sensors. *Sensor Review*, 22(4):322–327, 1999.

[33] Private communication with David Ables, PPS representative, May 2005.

[34] Private communication with Wayne Board, Novel representative, May 2005.

[35] Private communication with Karl Schilling, XSensor representative, June 2005.

[36] Private communication with Scott Fiss, XSensor representative, December 2005.

[37] F. Mitchell et al. Pressure Measurement Applications for Humans. Unpublished (supplied by Xsensor Inc.), June 2005.

[38] J. Blaya. Force-controllable ankle foot orthosis to assist drop foot gait. Master's thesis, Massachusetts Institute of Technology, 2003.

[39] G. A. Ateshian et al. A stereophotogrammetric method for determining in situ contact areas in diarthrodial joints, and a comparison with other methods. *Journal of Biomechanics*, 27(1):111–124, 1999.

[40] M. Manouel et al. A miniature piezoelectric polymer transducer for in vitro measurement of the dynamic contact stress distribution. *Journal of Biomechanics*, 25(6):627–633, 1992.

[41] H. P. Giele et al. Direct measurement of cutaneous pressures generated by pressure garments. *Burns*, 23(2):137–141, 1997.

[42] J. M. A. Waldie et al. Compression under a mechanical counter pressure space suit glove. *Journal of Gravitational Physiology*, 9(2):93–97, December 2002.

[43] N. Jared Keegan. Midé Bio-Suit July Tasks. Internal memo between Midé Technology Corporation and MIT Man Vehicle Laboratory, July 2005.

[44] L. Sim. Unpublished data, p65 of Lab Book 2, Massachusetts Institute of Technology (2005).

[45] NASA 2005 Small Business Technology Transfer (STTR) Program Phase 1 Award Selections. Published online at http://sbir.gsfc.nasa.gov/SBIR/sttr2005/phase1/awards/index.html, November 2005.

[46] J. Knudsen et al. Physiological effects of underpressure and overpressure in a study of mechanical counter pressure suits. SAE Paper 2002-01-2317, 2002.

[47] V. A. Convertino. Lower body negative pressure as a tool for research in aerospace physiology and military medicine. *Journal of Gravitational Physiologiy*, 8(2):1–14, 2001.

[48] G. T. Nola and L. M. Vistnes. Differential response of skin and muscle in the experimental production of pressure sores. *Plastic and Reconstructive Surgery*, 66(5):728–733, 1980.

[49] S. Patel et al. Temperature effects on surface pressure-induced changes in rat skin perfusion: implications in pressure ulcer development. *Journal of Rehabilitation Research and Development*, 36(3):189–201, 1999.

[50] V. Schubert and B. Fagrell. Local skin pressure and its effects on skin microcirculation as evaluated by laser-doppler fluxmetry. *Clinical Physiology*, 9:535–545, 1989.

[51] R. Stolk et al. A method for measuring the dynamic behavior of medical compression hosiery during walking. *Dermatologic Surgery*, 30(5):729–736, 2004.

[52] R. H. Hooper and G. R. Jones. Are interface pressure measurements a true reflection of skin contact pressure when made over different layers of clothing? (Unpublished; provided by Tekscan Inc., South Boston MA in June 2005.).

[53] Private communication with C. E. Carr, Massachusetts Institute of Technology, June 2005.

[54] J. Lundvall and T. Lanne. Transmission of externally applied negative pressure to the underlying tissue. a study on the upper arm of man. *Acta Physiologica Scandinavica*, 136:403–409, 1989.

[55] R. A. Wolthuis, S. A. Bergman, and A. E. Nicogossian. Physiological effects of locally applied reduced pressure in man. *Physiological Review*, 54(3):566–595, 1974.

[56] K. Skagen and O. Henriksen. Changes in subcutaneous blood flow during locally applied negative pressure to the skin. *Acta Physiologica Scandinavica*, 117:411–414, 1983.

[57] A. E. Lasheen et al. External tissue expansion successfully achieved using negative pressure. *Surgery Today*, 34:193–196, 2004.

[58] Private communication with A. Natapoff, Massachusetts Institute of Technology, September 2005.

[59] L. Macintyre et al. The study of pressure delivery for hypertrophic scar treatment. *International Journal of Clothing Science and Technology*, 16(1 and 2):173–183, 2004.

[60] J. Z. Wu, W. Herzog, and M. Epstein. Effects of inserting a pressensor film into articular joints on the actual contact mechanics. *Journal of Biomechanical Engineering*, 120(4):655–659, 1998.